



SMITHSONIAN INSTITUTION
CONSERVATION ANALYTICAL LABORATORY

**Development of an Evaluation
Methodology for Cleaning Damage Assessment**

FINAL REPORT

Prepared by:

A. Elena Charola

in collaboration with:

Carol A. Grissom

with the support of:

Melvin J. Wachowiak, Jr.
Evin Erder
Douglas Oursler, Johns Hopkins University

and contributions from:

Dale Bentz, NIST
John W. Roth, Zygo Corporation
Theodore Vorburger, NIST

through cooperative agreement (1443CA00194036) between:

The National Park Service and the Smithsonian Institution

June 1996

EXECUTIVE SUMMARY

The aim of the project was to determine an appropriate methodology for evaluation of damage induced during cleaning of masonry materials. Of the techniques used for the evaluation of surface changes, measurement of roughness appeared to be most promising.

After a literature survey was conducted, a number of methods were explored, including white light interferometry, thermographic imaging, reflectometry, laser triangulation profilometry, stylus profilometry, and reflected light image analysis. This was followed by careful evaluation of the last three techniques on a set of three samples prepared in the laboratory: polished marble, sawn limestone, and a brick paver. Portions of each sample were abraded with glass beads or alumina powder, and silicone rubber replicas were prepared for laser triangulation profilometry (LTP) and reflected light image analysis (RLIA). Results of testing these samples showed that stylus profilometry and RLIA gave results consistent with LTP, which seemed the most accurate technique except on polished surfaces, but was unavailable for further tests.

These two techniques were then used on a second, larger set of samples (polished marble, sawn marble, polished granite, flame finished granite, sawn limestone, sawn sandstone, quarry tile and glazed tile) blasted with water or powdered materials (walnut shells, glass beads, Black Beauty slag) at two pressures. In addition, reflectometry was used for evaluation of gloss on polished surfaces. To gain further insight about changes, a microdrop absorption test was used on porous surfaces, and visual and touch evaluations were also carried out.

Results showed that none of the instrumental techniques is ideal for assessing changes in roughness of masonry materials induced by blasting. Stylus profilometry, as measured with a portable instrument, cannot be used to measure very rough surfaces. RLIA has the advantage that large surfaces can be evaluated, but interpretation of results is complex and use of replicas is mandatory. Microdrop absorption tests confirmed damage induced by the harshest abrasives. Touch and especially visual evaluation of surfaces showed that if the appropriate standards were available, consisting of a range of samples for each type of stone, these methods could be applied successfully to evaluate change in roughness.

Surface roughness of masonry materials is in general irregular because of inhomogeneities in the material itself and inconsistent application of surface finishes. Finally, the evaluation of roughness does not necessarily reflect the damage that abrasive cleaning methods can induce on stone.

ACKNOWLEDGMENTS

Dr. Lambertus van Zelst, Director of CAL is gratefully acknowledged for helpful discussions and suggestions throughout the development of this project.

Thanks are specially due to E. Blaine Cliver, Anne Grimmer and Judy Jacob, from the National Park Service for discussions during the meetings that were held at various stages of the project.

Also to be thanked are Nick Veloz and the Statue Preservation Crew: Jessie Mallard, Jimmy Mauldin and Tim Boyd, of the National Park-Central, for their help in the blasting of the samples for Phase II of this project. Robert Stanton, Regional Director, and Arnold Goldstein, Superintendent of National Capitol Park-Central are hereby acknowledged for allowing the use of that facility to carry out the blasting.

Last but not least, Loretta Ester-Clark and Vernetta Williams, CAL, are thanked for their support in the practical aspects of this project.

Great Neck, June 1996

TABLE OF CONTENTS

EXECUTIVE SUMMARY	
ACKNOWLEDGMENTS	
I. GENERAL INTRODUCTION	1
1. Outline of the Problem	1
2. Surface Roughness Definition	2
3. Survey of Methodologies	3
3.1 Comparison with Standards	3
3.2 Tracer Point Analysers	4
3.3 Changes in Surface Air-flow	4
3.4 Light Measuring Devices	4
3.5 Thermographic Imaging	6
II. PHASE I: LABORATORY TESTS	7
1. Sample Preparation	7
2. Replica Preparation	8
3. Applied Methodologies	9
3.1 Methods tested in other Labs	9
3.2 Methods tested at CAL	11
4. Results	12
5. Conclusions	16
III. PHASE II: FIELD TESTS	17
1. Sample Preparation	17
2. Replica Preparation	19
3. Evaluation of Surfaces	19
3.1 Visual Assessment	20
3.2 Assessment by Touch	20
3.3 Gloss Measurements	20
3.4 Stylus Measurements	20
3.5 Microdrop Absorption Time	21
3.6 Reflected Light Image Analysis	21
4. Results	22
5. Discussion	27
5.1 General Comments	27
5.2 Comparison of Data	27
5.3 Discussion of Techniques	32
5.4 Roughness Standards for Stone	35
6. Conclusions	45
7. Summary	46
IV. BIBLIOGRAPHY	47

Appendix I.	Thermographic Imaging	50
Appendix II.	Scanning White Light Interferometry	58
Appendix III.	Laser Triangulation Profilometry	69
Appendix IV.	Gloss Measurements (Ph.I)	77
Appendix V.	Stylus Profilometry (Ph.I)	79
Appendix VI.	Reflected Light Image Analysis (Ph.I)	83
Appendix VII.	Paper submitted to '96 Stone Congress	88
Appendix VIII.	Gloss Measurements (Ph.II)	107
Appendix IX.	Stylus Profilometry (Ph.II)	110
Appendix X.	Microdrop Absorption Time	131
Appendix XI.	Reflected Light Image Analysis (Ph.II)	134

TABLES

I.	Roughness with LTP (Ph.I)	12
II.	Roughness with Stylus Profilometer (Ph.I)	13
III.	RLIA Pixel Counts (Ph.I)	14
IV.	Comparison of Results (Ph.I)	15
V.	Blasting Parameters	18
VIa-d.	Summary of Results (Ph.II)	23-26
VIIa-h.	Relative Changes (Ph.II)	28-31
VIII.	Roughness for Marble	36
IX.	Roughness for Limestone	39
X.	Roughness for Sandstone	42

FIGURES

1.	LTP Surface Profile on Flame Finished Granite	33
2.	LTP Surface Profile on Sandstone	32
3a-b.	RLIA Histograms for Marble	37-38
4a-b.	RLIA Histograms for Limestone	40-41
5a-b.	RLIA Histograms for Sandstone	43-44

RESEARCH PROJECT:

Development of an Evaluation Methodology
for Cleaning Damage Assessment

I. GENERAL INTRODUCTION

1. Outline of the Problem

Cleaning of exterior masonry can be considered one of the primary requirements in the non-routine maintenance of any building. For historic structures, it is probably one of the most important procedures since it can change the appearance of the building significantly. Stone cleaning methods are primarily based on two systems: those that act by chemical dissolution of the soiling or surface deposit, and those eliminating the dirt or deposit by mechanical erosion. In either case, there is a high probability that the actual surface skin of the stone will also be damaged or eliminated.

Cleaning procedures that cause visible surface loss of masonry materials need no sophisticated methodology for determining that damage has been done. The difficulty lies in assessing damage caused by those cleaning techniques which apparently do not induce visible surface loss.

Methodologies for evaluation of changes in highly polished surfaces, such as reflectometry, have been developed and are currently in use. The problem is more complex when the changes occur on surfaces that are rough to begin with, such as stones with a stugged, droved or rockfaced finish, or the surface of bricks; or where the surface is weathered. The phenomenon can be compared to trying to hear low music in an environment with a loud background.

The techniques which have been used for the evaluation of surface changes are based on the measurement of:

- weight loss
- surface gloss changes
- changes in surface roughness
- differential surface loss

Weight loss measurements are not accurate enough to establish damage when damage is slight. Changes in surface gloss can only be applied for polished surfaces and are measured by changes in the specular reflectance. Changes in roughness can be measured through various techniques described in the section following the brief definition of terms that are used to describe surface texture. Some of these techniques can also be used for measuring differential surface loss.

2. Surface Roughness Definition

Surface texture results from the fine topography (peaks and valleys) present in a surface. By convention, texture is divided into two components: roughness and waviness. Roughness consists of the finer irregularities which are closely spaced, whereas waviness consists of the more widely spaced irregularities. However, because roughness is the parameter measured most frequently, the terms surface roughness and texture are interchangeable (Song & Vorburger, 1992).

To completely describe the topography of a surface other terms are also required. These are *lay*, which is the predominant direction of the surface pattern; *flaws*, which are unintentional and unexpected interruptions in the typical topography, and *form* or *error of form*, which are widely spaced deviations on machined surfaces, such as out-of-flatness.

For the purpose of describing changes in a stone surface, surface roughness has been considered sufficient. Profile methods, which measure the height changes along a line, or raster area methods, which measure the changes over an area, are used.

Surface textures are highly complex because they result from finishing processes, such as polishing and grinding, which are statistical by nature. Statistical parameters are used to characterize these textures. The most frequently used are:

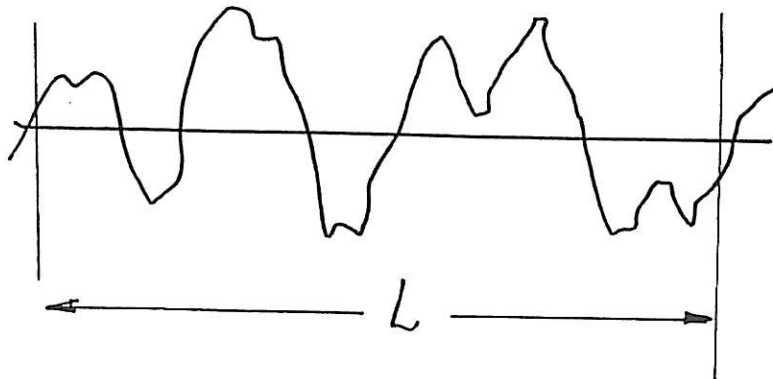
R_a roughness average

$$R_a = 1/L \int_0^L |y(x)| dx$$

R_q or rms (root mean square) roughness

$$R_q = [1/L \int_0^L y^2(x) dx]^{1/2}$$

where $y(x)$ is the surface profile, sampled by a set of N points y_i over the length L as shown in the diagram below:



Other parameters are:

mean peak spacing, S_m , the mean spacing between profile peaks (the highest part of the profile between an upwards and downwards crossing of the mean line), measured over the assessment length L , is the most useful wavelength parameter;

$$S_m = 1/n \sum_{i=1}^{i=n} S_i$$

skewness, R_{sk} , a shape parameter, is the measure of the symmetry of the profile about the mean line and is defined as:

$$R_{sk} = 1/NR_q^3 \sum_{i=1}^N Y_i^3$$

Since stone and ceramic surfaces are porous they are characterized by deep holes which result in negative skewness.

3. Survey of Methodologies

Research was done on the applicability of methods of roughness measurement on stone, either through literature review or, when possible, by actual experimentation.

3.1 Comparison with Standards

Metal profile comparators are used for measuring roughness of abraded metals, but have not been used for stone. These consist of metal plates divided into different areas (usually one square inch), each with a different profile of known depth. The comparison is done visually, with or without magnification of 5 to 10X; by touch; or by means of a dial depth gauge (ASTM D 4417-84). A CLEMCO surface profile comparator (Hodge Clemco Limited, Orgreave Drive, Sheffield, S13 9NR, Great Britain; 0742-697351) was borrowed from Mary McKnight at NIST. Attempts were made to use the comparator to measure the roughness of Indiana limestone, but it proved difficult to compare stone to metal. However, the concept of comparison has considerable potential, although it is anticipated that comparative samples would have to be developed for each type of stone.

3.2 Tracer Point Analysers

Dial Depth Gauges: A needle, attached to a dial gauge is used to measure depth at given points. The depth can be measured with a single point or between a two-point reference plane (Baer et al. 1983; Livingston et al. 1985/86). For larger surfaces, a set of points on a fixed grid can be measured before and after the cleaning and the differences plotted for all points (Binda et al. 1992; Baronio et al. 1992). To measure rock erosion, a dial gauge is set on a tripod support which requires the installation of pins in the surface to measure exactly the same spots (High et al. 1970, Trudgill et al. 1981; Cann 1974; ASTM D 4417-84). The requirement of measuring exactly the same spot limits practical application of this method.

Stylus Profilometers: A pointed stylus, usually a diamond-tipped needle, is passed in a line over the surface, the vertical motion of the needle following the roughness of the surface. If the exact line is to be measured before and after cleaning, bushings have to be glued to the surface to have the instrument located at the same point (Hoffmann et al. 1992 & 1993). Otherwise, many measurements over the surface have to be made to obtain an average value and to achieve statistical validity (Grimm 1983; Grimm and Völkl 1983; Stonecleaning in Scotland, 1992; Veloz 1994). This is one of the techniques that was tested in this study.

3.3 Changes in Surface Air-flow

The methods (Sheffield and Bekk) are based on the measurement of the time required to draw air through a specimen when suction is applied to one side of it. They are comparative methods mainly used to determine smoothness of paper (TAPPI 1988, 1991) but no information regarding the application to stone surfaces was found.

3.4 Light Measuring Devices

Macrosteriophotography: The method is based on measuring the relief on a pair of stereoscopic photographs by means of a "heightfinder" attached to a stereoviewer. The stringent requirements of stereo photography limit the applicability of this technique (Winkler 1986).

Reflectometer: This instrument, which measures the reflectance of light from a polished surface, gives a comparative value of surface gloss. The instrument can be used to determine changes in reflectance upon loss of polish (Lauffenburger et al. 1992). Because reflection is dependent on the index of refraction, the values obtained can only be compared when measured on the same material. This technique was used on polished surfaces in this study.

Line Grid Profilometer: A line grid is projected at 45° onto the object. The degree of distortion of the grid is directly proportional to the roughness of the surface. Zeiss equipment has been used on stone (Aires-Barros et al. 1994) but is no longer commercially available.

Speckle Interferometry: Speckles appear whenever an optically rough surface is illuminated with highly coherent light. The roughness of the surface needs to be of the order of the wavelength of the light used or coarser. The interference of secondary wavelets results in a granular pattern of intensity that is termed speckle. Light sources ranging from laser (Realini et al. 1994) to microwave (Oursler et al. 1994) have been used to measure the roughness of stone and metal objects.

Laser Triangulation Profilometry: Laser triangulation is based on a laser beam linearly scanning the surface of an object and measuring changes in reflection. The distance of any point on the surface (x-y position) from the position of a plane surface is evaluated by measuring small differences in the position of the profile with respect to a reference plane (z position) (Cielo, 1988). From this data the surface roughness of the area can be calculated or plotted (Berra et al., 1993; Fairbrass & Williams, 1995). This method was tested in this study.

White Light Interferometry: The technique is based on phase-shifting interferometry. A scanning technique (SWLI) can be applied for measuring surface roughness. An interferometric objective is mounted in a precision piezo scanning device which moves vertically (Z direction) over the sample. The phase relationships of individual components of the white light spectrum in the interferogram are analyzed giving a surface map with ultra high Z resolution (Deck & de Groot, 1994). One sample in this study was tested with this method, but it does not perform well on rough surfaces.

Reflected Light Image Analysis: computer image analysis of the reflected light from a surface can be used for qualitative measurement of its texture (Cielo, 1988). In raking light a highly reflecting surface appears dark because light reflects at an angle away from the detector (camera's chip) perpendicular to the surface. A rough surface scatters light in all directions and results in a brighter field. Comparison with standards could serve to assign a relative roughness value. The determination of absolute measurements of the z-axis could be carried out but would require complex data processing. A replica of the surface in a transparent material could also be measured in transmission mode. Light reflectance image analysis was tested in this study.

SEM-BS or x-ray mapping imaging: Elemental mapping or back-scattered electron images of polished cross-sections of epoxy impregnated stones can be used to assess changes in surface roughness (Mossotti et al. 1992). This technique was not considered practical for inclusion in this study.

3.5 Thermographic Imaging

The method is based on imaging the thermal emission of a sample uniformly heated from the backside. For a homogeneous panel, the temperature in the surface valleys is slightly higher than at the peaks and therefore emit more radiation which can be detected by a thermographic camera. The camera transforms them into a greyscale intensity image (Martin & Bentz, 1987; Bentz et al. 1991). Tests carried out with this method seem to indicate that because of their homogeneity replicas would perform better than stone samples.

II. PHASE I: TESTS ON LABORATORY SAMPLES

After initial experimentation with miscellaneous samples readily available in the laboratory, three masonry samples were prepared to be used for testing some of the above-mentioned techniques. Surfaces of these materials were intended to represent a range from highly polished (polished Carrara marble) to rough (brick paver). The surfaces were modified by abrasion to different degrees by means of a laboratory air abrasive unit [S.S.White Airbrasive Unit Model-K].

1. Sample Preparation

Carrara Marble: The marble sample [#14] was a square approximately 6" x 6" and 7/16" thick. It had been cut with a water-cooled saw blade from a commercial tile (12" x 12" x 7/16") obtained from the Morris Tile Company. Half the tile was left as the polished control by covering it with 2" wide plastic tape during the blasting. The second half was divided into two equal areas, with each protected by tape while the other was blasted. One area was blasted with glass beads [S.S. White abrasive powder #9, 44 μm in average diameter] at 60 psi [flow rate approx. 9 g/min]. The other was blasted with aluminum oxide powder [S.S. White abrasive powder #3, 50 μm in average diameter] at the same pressure [flow rate approx. 10 g/min]. The tip of the nozzle ($\phi = 0.018$ ") was held approximately 3/4" from the surface, and the blasting was carried out by scanning first in horizontal and then in vertical lines using a circular motion. Blasting the polished marble with glass beads required extra passes to produce an even surface.

Indiana Limestone: The Indiana limestone sample [#12] was a 2" thick prism with a 2 3/8" x 9" top sawn surface, obtained from Cathedral Stone. The center 3" of the top surface served as control and was covered with 3" wide clear packing tape during the blasting. Of the two side areas, one area was blasted with glass beads and the other with aluminum oxide powder, using the same conditions described above for the marble sample.

Brick paver: The brick sample [#13] was a paver (8" x 3 7/8" x 1 7/16") obtained from L.C. Smith. The center area served as control and was covered with 2" wide packing tape on both the narrow and wide (bedding) face, but because the wide face had deep pits, all measurements reported here were made on the narrow face. The side areas were abraded, one with glass beads and the other with aluminum oxide powder, using the same procedure described above for the marble sample.

2. Replica Preparation

The first attempts at obtaining replicas were carried out using a silicone rubber from Dow Corning [3110 RTV with standard cure catalyst #1]. Most replicas were prepared with the white product, but for one limestone specimen, a small amount of carbon powder [Winsor & Newton Lamp Black] was added to obtain a grey coloured mass. However, the carbon powder remained in discrete clumps visible under low magnification, and the replicas could therefore not be used for reflectance measurements. The silicone rubber was found to trap air-bubbles. To avoid this problem subsequent molds were made under vacuum.

It was found that the silicone material stained the stone, most noticeably the limestone samples. Intending to reduce or eliminate staining and facilitate removal of the silicone, tests were made in which samples were coated with Acryloid B72 [Rohm & Haas] 5% solution in acetone before moldmaking. Staining was not apparent after the coating was removed. However, it was later discovered that the acrylic resin applied to polished surfaces, such as the marble, was apparent in reverse on the silicone replicas, and the practice of coating was eventually discontinued.

It should be noted that after removal of the silicone rubber, rough surfaces, particularly of the limestone, retained some silicone rubber. This gave a distinctly reddish coloration to the sample when the red silicone rubber was used.

Replica material which consisted of methyl-methacrylate [Facsimile from Flexbar Machine Corp.] powder with a liquid catalyst was also tested. The replicas obtained were hard and in principle suitable for stylus measurements. However, they did not reproduce as fine detail as the silicone replicas, and the matrix of the material still contained unreacted powder particles which preclude accurate reflectance measurements.

Since image analysis can also be done with transmitted light through positive transparent casts, Tra-con epoxy resin [Bipax Tra-bond BB-2113] was cast into some silicone molds. However, many air bubbles were retained in these transparent molds which could not be eliminated by drawing a vacuum, and these bubbles would preclude accurate measurements.

After these tests were carried out, it was decided that white silicone rubber replicas would be made of the three masonry materials. The surfaces were pre-coated with a 5% w/v solution of B72 in acetone.

White replicas: white replicas were made with Dow Corning silicone rubber [3110 RTV with standard cure catalyst #1 in a 10:1 w/w ratio]. The silicone was poured onto the marble surface, which had been framed with a plasticine "dam" to hold the liquid resin, and a vacuum was drawn to de-air the silicone. The vacuum was drawn approximately ten times. The silicone was allowed to cure for 24 hours and removed from the surface of the stone.

In the case of the marble tile [#14], the surface was first cleaned with toluene to remove the uneven B72 coating. A second replica was made, identified as S-27. The replicas of the Indiana limestone sample [#12] and the narrow face of the brick paver [#13] are identified as S-23 and S-24, respectively.

Experimentation with the laser and the reflected light image analysis technique showed the white replica material to be too reflective for good results. Red silicone material was then used to prepare a second set of replicas.

Red replicas: red replicas were prepared with Dow Corning silicone rubber [3120 RTV with standard cure catalyst #1 in a 10:1 w/v ratio]. The preparation followed the same procedure described above for the white replica.

The red replica for the marble tile is identified as S-29, for the Indiana limestone as S-33, and the narrow face of the brick paver as S-31.

3. Applied Methodologies

Some methodologies were tested at other laboratories where instrumentation was available. Other methods were tested in-house at CAL.

3.1 Methods Tested in Other Laboratories

Stylus Profilometry: tests were carried out with different equipment on miscellaneous samples or the three prepared specimens of masonry material. Stylus measurements were carried out on a sandblasted Indiana limestone sample [#2] with a large bench model of a Form Talysurf apparatus through the courtesy of Dr. T. Vorburger at NIST. Other tests were carried out with portable instruments, i.e., Pocketsurf III (Federal), Surtronic 10 (Rank Taylor Hobson) and Surtronic 3+ (Rank Taylor Hobson) on the Carrara marble [#14], Indiana limestone [#12] and brick paver [#13]. The results of these preliminary measurements are to be found in Appendixes I and II of the Phase I Report for this

project. However, these results should be considered less accurate than subsequent tests performed at CAL.

Thermographic Imaging: this technique was tested on both the polished and fractured surfaces of a marble sample [#9a] and on a silicone replica [S-2] from an Indiana limestone sample [#2]. The tests were carried out at NIST by courtesy of Dr. D. P. Bentz. The actual stone may not serve for this technique because of different thermal emissivity of the calcite crystals. The silicone replica does not present this problem and the image obtained could be quantified. However, this requires calibration and data processing. The results obtained are summarized in Appendix I.

Scanning White Light Interferometry: this technique was used by Dr. J. W. Roth at Zygo Corporation to analyze a silicone replica [S-8] of a limestone sample [#2]. The results obtained, including the average roughness, Ra [μm], are summarized in Appendix II.

Laser Triangulation Profilometry (LTP): the technique was applied by Dr. D. Oursler at Johns Hopkins University with custom-made equipment consisting of an Aromat laser distance sensor (LM200RAC) mounted on an x-y translation stage coupled to a computer with an analog to digital board to digitize the laser distance sensor's signal. The computer also controlled the stage positioning and processed the surface profile. The red laser (670 nm) projects a beam of low power light (<1.9 mW) perpendicular to the specimen surface and the sensor triangulates the position by imaging the laser spot with an adjacent lens to a position sensitive detector. The device is calibrated by translation with the precision stage towards a stationary surface.

The samples themselves [#14, #12, #13] and both white [S-27, S-23, S-24] and red [S-29, S-33, S-31] silicone replicas were measured. Differences in color of the masonry materials interfered with assessment of surface roughness. In the case of the marble sample, care was taken to read only in the white areas, avoiding the black veins in the stone. The white silicone replica proved to be too reflective, distorting interpretation of the signal produced by the surface roughness. It was found that the red silicone replica gave the best results.

The results, expressed in Ra [μm], represent the average of each area measured (1 cm^2). Each area was scanned in ten lines, each line containing 5 blocks, resulting in 50 determinations of 40 reading points each (2000 points/ cm^2). The reproducibility of each area was excellent. Since the standard deviations calculated for the average roughness of each area (from 50

determinations) have a certain overlap, the results were subjected to an analysis of variance which confirmed that real differences exist between the means of each area. The average results for each area, the analysis of variance table for the data of the limestone red replica and the contour maps and line graphs for the limestone [#12] and the brick paver [#13] are presented in Appendix III. The results for the samples and the white and red silicone replicas are presented in Table I. The red replica measurements can be compared with those for other techniques in Table IV.

3.2 Methods Tested at CAL

Reflectometry: the gloss of the polished marble sample [#14] was measured [ASTM D 523-85] by means of a reflectometer [Lange Labor-Reflektometer] using a 20° geometry, found to be most appropriate for the gloss values measured. Data are presented in Appendix IV and summarized in Table IV.

Stylus Profilometry: measurements on the Carrara marble [#14], Indiana limestone [#12] and brick paver [#13] surfaces were repeated with a Surtronic 3+ profilometer after careful calibration of the instrument. The measurements were obtained over an evaluation length [Ln] of 4.00 mm, using 5 cut-offs (sampling or cut-off length [Lc] 0.80 mm) and a gauge range of 100 μm. Data for these measurements, given in Ra [μm], are presented in Appendix V. Since the Ra may change significantly depending on the Lc, the samples were remeasured using an Ln of 25 mm and an Lc of 2.5 mm, the maximum available for the Surtronic +3. However, the computer software can recalculate the roughness for an Lc of 8 mm. These results are summarized in Table II. Results for the Lc of 8 mm can be compared to other methods in Table IV.

Reflected Light Image Analysis (RLIA): the white silicone replica of the marble [S-27] and the red silicone replicas [S-29, S-33, S-31] of all three samples were measured by reflected light image analysis (RLIA). A video camera (World Video Automaticam with a single 1/2" CCD chip) was set perpendicular to the surface of the sample. The area measured with a 50mm video macro-lens was 22x32 mm. The surface was evenly illuminated with raking light at approximately 24° produced by two fixed fiber optic lights in a line array (Fostec fiber optic 21V 259W tungsten halogen EJA lamps). These were controlled by a rheostat set at 50%, with the iris diaphragm open. Shutter speed was 1/1000 sec. The image analysis package was Leica Quantimet 500. Histograms and relevant data were given in the Phase I Report and its Appendix VII.

After the Phase I report had been written, the RLIA system was modified and the red replicas were remeasured. The new system was assembled with a 55mm Micro-Nikkor lens (set at f4) instead of the 50mm video macro-lens. This resulted in lower light intensity on the samples. The rheostat was also altered to 60%.

An area of 5.43 cm² was captured in monochrome in a frame of 538x394 pixels (211,972 total); each pixel corresponded to 2500 μm². The software distributes pixels on a grey scale, where the pixel at 0 is black and at 256, white, and the distribution of the grey values are given in a table and a histogram. The value of the highest bar is indicated in the pixel (y) axis of the histogram. At least three different areas were randomly selected and measured on each sample. Results of representative runs of red silicone replicas, including histograms, are presented in Appendix VI. The pixel count of the highest bar in the peak of the histogram is considered an indicator of surface roughness. These values are presented in Table IV for comparison with results for other techniques.

4. Results

4.1 Laser Triangulation Profilometry

The roughness averages obtained through laser triangulation profilometry (LTP), measured directly on the surface of the samples, white and red silicone replicas, are presented in Table I.

TABLE I. Average roughness measured with LTP on the three samples, white and red silicone rubber replicas. Standard deviations are given in parentheses.

	Roughness Ra [μm]		
	Masonry surface	White replica	Red replica
Polished Marble	50 (±11)	2.5 (±0.5)	5.5 (±1.0)
PM/Glass Beads	42 (±10)	5.1 (±1.4)	7.1 (±1.5)
PM/Alumina	35 (± 8)	3.5 (±0.8)	6.2 (±1.2)
Limestone Sawn	18 (± 9)	13 (± 5)	24 (±13)
LS/Glass Beads	26 (±11)	20 (±10)	44 (±20)
LS/Alumina	30 (±12)	21 (± 8)	50 (±24)
Brick Paver	9 (± 3)	7 (± 3)	9 (± 3)
BP/Glass Beads	11 (± 5)	8 (± 4)	12 (± 7)
BP/Alumina	12 (± 6)	9 (± 3)	12 (± 4)

4.2 Stylus Profilometry

For stylus profilometry, a long evaluation length [Lc], such as 8 mm, is considered appropriate for accurate measurement of rough surfaces. Table II presents the different Ra measured with two Lc, 0.80 mm and 2.5 mm, as well as the latter recalculated at an 8.0 mm evaluation length. It is noteworthy that measurements made consistently with the shorter evaluation lengths produce correct trends in surface roughness. Data calculated with the longest evaluation length are summarized in Table IV for comparison with other methods.

TABLE II. Summary of roughness averages measured with the stylus profilometer at different evaluation or cut-off lengths [Lc]. Standard deviations are given in parentheses.

	Ra [μm]		
	@ Lc 0.80 mm	@ Lc 2.5 mm	@ Lc 8.0 mm
Polished Marble	0.6 (± 0.5)	0.74 (± 0.38)	0.85 (± 0.43)
PM/Glass beads	4.3 (± 1.0)	7.01 (± 0.62)	7.85 (± 0.78)
PM/Alumina	3.5 (± 0.8)	5.45 (± 0.94)	7.8 (± 1.5)
Limestone sawn	16.9 (± 3.5)	30.4 (± 3.7)	36.8 (± 4.5)
LS/Glass beads	30 (± 4.0)	38.6 (± 2.2)*	46.0 (± 3.1)*
LS/Alumina	42 (± 4.0)	38.1 (± 2.9)*	46.8 (± 4.0)
Brick paver	6.9 (± 1.0)	12.1 (± 1.3)	21.8 (± 1.4)
BP/Glass beads	12.2 (± 3.5)	16.4 (± 1.8)	26.6 (± 7.3)
BP/Alumina	12.8 (± 3.7)	17.9 (± 4.7)	26.5 (± 7.4)

NOTE:

Averages with (*) signify that instrument failed to read some areas because roughness was too high.

4.3 Reflected Light Image Analysis

Reflected light image analysis (RLIA) can provide, apart from the histograms used to characterize the samples in this study, a line profile and an image of the surface. The position and shape of the histogram obtained provide a qualitative measure of the texture of the surface. It was found that the pixel count for the highest bar in the central peak of the histogram gives a semiquantitative value of the roughness. The data for the pixel counts of the samples are reported in Table III and summarized in Table IV for a comparison with the other methods.

TABLE III Pixel count of the highest bar in the central peak of histograms obtained by RLIA from the red silicone replicas. Standard deviations are given in parentheses. (complete data can be found in Appendix VI)

	PM	PM/GB	PM/A1
	26,187	20,411	23,525
	23,084	19,642	22,175
	23,671	22,090	23,691
Average	24,314 ($\pm 1,648$)	20,714 ($\pm 1,251$)	23,120 (± 831)
	LM	LM/GB	LM/A1
	9,134	5,973	5,332
	8,657	6,368	5,396
	8,419	5,785	5,081
Average	8,736 (± 364)	6,042 (± 297)	5,269 (± 166)
	BP	BP/GB	BP/A1
	20,377	17,658	12,353
	21,740	18,563	14,217
	18,910	17,264	12,228
Average	20,342 ($\pm 1,415$)	17,828 (± 666)	12,932 ($\pm 1,114$)

4.4 Summary of Data

Table IV summarizes the results obtained with the four methods used to assess surface roughness. A discussion of stylus profilometry, LTP, and RLIA is presented in a paper that has been submitted for presentation and publication at the 8th Congress on the Deterioration and Conservation of Stone, Berlin, 9/30-10/4/96. A copy of this paper is in Appendix VII.

TABLE IV. Comparison of results obtained with four methods used to assess surface roughness

Sample	Method	Gloss [@ 20°]	Stylus @Lc 8.0mm [Ra μm]	LTP (red replica) [Ra μm]	RLIA pixel count x10 ⁻³ highest bar/peak
Polished Marble # 14	Polished Marble # 14	79 (± 6)	0.85 (±0.4)	5.5 (±1.1)	24.3 (±1.6)
	Marble/glass beads	1.6 (±0.6)	7.8 (±0.8)	7.1 (±1.5)	20.7 (±1.3)
	Marble/alumina	1.4 (±0.2)	7.8 (±1.5)	6.2 (±1.2)	23.1 (±0.8)
Sawn Limestone # 12	Sawn Limestone # 12		36.3 (±4.5)	24 (± 13)	8.7 (±0.4)**
	Limestone/glas beads		46.0 (±3.1)*	44 (± 20)	6.0 (±0.3)**
	Limestone/alumina		46.8 (±4.0)*	50 (± 24)	5.3 (±0.2)**
Brick Paver # 13	Brick Paver # 13		21.8 (±1.4)	9 (± 3)	20.3 (±1.4)
	Brick/glass beads		26.6 (±7.3)	12 (± 7)	17.8 (±0.7)
	Brick/alumina		26.5 (±7.4)	12 (± 4)	12.9 (±1.1)

NOTE:

- (*) indicates that instrument failed to read some points due to high roughness;
- (**) indicates that a spike is present at the black end of the histogram.

5. Conclusions

Thermographic imaging is a technique that still has to be developed for masonry materials. It requires further exploration to determine practicality. Use of replicas is necessary.

Scanning white light interferometry requires expensive instrumentation and may not be practical for evaluation of the roughness of masonry materials because it cannot measure the large areas required to capture their variability.

Laser triangulation profilometry (LTP) is one of the most promising techniques tested. However, commercial equipment, similar to the instrument tested, is also expensive. For accurate and comparative evaluation, replicas have to be prepared of the surfaces.

Reflectometry can only measure the gloss of polished surfaces. Even then, it is only valid for comparing data obtained from the same material, given the influence refractive index and color have on measurements.

Stylus profilometry can be used directly on the surface of masonry materials and can be used to compare roughness between different materials. However, the smaller portable models are not adequate to measure accurately rough surfaces such as are encountered in most masonry materials exposed out-doors. Nevertheless, values obtained, even if not accurate, do reflect changes in roughness, as long as these are under a certain value, estimated at 50 μm .

Reflected light image analysis appears to be a promising technique, although interpretation of results requires further study. It requires use of replicas and the technique is highly susceptible to variations in tilt of the surface, lighting, and lens set-up.

Of the techniques tested in Phase I, stylus profilometry and RLIA were selected for measuring the surfaces of the samples obtained in field conditions for Phase II of the study. To complement the data, gloss measurements for polished surfaces and microdrop water absorption tests for porous surfaces, as well as visual and touch evaluation of the roughness of all surfaces, were also proposed.

III. PHASE II: TESTS ON FIELD SAMPLES

On the basis of discussions during review meetings held with Lambertus van Zelst, CAL, and E. Blaine Cliver, Anne Grimmer and Judy Jacob of the National Park Service (March 8th, June 13th and September 7th, 1995) and results from Phase I of the project, the following program for field sample preparation was determined. Four types of abrasives were used to "blast" eight samples of different materials and/or finishes at two different pressures. The roughness of the resulting 64 treated surfaces and eight untreated "control" surfaces, totalling 72 surfaces, was to be measured by reflected light image analysis [RLIA]. Wherever applicable, roughness would also be measured with a stylus profilometer. Measurement of micro-drop absorption time on the most porous samples was also proposed and measurement of gloss with a reflectometer on the smoothest samples. In addition, the roughness of all surfaces would be ranked both visually and by touch.

1. Sample Preparation

Six materials were used in this part of the study. They were Carrara Marble, North Dakota granite, Indiana limestone, Seneca Creek red sandstone, smooth finish quarry tile and Brazilian glazed tile. For marble and granite, samples with two different surface finishes were obtained. These were highly polished and sawn samples for marble, and highly polished and flame-finished samples for granite. Stone was cut into squares measuring 6 inches on a side, while the tiles measured approximately the same dimensions as purchased. The samples, 8 in total, were identified by the following abbreviations: polished marble (PM); sawn marble (SM); sawn limestone (SL); sawn sandstone (SS); polished granite (PG); flame finished granite (FG); quarry tile (QT) and glazed tile (GT).

Each of the eight samples was constituted by 8 specimens, which were subjected to blasting by four materials at two pressures. To protect the original finish during blasting, half of each specimen was covered with an adhesive rubber layer used to protect tombstones during inscription blasting. These protected areas served as controls for laboratory measurements.

The specimens of each material were blasted with four different materials: water [W], milled walnut shells [N], glass beads [G] and Black Beauty [B], a glassy slag obtained from power plants. The walnut shells (Shelblast AD 10.5 B Nutshell) were packaged by Agrashell, Inc., Los Angeles, CA 90040; 90% passed through a 60

mesh but not 200 mesh. The glass beads (MS-XL) were manufactured by Cataphote, Inc. of Jackson, Mississippi (601/939-4612) and were finer than 270 mesh, measuring less than $53\mu\text{m}$ or .0021-.0005 inches. Black Beauty (2040) was packaged by Reed Minerals Harsco Corporation, Highland, Indiana (219/923-4200); 90% passed through 20 mesh (.85 mm or .0331 inches) but not 40 mesh (.425 mm or .0165 inches).

Except for the water, blasting was done with a Lindsay 35 sandblasting unit with a 5/16" nozzle. The nozzle was held at an approximately 15° from the perpendicular during blasting, and several passes were made on each sample, with each pass slightly overlapping the previous in order to achieve even coverage. The compressor (a 185 CFM Ingersoll-Rand) was maintained at about 100 psi (690 kPa) for the high pressure and around 50psi (345 kPa) for the low pressure. Abrasive flow rate was adjusted to maximize effectiveness at the given pressure.

A water jet was obtained by means of Hydroteck 25055 equipment with a tip of 25° ; the flow rate was 5.5 gal/min. Pressure was maintained at 2000psi (14×10^3 kPa) for the high pressure and 1000psi (7×10^3 kPa) for the low pressure. Other practical details of the blasting are summarized in Table V.

TABLE V. Blasting parameters for the four materials. Distance from the nozzle to the surface and the spray width were estimated by both the operator and observers while dwell time was measured with a stop watch.

Material	Pressure	Distance tip to surface	Spray Width @ surface	Dwell time average
N I	90 psi	7"	1"	7 sec
N II	50 psi	6"	1"	5 sec
G I	100 psi	9"	3/4" - 5/8"	5 sec
G II(*)	50 psi	8"	3/4" - 5/8"	(*)6 sec
BI	100 psi	7"	1½"	5 sec
BII	50 psi	6"	1½"	5 sec
WI	2000 psi	10"-15"	-	2 sec
WII	1000 psi	10"-15"	-	2 sec

NOTE:

(*) indicates that sample was blasted twice. Time listed corresponds to the second run.

Blasting was performed by Nicholas Veloz with the assistance of the Statue Preservation Crew of the National Park Service (Jessie Mallard, Jimmy Mauldin and Tim Boyd) at the Brentwood Maintenance Facility of the National Capitol Park-Central on August 4, 1995.

Blasting with the higher pressure was performed first in each case. After blasting samples with glass beads at high pressure, the equipment seemed to be hardly operating when samples were blasted at low pressure. As a result, the tank was refilled with glass beads, and the samples were blasted a second time.

2. Replica Preparation

Red replicas were prepared of all surfaces using Dow Corning silicone rubber [3120 RTV with standard cure catalyst #1 in a 20:1 w/v ratio]. The silicone was poured onto the sample surface, which had been framed with a plasticine "dam" to hold the liquid resin, and a vacuum drawn to de-air the silicone. The vacuum was drawn approximately ten times. The silicone was allowed to cure for 24 hours and removed from the surface of the masonry sample.

The removal of the replicas posed no problems except in the case of the sandstone specimens, where because of the chemical affinity of the silicone resin for the sandstone, the replica stuck to the surface and could not be removed in one piece. The surfaces of the sandstone were subsequently cleaned by submersion overnight in the AMTEX-CCR Silicone Dissolving Solution [AMTEX Chemical Company, PA]. Residues were brushed off from the surface under running water as the cleaning solution was rinsed off.

The surface of the sandstone specimens was then treated by brushing on a B72 solution (2% B72 in 1:1 acetone:ethanol). This served as releasing agent and the new set of replicas could be removed from these surfaces without any problems.

Since the set-up for RLIA required replicas of uniform thickness, a silicone rubber caulk was applied to the reverse side of the silicone rubber. This was then placed between heavy Plexiglas sheets clamped together with 3/16" spacers in between.

3. Evaluation of the surfaces

The evaluation of the surfaces before (control) and after blasting was carried out by different techniques, including surface roughness, gloss measurement and reflected light image analysis, as well as by visual comparison or touch differences.

3.1 Visual Assessment

Visual comparison of each set of eight specimens was conducted by two observers using a scale from 1 to 6. The values of the scale were be defined as follows:

- 1 = no visible change
- 2 = slight change visible, mainly the dividing line between control and abraded areas
- 3 = some change visible
- 4 = moderate change but no dislevel at interface
- 5 = definite erosion with minimal dislevel at the interface
- 6 = extreme erosion with marked dislevel at interface

3.2 Assessment by Touch

The samples were compared by touch by three observers using a scale from 1 to 6. The values of the scale were defined as follows:

- 1 = no difference between control and abraded areas
- 2 = slight difference between the two areas detected by some observers
- 3 = some change detected by all observers
- 4 = moderate change between areas with interface detected
- 5 = significant change between areas with marked dislevel detected at the interface
- 6 = extreme difference with marked dislevel detected at interface

3.3 Gloss Measurements

The gloss of sufficiently reflecting surfaces was measured [ASTM D 523-85] by means of a reflectometer [Lange-Labor Reflektometer] using a 20° geometry. The data are presented in Appendix VIII and summarized in Table VI.

3.4 Stylus Measurements

The surface roughness was measured by means of a stylus profilometer (Surtronic 3+ made by Rank Taylor Hobson Ltd). The evaluation length [Ln] was of 4.00 mm, the sampling or cut-off length [Lc] was 0.80 mm and the gauge range 100 μm . The calculation resolution selected for the roughness parameter [Ra] was 0.02 μm . Although the cut-off was not optimal for rougher surfaces, data show correctly trends of change in roughness. Data and line profiles for representative samples are presented in Appendix IX and summarized in Table VI.

3.5 Microdrop Absorption Time

Microdrop absorption time was used as an additional method to measure changes resulting from blasting. This is based on the principle that the roughness of a surface increases the speed of absorption of water for a given material and constant porosity. Prior to testing, samples were stabilized at room conditions (21°C and 45% RH) for over 10 days. RILEM Test II.8b Water Drop Absorption (UNESCO/RILEM International Symposium, 1978) was used with the following modifications:

drop size	10 μ l \pm 2 μ L
dropping distance	2.5 cm

Furthermore, absorption times are given directly rather than as a percentage of the absorption time of the reference material (glass surface) because these times proved to be so much shorter than those for the reference material (32 min \pm 1 min). The absorption times for polished materials were not measured specifically because they were found to fall within this time range. Data are presented in Appendix X and Table VI.

3.6 Reflected Light Image Analysis

The RLIA system with the 55-mm Micro Nikkor lens and the rheostat set at 60% was used in the same configuration as for the second set of samples measured in Phase I. The single 1.2" RGB chip camera (World Video Automaticam) was mounted on a fixed stand with its optical axis perpendicular to the sample surface. The light source was the Fostec fiber optic 21V 250 W tungsten halogen EJA lamp, controlled by a rheostat and with the iris diaphragm open, distributed through two 2" fiber optic line generators. These were set at a fixed angle (24°), illuminating the sample with even raking light. Shutter speed was 1/1000 sec. The image analysis workstation was a Leica Quantimet 500. An area of 5.43 cm² was captured in monochrome in a frame of 538x394 pixels (211,972 total); each pixel corresponding to 2500 μ m².

Representative histograms of all samples are presented in Appendix XI. Pixel counts for the highest bar of the peak of towards the center of the histogram, which give semiquantitative values for the roughnesses of surfaces, are also tabulated in Appendix XI.

4. Results

Data obtained from the various evaluation methods on the samples or their silicone replicas, are summarized in Table VI for comparison between methods and blasting materials. The table is divided into four sections: a) water, b) walnut shells, c) glass beads, and d) Black Beauty slag.

Data for "controls" used for visual and touch assessment, gloss measurement, and stylus profilometry are averaged from all eight unblasted areas of each sample set. It should be noted that control areas for the sawn samples vary significantly in some cases.

On the other hand, not all control samples were measured with RLIA. Data for RLIA controls are reported in italics when the average of unblasted areas on other samples is presented for comparison. Similarly, the microdrop absorption time was not always measured on polished samples. In these cases the average measure from the glass slide control is presented, in italics, for comparison.

TABLE VI a. Summary of results obtained with the different evaluation methods for samples blasted with water at high (2000 psi) and low (1000 psi) pressures. Standard deviation is indicated between parenthesis.

		Visual	Touch	Gloss (@ 20°)	Microdrop (min)	Stylus Ra (μm)	RLIA pixel count (10 ³)
PM	C	1	1	67.3 (±3.5)	<i>32.0</i> (±1.0)	0.22 (±0.16)	28.4 (±2.8)
	I	1	1	60.0 (±1.4)	20.2 (±2.7)	0.23 (±0.20)	29.6 (±3.7)
	II	1	1	63.8 (±2.0)		0.18 (±0.08)	29.8 (±1.3)
SM	C	1	1		21.1 (±1.7)	5.9 (±0.8)	22.0 (±2.4)
	I	3	1		16.0 (±1.2)	4.9 (±0.4)	23.1 (±0.5)
	II	3	1		12.1 (±1.9)	4.8 (±0.9)	24.4 (±2.5)
PG	C	1	1	73.8 (±4.7)		0.22 (±0.21)	28.4 (±2.2)
	I	1	1	69.4 (±2.5)		0.32 (±0.4)	32.6 (±3.5)
	II	2	1	68.8 (±3.3)		0.15 (±0.06)	31.0 (±2.2)
FG	C	1	1		9.8 (±2.3)		14.4 (±0.3)
	I	1	1		13.9 (±2.2)		14.8 (±0.7)
	II	1	1		13.8 (±0.9)		14.7 (±0.6)
SL	C	1	1		1.8 (±0.4)	13.1 (±3.5)	13.3 (±0.4)
	I	3	3		0.12 (±0.11)	20.5 (±3.7)	10.5 (±1.0)*
	II	1	1		0.11 (±0.09)	13.3 (±1.9)	12.6 (±0.3)*
SS	C	1	1		0.15 (±0.07)	18.8 (±2.6)	7.7 (±0.5)
	I	2	1		0.13 (±0.07)	21.7 (±1.3)	7.9 (±0.3)*
	II	2	1		0.06 (±0.02)	19.2 (±2.5)	7.8 (±0.3)*
GT	C	1	1	81.3 (±2.0)		0.10 (±0.07)	34.5 (±5.1)
	I	1	1	78.5 (±1.4)		0.47 (±0.55)	31.8 (±4.3)
	II	1	1	78.3 (±2.2)		0.07 (±0.03)	28.2 (±3.0)
QT	C	1	1			3.8 (±0.7)	25.5 (±1.1)
	I	1	1			4.8 (±0.4)	26.7 (±1.9)
	II	1	1			4.7 (±1.3)	24.9 (±0.5)

NOTE:

Italics indicate that measurements were done on control areas of other samples and are presented for comparison;
 (*) indicates the appearance of a spike at the black end of the histogram.
 For visual and touch assessment increasing numbers indicate increasing roughness.

TABLE VI b. Summary of results obtained with the different evaluation methods for samples blasted with walnut shells at high (100 psi) and low (50 psi) pressures. Standard deviation is indicated between parenthesis.

		Visual	Touch	Gloss (@ 20°)	Microdrop (min)	Stylus Ra (μm)	RLIA pixel count (10 ³)
PM	C	1	1	67.3 (±3.5)		0.22 (±0.16)	28.4 (±2.8)
	I	1	1	58.6 (±1.4)		0.24 (±0.08)	31.1 (±2.9)
	II	1	1	79.7 (±1.3)		0.21 (±0.2)	30.4 (±0.3)
SM	C	1	1		21.2 (±1.7)	5.9 (±0.8)	22.0 (±2.4)
	I	3	1		15.3 (±1.1)	6.5 (±1.2)	18.6 (±2.2)
	II	3	1		16.9 (±2.2)	5.7 (±0.7)	21.4 (±1.2)
PG	C	1	1	73.8 (±4.7)		0.22 (±0.21)	28.4 (±2.2)
	I	1	1	68.3 (±5.8)		0.11 (±0.09)	29.1 (±0.5)
	II	1	1	70.8 (±3.5)		0.2 (±0.2)	30.5 (±3.3)
FG	C	1	1		9.8 (±2.3)		14.4 (±0.3)
	I	2	1		22.9 (±2.3)		14.3 (±0.05)
	II	1	1		21.3 (±2.8)		14.0 (±0.5)
SL	C	1	1		1.8 (±0.4)	13.1 (±3.5)	12.2 (±1.4)
	I	3	1		0.41 (±0.09)	18.0 (±2.9)	8.2 (±0.2)*
	II	1	1		0.37 (±0.05)	13.3 (±1.5)	14.0 (±1.5)
SS	C	1	1		0.15 (±0.07)	18.8 (±2.6)	7.5 (±0.4)
	I	3	2		1.5 (±0.4)	23.5 (±1.8)	6.5 (±0.3)*
	II	2	1		1.3 (±0.2)	21.1 (±3.6)	7.0 (±0.2)*
GT	C	1	1	81.3 (±2.0)		0.10 (±0.07)	34.5 (±5.1)
	I	1	1	66.0 (±4.1)		0.07 (±0.02)	32.1 (±2.4)
	II	1	1	78.2 (±2.0)		0.09 (±0.05)	28.0 (±2.5)
QT	C	1	1			3.8 (±0.7)	25.5 (±1.1)
	I	3	1			3.5 (±0.6)	29.7 (±2.9)
	II	2	1			3.9 (±0.5)	26.3 (±0.4)

NOTE:

Italics indicate that measurements were done on control areas of other samples and are presented for comparison;
 (*) indicates the appearance of a spike at the black end of the histogram.
 For visual and touch assessment increasing numbers indicate increasing roughness.

TABLE VI c. Summary of results obtained with the different evaluation methods for samples blasted with glass beads at high (100 psi) and low (50 psi) pressures. Standard deviation is indicated between parenthesis.

				Visual Touch	Gloss (@ 20°)	Microdrop (min)	Stylus Ra (μm)	RLIA pixel count (10 ³)
PM	C	1	1	67.3 (±3.5)	32 (±1)	0.22 (±0.16)	28.4 (±2.8)	
	I	1	1	68.7 (±0.8)	21.4 (±1.4)	0.36 (±0.2)	31.3 (±3.0)	
	II	4	1	6.2 (±3.4)	18.2 (±1.5)	6.4 (±1.2)	21.2 (±3.5)	
SM	C	1	1		21.2 (±1.7)	5.9 (±0.8)	22.0 (±2.4)	
	I	4	1		11.2 (±0.7)	6.5 (±1.1)	21.0 (±0.3)	
	II	3	3		5.6 (±0.8)	9.9 (±1.10)	15.5 (±0.4)	
PG	C	1	1	73.8 (±4.7)	32 (±1)	0.22 (±0.21)	28.4 (±2.2)	
	I	2	1	68.4 (±6.8)		0.6 (±0.8)	33.8 (±3.7)	
	II	2	1	70.1 (±2.2)	19.6 (±2.2)	0.31 (±0.30)	29.7 (±1.8)	
FG	C	1	1		9.8 (±2.3)		14.4 (±0.3)	
	I	2	1		16.7 (±1.3)		14.8 (±0.6)	
	II	1	1		18.7 (±1.7)		14.4 (±0.2)	
SL	C	1	1		1.8 (±0.4)	13.1 (±3.5)	11.1 (±0.9)	
	I	3	1		0.6 (±0.1)	14.5 (±1.4)	11.1 (±1.0)	
	II	4	3		0.04 (±0.02)	19.8 (±5.7)	8.7 (±0.4)*	
SS	C	1	1		0.15 (±0.07)	18.8 (±2.6)	8.0 (±0.5)	
	I	2	2		0.38 (±0.14)	19.9 (±2.0)	7.4 (±0.1)*	
	II	3	2		0.025 (±0.003)	21.8 (±2.9)	6.4 (±0.1)*	
GT	C	1	1	81.3 (±2.0)		0.10 (±0.07)	34.5 (±5.1)	
	I	1	1	83.6 (±0.5)		0.12 (±0.07)	32.1 (±4.5)	
	II	1	1	75.4 (±0.8)		0.10 (±0.05)	30.9 (±1.6)	
QT	C	1	1		21.1 (±1.1)	3.8 (±0.7)	25.5 (±1.1)	
	I	2	1		29.3 (±0.5)	3.6 (±0.6)	24.5 (±0.8)	
	II	3	1		21.3 (±1.1)	4.0 (±0.6)	27.2 (±1.3)	

NOTE:

Italics indicate that measurements were done on control areas of other samples and are presented for comparison;
 (*) indicates the appearance of a spike at the black end of the histogram.
 For visual and touch assessment increasing numbers indicate increasing roughness.

TABLE VI d. Summary of results obtained with the different evaluation methods for samples blasted with Black Beauty at high (100 psi) and low (50 psi) pressures. Standard deviation is indicated between parenthesis.

		Visual	Touch	Gloss (@ 20°)	Microdrop (min)	Stylus Ra (μm)	RLIA pixel count x10 ³
PM	C	1	1	67.3 (±3.5)	32 (±1)	0.22 (±0.16)	28.4 (±2.8)
	I	6	1	1.4 (±0)	2.6 (±0.5)	11.7 (±0.9)	13.1 (±0.3)
	II	5	5	1.5 (±0)	5.6 (±1.1)	10.0 (±0.9)	14.8 (±0.4)
SM	C	1	1		21.1 (±1.7)	5.9 (±0.8)	22.0 (±2.4)
	I	5	1		1.0 (±0.2)	13.3 (±2.6)	13.6 (±0.6)
	II	5	3		1.4 (±0.2)	10.9 (±1.7)	15.5 (±0.05)
PG	C	1	1	73.8 (±4.7)	32 (±1)	0.22 (±0.21)	28.4 (±2.2)
	I	4	2	1.3 (±0.4)	20.0 (±0.7)	8.7 (±3.1)	19.7 (±1.5)
	II	4	3	15.4 (±4.0)	21.2 (±2.0)	2.0 (±0.8)	25.9 (±0.8)
FG	C	1	1		9.8 (±2.3)		14.4 (±0.3)
	I	4	1		15.6 (±2.3)		12.9 (±0.1)
	II	4	1		18.5 (±1.9)		13.5 (±1.3)
SL	C	1	1		1.8 (±0.4)	13.1 (±3.5)	12.2 (±1.4)
	I	6	6		0.030 (±0.003)	***	7.5 (±0.1) *
	II	5	5		0.027 (±0.003)	17.2 (±3.5)	8.3 (±0.2) *
SS	C	1	1		0.15 (±0.07)	18.8 (±2.6)	7.7 (±0.5)
	I	6	5		0.023 (±0.003)	19.0 (±1.5)	7.3 (±0.2)
	II	5	3		0.030 (±0.005)	22.1 (±2.3)	7.4 (±0.06)
GT	C	1	1	81.3 (±2.0)		0.10 (±0.07)	34.5 (±5.1)
	I	5	4	3.8 (±0.4)		2.8 (±1.2)	27.6 (±1.8)
	II	5	3	29.1 (±0.6)		1.1 (±0.4)	30.7 (±3.2)
QT	C	1	1		21.1 (±1.1)	3.8 (±0.7)	25.5 (±1.1)
	I	5	2		12.1 (±1.4)	12.9 (±2.9)	13.7 (±0.1)
	II	4	1		20.2 (±1.8)	9.3 (±0.9)	19.0 (±2.2)

NOTE:

Italics indicate that measurements were done on control areas of other samples and are presented for comparison;
 (*) indicates the appearance of a spike at the black end of the histogram.
 For visual and touch assessment increasing numbers indicate increasing roughness.

5. Discussion

5.1 General Comments

This discussion begins with a few general comments about changes induced by blasting, most of which were expected. First of all, when changes occurred after blasting, data showed that higher pressure blasting produced greater changes. An exception is presented by glass bead blasting, which generally showed greater damage at the lower pressure, apparently because of the reblasting of the samples. This confirms that pressure is not the only factor inducing changes in surface texture. Dwelling time, flow rate, and the air/abrasive ratio are also factors.

Secondly, data showed that water and walnut shells induced little or no change on the samples, while glass beads could induce moderate changes, and Black Beauty produced the most extreme changes.

Finally, data reflected that sawn limestone and sawn sandstone showed most changes. Fewer changes were shown for sawn marble followed by polished marble. Data for granite, apart from some particular results for flame-finished granite, showed changes mostly for blasting with Black Beauty and to a lesser extent, glass beads. Similar results, slightly less marked, were observed for both types of tiles.

5.2 Comparison of Data

To facilitate the comparison of data between the various measuring methods, relative changes induced by the abrasion procedures are summarized in Table VII. Changes shown in the table have been derived from data in Table VI. Roughness (Ra) is based on stylus profilometry measurements. When describing changes in RLIA, histograms have been taken into consideration in addition to data in Table VI.

Tables VII a and b list changes observed for the polished and sawn marble samples. Although only sawn marble seems to be affected by water blasting, small changes on the polished marble appeared to be measured by the reflectometer (see Table VIa). Changes induced by abrasion with the powdered materials increased as expected, from the walnut shells to the Black Beauty.

Tables VII c and d list changes observed for the polished and flamed-finished granite samples. The latter presented a high micro-drop absorption rate, probably because of microfissures induced during the heat-treatment. Abrasion with all four materials decreased its absorption of water.

TABLE VII a. Relative changes induced by the abrasion on the polished marble surface.

	Vis./Touch		Wat. Absorp.		Roughness [Ra]		RLIA	
W low	o		n.d.		o		o	
W high		o		++		o		o
N low	o		n.d.		o		o	
N high		o		n.d.		o		o/-
GB low	++		++		++		++	
GB high		o		++		+		o/-
BB low	+++		+++		+++		++	
BB high		>+++		+++		+++		+++

TABLE VII b. Relative changes induced by the abrasion on the sawn marble surface.

	Vis./Touch		Water Absorp.		Roughness [Ra]		RLIA	
W low	+		+		o/-		o	
W high		+		++		o/-		o
N low	+		++		o		o	
N high		+		++		+		o
GB low	+		+++		++		+	
GB high		++		++		+		o
BB low	+++		>+++		++		+	
BB high		>+++		>+++		+++		++

where:

- o = no change with respect to the control;
- o/+ = uncertain change with possible increase in roughness;
- + = increase in roughness; degree of change is indicated by number of signs;
- o/- = uncertain change with a possible "polishing" effect;
- = slight "polishing" effect or increase in water absorption; degree of change in water absorption is indicated by number of signs.

TABLE VII c. Relative changes induced by the abrasion on the polished granite surface.

	Vis./Touch		Water Absorp.		Roughness [Ra]		RLIA	
W low	o		n.d.		o/-		o	
W high		+		n.d.		o/+		o
N low	o		n.d.		o		o	
N high		o		n.d.		-		o
GB low	+		++		+ / ++		o	
GB high		+		n.d.		+		-
BB low	++		++		++		o	
BB high		++		++	.	+++		++

TABLE VII d. Relative changes induced by the abrasion on the flamed finished granite surface.

	Vis./Touch		Water Absorp.		Roughness [Ra]		RLIA	
W low	o		-		o.r.		o	
W high		o		-		o.r.		o
N low	+		---		o.r.		o	
N high		o		---		o.r.		o
GB low	o		--		o.r.		o	
GB high		+		---		o.r.		o
BB low	++		--		o.r.		o	
BB high		++		---		o.r.		o

where:

- o = no change with respect to the control;
- o/+ = uncertain change with possible increase in roughness;
- + = increase in roughness; degree of change is indicated by number of signs;
- o/- = uncertain change with a possible "polishing" effect;
- = slight "polishing" effect or increase in water absorption; degree of change in water absorption is indicated by number of signs;

TABLE VII e. Relative changes induced by the abrasion on the
sawn limestone surface.

	Vis./Touch		Water Absorp.		Roughness [Ra]		RLIA	
W low	○		++		○		+*	
W high		+		++		++		+*
N low	+		+		○		-	
N high		+		+		++		++*
GB low	++		+++		+++		++*	
GB high		+		+		+		+
BB low	+++		+++		+++		++*	
BB high		>+++		+++		o.r.		+++*

TABLE VII f. Relative changes induced by the abrasion on the
sawn sandstone surface.

	Vis./Touch		Water Absorp.		Roughness [Ra]		RLIA	
W low	+		+++		+		+*	
W high		+		○		++		+*
N low	+		--		++		+*	
N high		++		--		++		++*
GB low	++		+++		++		+*	
GB high		+++		-		+		+*
BB low	+++		+++		++		+	
BB high		>+++		+++		+		+

where:

- = no change with respect to the control;
- /+ = uncertain change with possible increase in roughness;
- + = increase in roughness; degree of change is indicated by number of signs;
- /- = uncertain change with a possible "polishing" effect;
- = slight "polishing" effect or increase in water absorption; degree of change in water absorption is indicated by number of signs.
- * = indicates bar at the black end of the histogram.

TABLE VII g. Relative changes induced by the abrasion on the glazed tile surface

	Vis./Touch		Water Absorp.		Roughness [Ra]		RLIA	
W low	o		n.d.		o/-		+	
W high		o		n.d.		+		+
N low	o		n.d.		o/-		+	
N high		o		n.d.		o/-		+
GB low	o		n.d.		o/+		+	
GB high		o		n.d.		o		+
BB low	+++		n.d.		++		+	
BB high		+++		n.d.		+++		++

TABLE VII h. Relative changes induced by the abrasion on the quarry tile surface

	Vis./Touch		Water Absorp.		Roughness [Ra]		RLIA	
W low	o		n.d.		+		o/-	
W high		o		n.d.		+		o
N low	+		n.d.		o		o	
N high		++		n.d.		o/-		o
GB low	++		o		o/+		o	
GB high		+		-		o/-		o
BB low	+++		o		++		+	
BB high		>+++		++		+++		++

where:

- o = no change with respect to the control;
- o/+ = uncertain change with possible increase in roughness;
- +
- o/- = uncertain change with a possible "polishing" effect;
- = slight "polishing" effect or increase in water absorption; degree of change in water absorption is indicated by number of signs.

Table VII e and f list changes observed for the limestone and sandstone samples. In general the results, especially the stylus profilometry measurements, do not reflect substantial changes produced by Black Beauty which are apparent to the naked eye as marked dislevels at the interfaces of blasted and control areas. However, Black Beauty did produce at least 10-fold decreases in water absorption times indicative of damage. Like the granite, sandstone showed increases in the microdrop absorption time for walnut shells and the generally less damaging high pressure glass beads. RLIA results are difficult to interpret particularly sandstone. Spikes appear at the black end of the spectra after blasting with nearly all media, attributed to increased pitting. However, no spike was apparent for the sandstone blasted with Black Beauty.

Tables VII g and h list changes observed for glazed and quarry tile. These resistant samples were mainly affected by blasting with the Black Beauty. Like the granite, the micro-drop absorption time increased for the quarry tile blasted with glass beads at high pressure.

5.3 Discussion of Techniques

Measurement of the micro-drop absorption time served to determine the porosity available to water and can be considered an indicator of damage at a microscopic level. As mentioned, the flame finished granite improved its resistance to water penetration even after blasting with Black Beauty as well as other abrasive materials, suggesting polishing. Figure 1 shows the surface profile for the interface between the control and an area blasted with Black Beauty, obtained from LTP (see Phase I). Decrease in surface topography confirms decrease in roughness.

Relative increases in roughness may be different for each material, and in some cases may be negligible even though considerable loss of stone or damage has occurred. For example, sawn sandstone would not appear to be damaged significantly during any of the blasting if only the values of the surface roughness are considered. However, a definite loss of material can be seen in Figure 2, showing surface profile for the interface of the control and Black Beauty-blasted areas obtained with the LTP (see Phase I); this is corroborated by visual observations. In addition, the ten-fold decrease in water absorption time for Black Beauty suggests not just loss of stone, but serious micro-damage.

Monitoring damage induced by abrasion techniques cannot be accomplished by simply measuring changes in surface roughness, because no change in roughness does not signify that no damage has been induced. On the other hand, if surface roughness changes significantly, blasting is obviously damaging.

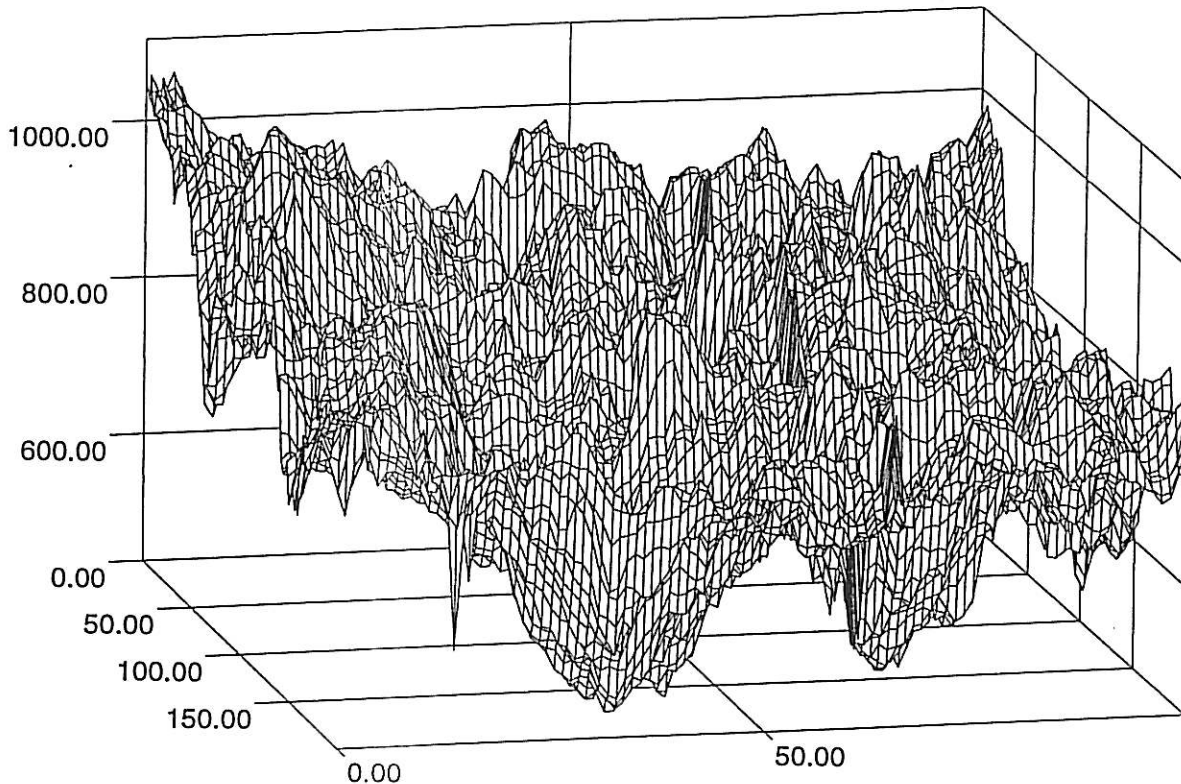


FIGURE 1. Surface profile of an area encompassing part of the control and part of the blasted area. The measurements were taken on a red replica of the flame finished granite sample (FGBI) blasted with Black Beauty at high pressure (100 psi).

The surface represented is 8 cm² and it was scanned along 4 cm (200 points) bridging the interface between the control and the blasted areas and along 2 cm (100 points) in the other direction. Each point measured was 200 μm.
(Courtesy of D.Oursler at Johns Hopkins University).

The interface runs parallel to the z-axis at about the 50.00 value on the x-axis. The right side is the control area and the left side is the blasted area. The deep peaks and pits that result from the flamed finish are lost and the surface is actually smoother after the blasting.

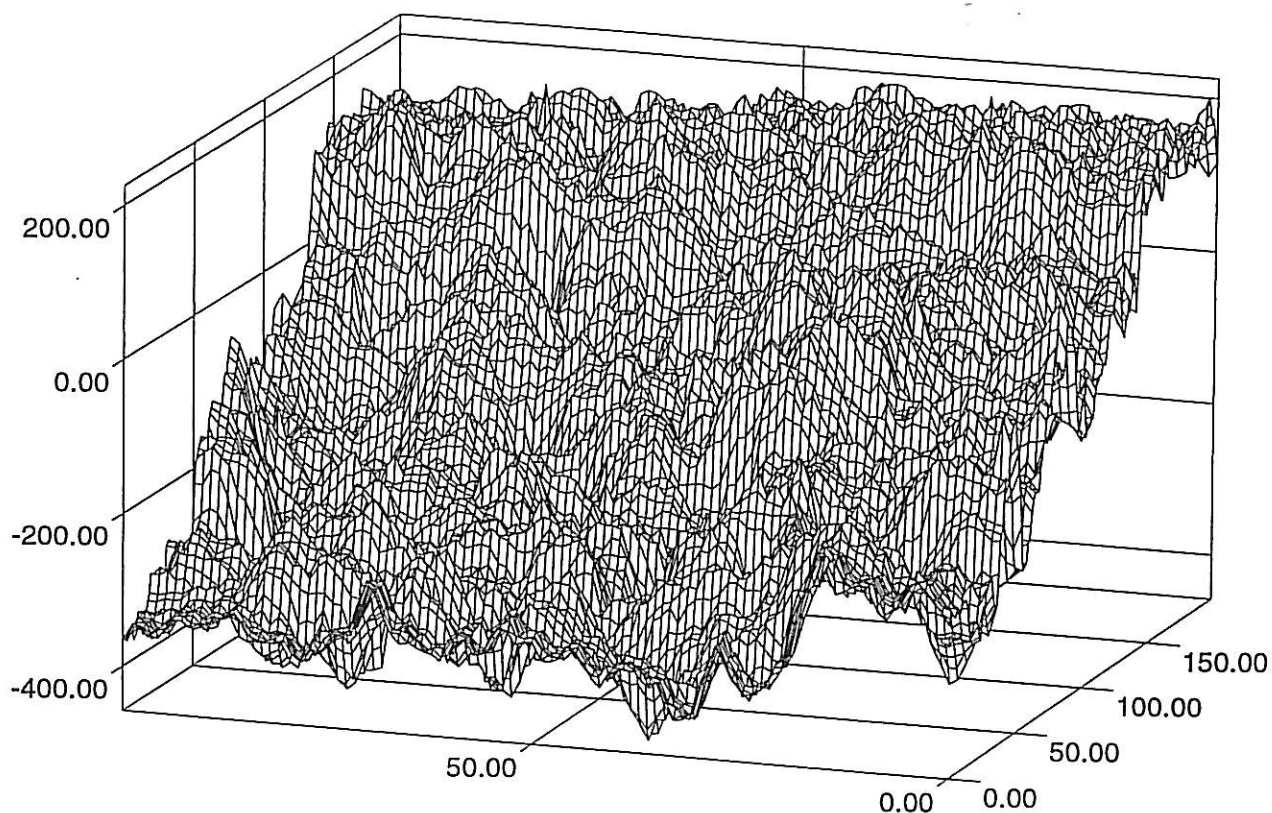


FIGURE 2. Surface profile of an area encompassing part of the control and part of the blasted area. The measurements were taken on a red replica of the sawn sandstone sample (SSBI) blasted with Black Beauty at high pressure (100 psi).

The surface represented is 0.5 cm^2 and it was scanned along 1 cm (200 points) bridging the interface between the control and the blasted areas, and along 0.5 cm (100 points) in the other direction. Each point measured was $50 \mu\text{m}$.
(Courtesy of D.Oursler at Johns Hopkins University).

The interface runs parallel to the x-axis at about the 0.00 value on the y-axis. The back part is the control, while the front is the surface eroded by the blasting. Only a relatively small difference in the roughness can be appreciated between the two areas, confirming the relatively low differences measured with the stylus profilograph.

The amount of damage done depends strongly on the abrading substance, the material in question, and its original roughness. Abrasive materials softer than the masonry tend to "polish" the surface and decrease its roughness. Because of this, the use of softer abrasive materials has not been encouraged. However, a softer abrasive could conceivably be used as a "sealing" finish after an abrasive cleaning operation. Harder materials, such as quarry and glazed tile, were only slightly affected by blasting, the largest effect being observed with the Black Beauty at higher pressure. Blasting with glass beads at higher pressure seemed to smooth the surface of the quarry tile as evidenced by the increased microabsorption time, although roughness did not change significantly as measured with the stylus or by RLIA.

Blasting with water does not appear to change any of the surfaces significantly, if only stylus roughness data or RLIA measurements are considered. However, the microdrop absorption time decreases indicating microstructural damage, and gloss measurements confirm that some changes have been induced on polished surfaces, even on hard ones such as polished granite.

The methods tested in this study for the evaluation of changes in roughness have shown that so far there is no perfect method available. Stylus profilometers have been developed for measuring roughness on metals, and the presence of deep pits in the surface of stone might require the use of other statistical parameters, such as the skew, to characterize the surface roughness appropriately. For rougher surfaces, such as found on outdoor buildings, a more sophisticated bench model is required. Portable instruments mainly give a trend in the change in roughness.

Laser triangulation profilometry is probably the most accurate method. However it requires the preparation of replicas, and the instrumentation required is expensive.

Reflected light image analysis has been applied for the first time to evaluate surface roughness. It also requires the preparation of surface replicas and extreme care in making them level. Although further tests are required to determine all the information that can be obtained from this procedure it is evident that the histograms reflect changes in texture observed visually. However, quantification procedures have to be developed to characterize these changes adequately.

5.4 Roughness Standards for Stone

Data confirmed that touch and visual assessment could be used to advantage for measuring roughness of some materials. It is considered that "standard roughness" samples could be prepared,

similar to the ASTM surface profile comparator for metals. For masonry materials, however, each type of material would require its own set.

To illustrate the point and to better understand data obtained in this study, selected samples of marble, limestone and sandstone were organized by increasing roughness differentiated by touch. The Ra values obtained by stylus profilometry and the pixel count of the highest bar in the RLIA histograms are presented in Table VIII for marble, Table IX for limestone and Table X for sandstone. The corresponding RLIA histograms are presented behind each table as Figures 3 to 5.

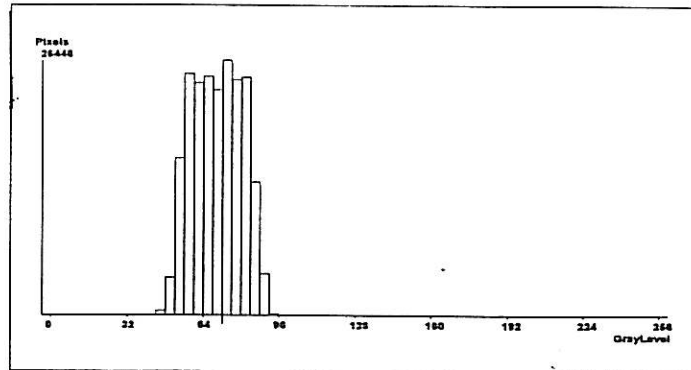
Marble: the shape and position of peaks in the histogram provide a qualitative measure of surface texture. For polished surfaces, the peak of the histogram appears as a high block of reflected light (see Figure 3a). As the surface roughens, the block becomes a relatively symmetrical bell-shaped peak, and with increased roughness, the peak broadens while losing height (Figure 3b).

TABLE VIII Scale of roughness that can be differentiated by touch for marble. Roughness was re-measured by stylus profilometry (@ Ln 25 mm, Lc 2.5 mm and recalculated for an Lc of 8 mm) and is given in Ra [μm]. RLIA is given in pixel count for the highest bar in the histogram peak which are shown in Figures 3a-b.

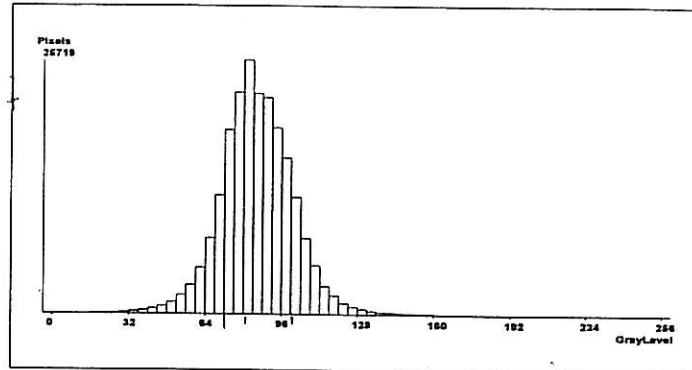
Marble Surface	Touch scale	Ra [μm]	RLIA
Polished	1	0.85 (± 0.43)	28.3 (± 2.8)
Sawn			
SM/NIIC	2	6.5 (± 0.7)	23.5 (± 0.07)
Marble/GB PhI		7.8 (± 0.8)	20.7 (± 1.3)
Marble/Al PhI		7.8 (± 1.5)	23.1 (± 0.8)
SM/NIc		10.5 (± 2.1)	20.7 (± 0.7)
SM/GII	3	13.8 (± 2.1)	15.5 (± 0.4)
PM/BII	4	17.0 (± 1.4)	14.8 (± 0.4)
SM/BII			15.5 (± 0.05)
PM/BI	5	29.2 (± 2.3)	13.1 (± 0.3)
SM/BI			13.6 (± 0.6)

FIGURE 3 a. RLIA histograms for marble samples of increasing roughness. Pixel count corresponds to highest bar in the peak.

Polished [PM/BI c] (26446 pixels)



Smooth sawn [SM/NII c] (26719 pixels)



Rough sawn [SM/NI c] (19935 pixels)

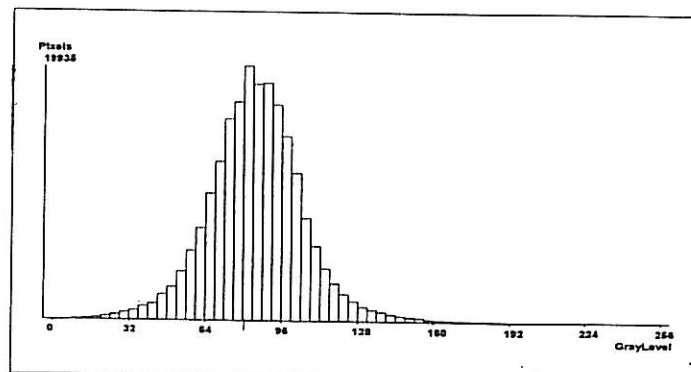
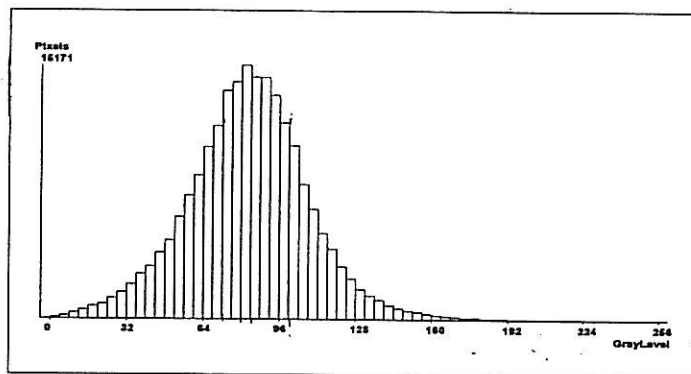
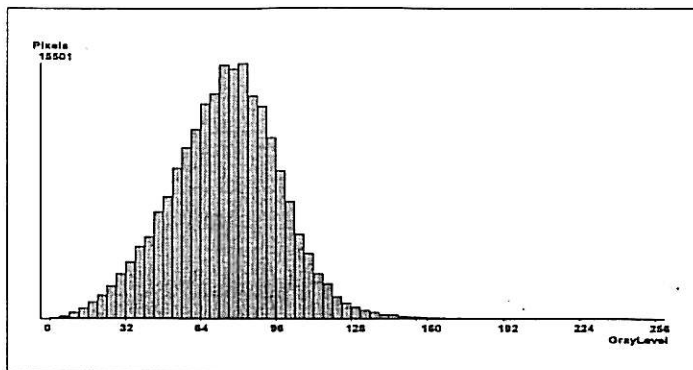


FIGURE 3 b. RLIA histograms for marble samples of increasing roughness. Pixel count corresponds to highest bar in the peak.

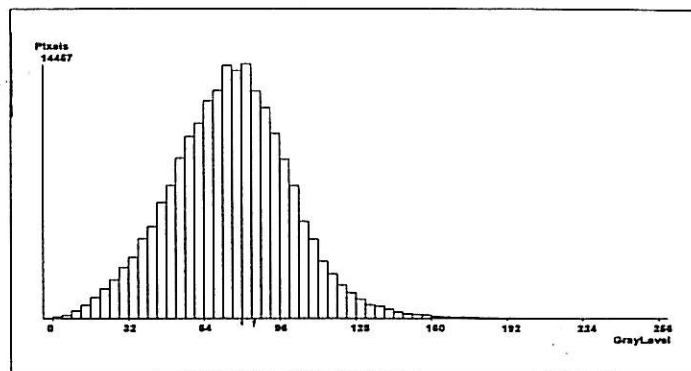
SM/GII (15171 pixels)



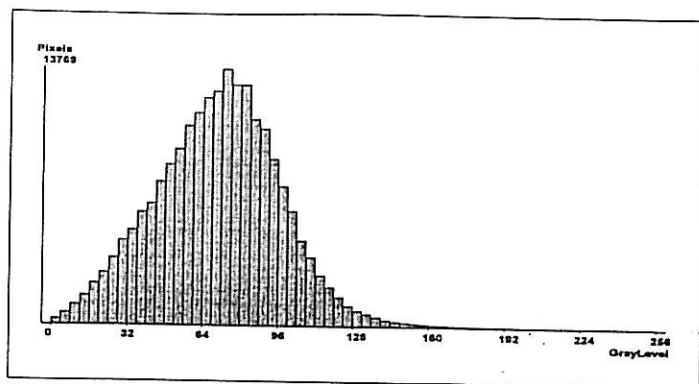
SM/BII (15501 pixels)



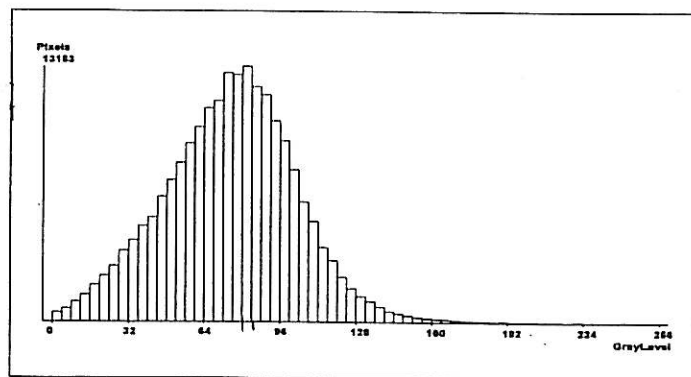
PM/BII (14457 pixels)



SM/BI (13769 pixels)



PM/BI (13183 pixels)



Limestone: the RLIA histograms for the selected limestone samples show both the problems and information possibilities of this technique. A smooth-sawn limestone surface shows a bell-shaped histogram, which as the surface roughens, broadens and flattens (Figure 4a). With increasing roughness, a spike at the black end of the spectrum makes its appearance.

The silicone replicas of the Phase I limestone samples abraded with glass beads and alumina, show a flatter curve with a larger spike at the black end compared with samples from Phase II blasted with glass beads or high pressure water. Part of the problem may be attributed to the inadequate levelling of the replica surface during the measurements, but the rest may well reflect differences in texture due to unevenness in abrasion. It is possible that the stylus profilometer measures the same roughness on two samples which have different texture, i.e., fewer but deeper pits. If the pits are too deep, the stylus profilometer "skids" over the sample and does not measure it, but RLIA will "see" a large increment in shadows. For example, the limestone sample blasted with walnut shells at high pressure also shows a large spike at the black end of the histogram, however, roughness evaluated by touch or measured with the profilometer, does not "see" these.

TABLE IX Scale of roughness that can be differentiated by touch for limestone. Roughness was re-measured by stylus profilometry (@ Ln 25 mm, Lc 2.5 mm and recalculated for an Lc of 8 mm) and is given in Ra [μ m]. RLIA is given in pixel count for the highest bar in the histogram peak which are shown in Figures 4a-b.

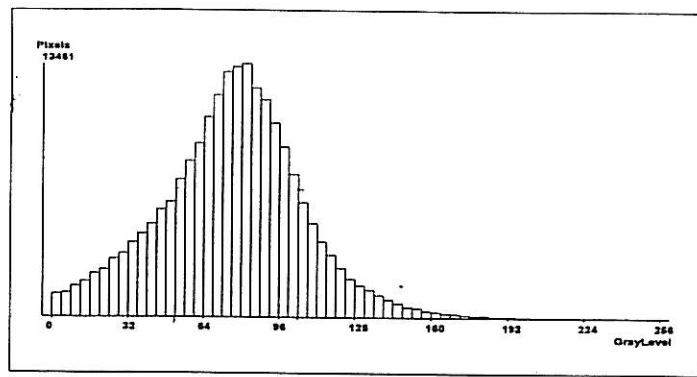
Limestone Surface	Touch scale	Ra [μ m]	RLIA
Smooth sawn LS/WIIc	1	17.3 (\pm 3.3)	13.3 (\pm 0.4)
Rough sawn LS/GIc	2	24.7 (\pm 3.9)	11.1 (\pm 0.9)
LS/GII	3	37.2 (\pm 5.7)	8.7 (\pm 0.4)*
LS/WI		39.4 (\pm 3.7)	10.5 (\pm 1.0)*
Limestone/GB PhI	4	46.0 (\pm 3.7)	6.0 (\pm 0.3)*
Limestone/Al PhI		46.8 (\pm 4.0)	5.3 (\pm 0.2)*
SL BII	5	51.8 (\pm 7.8)♦	8.3 (\pm 0.2)*
SL BI	6	52.73 (\pm 6.1)♦♦	7.5 (\pm 0.1)*

NOTE:

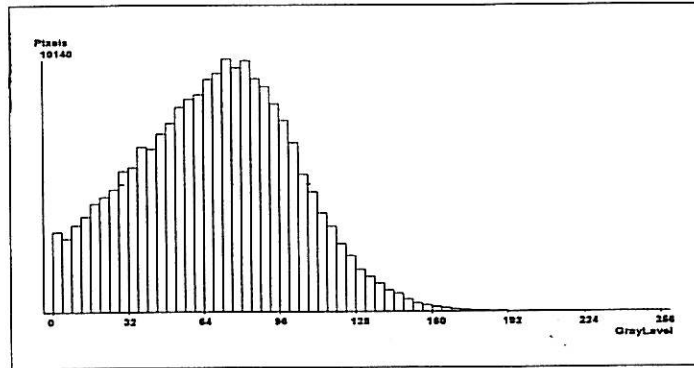
- (♦) denotes that one third, and (♦♦) that one half, of the measurements were out of range for this instrument;
- (*) indicates a spike at the black end of histogram.

FIGURE 4 a. RLIA histograms for selected limestone samples of increasing roughness. Pixel count corresponds to highest bar in the peak.

Smooth sawn [SL/WII c] (13461 pixels)



Rough sawn [SL/GI c] (26719 pixels)



Slightly abraded [LM/WI] (9696 pixels)

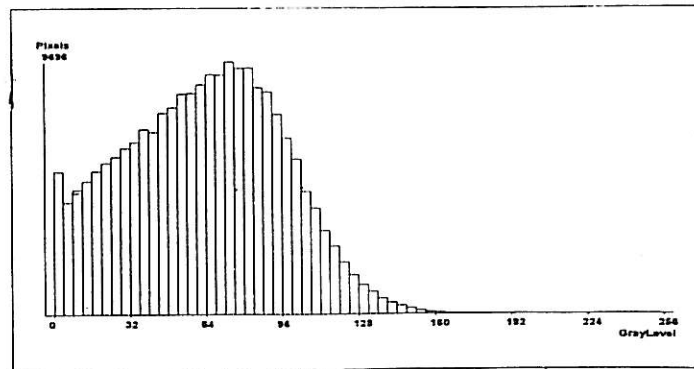
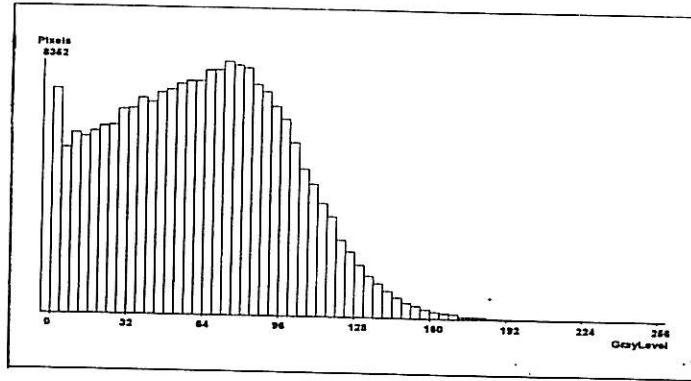


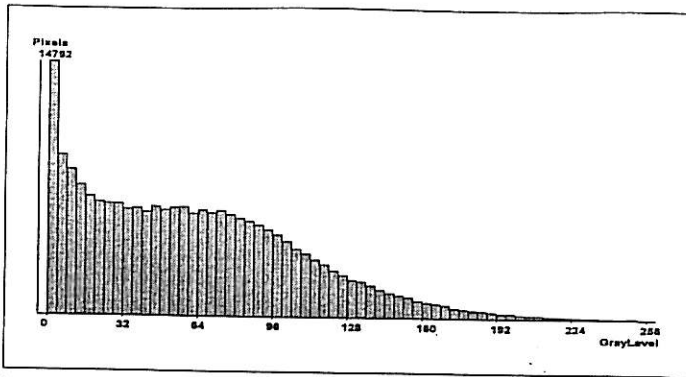
FIGURE 4 b.

RLIA histograms for selected limestone samples of increasing roughness. Pixel count corresponds to highest bar in the peak.

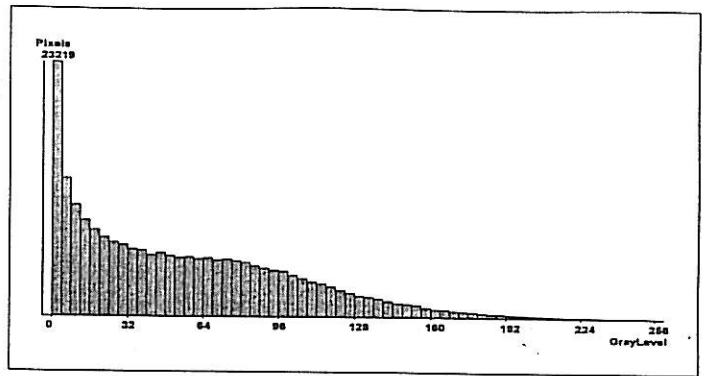
SL/GII (8352 pixels)



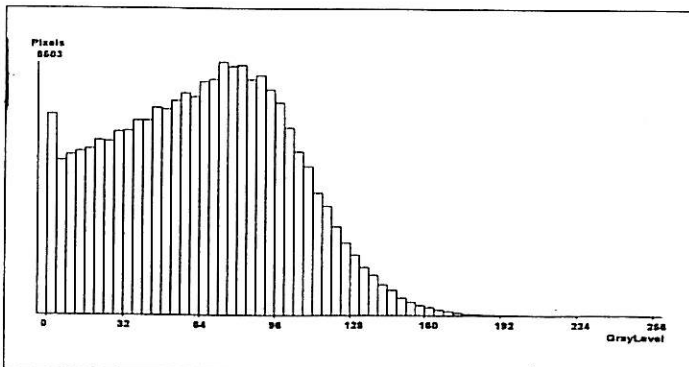
Phi LS/GB (6368 pixels)



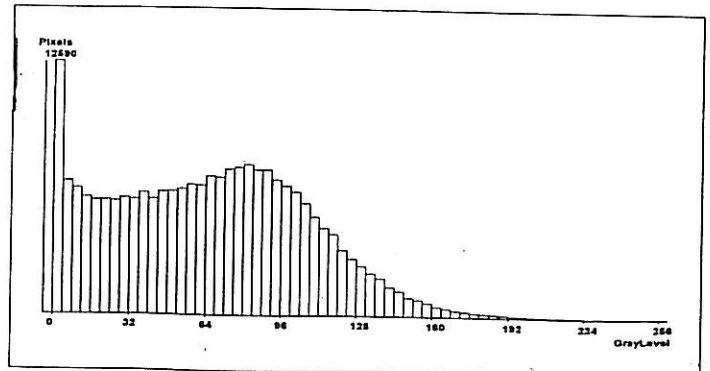
Phi LS/AI (5396 pixels)



SL/BII (8503 pixels)



SL/BI (7456 pixels)



The surfaces abraded with Black Beauty at low and high pressure follow the pattern described: flattening with an increased spike at the black end of the histogram.

Sandstone: the sandstone surfaces illustrate yet a different case. The surface of the sawn sandstone is rough, and in the RLIA histograms appears as a very broadened and distorted bell-shaped curve (Figure 5a). With increased roughness, the curve mainly flattens and it is interesting to note that a relatively small black spike appears for the surface blasted with the glass beads, while not spike is evident for samples blasted with Black Beauty.

The increased roughness in the sandstone samples selected can be differentiated by touch and by the Ra measured. However, the pixel count for the highest peak bar does not follow exactly the pattern.

TABLE X Scale of roughness that can be differentiated by touch for sandstone. Roughness was re-measured by stylus profilometry (@ Ln 25 mm, Lc 2.5 mm and recalculated for an Lc of 8 mm) and is given in Ra [μm]. RLIA is given in pixel count for the highest bar in the histogram peak which are shown in Figures 5a-b.

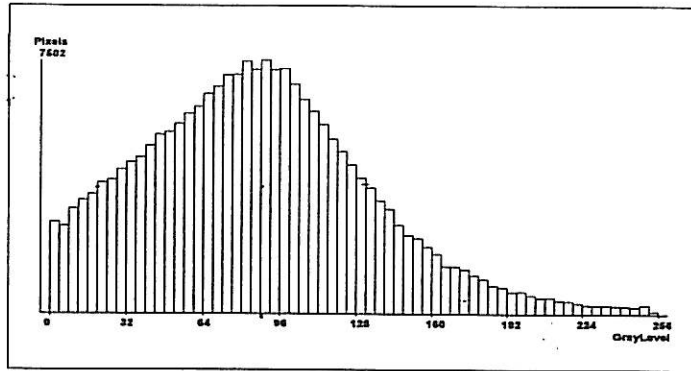
Sandstone Surface	Touch scale	Ra [μm]	RLIA
Smooth Sawn SS/GIc	1	28.6 (± 2.8)	8.0 (± 0.5)
Rough Sawn SS/NIIC	2	29.8 (± 1.8)	7.5 (± 0.4)
SS/GII	3	38.5 (± 2.5)	6.4 (± 0.1)*
SS BII	4	40.1 (± 6.6)	7.4 (± 0.06)
SS BI	5	61.7 (± 6.1) $\blacklozenge\blacklozenge$	7.3 (± 0.2)

NOTE:

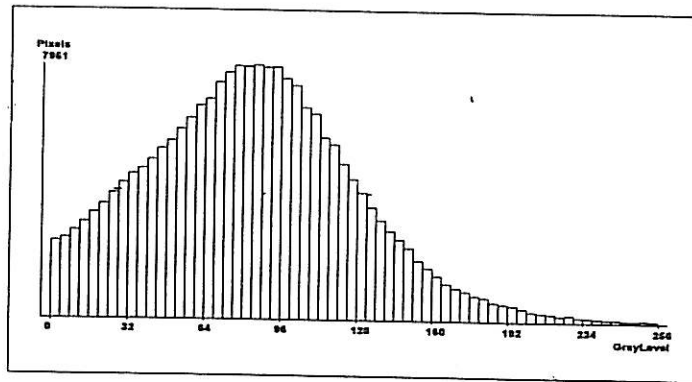
- (\blacklozenge) denotes that one third, and ($\blacklozenge\blacklozenge$) that one half, of the measurements were out of range for this instrument;
- (*) indicates a spike at the black end of the histogram.

FIGURE 5 a. RLIA histograms for selected sandstone samples of increasing roughness. Pixel count corresponds to highest bar in the peak.

Smooth sawn [SS/GI c] (7502 pixels)



Rough sawn [SS/NII c] (7951 pixels)



Slightly abraded [SS/GII] (6226 pixels)

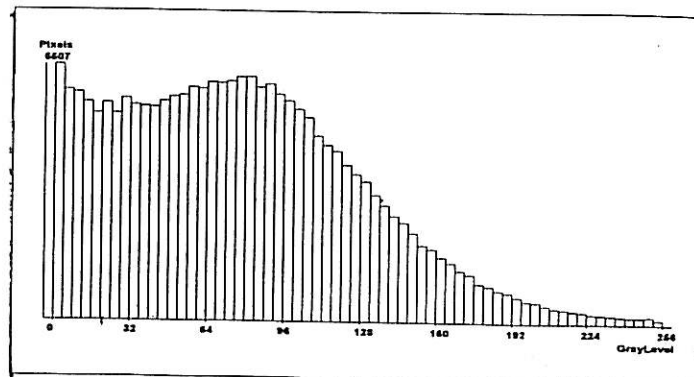
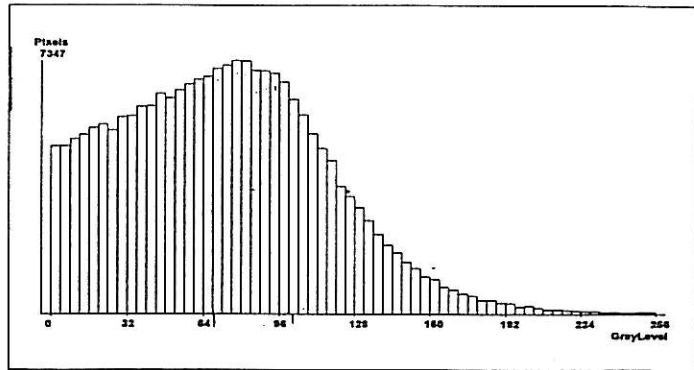
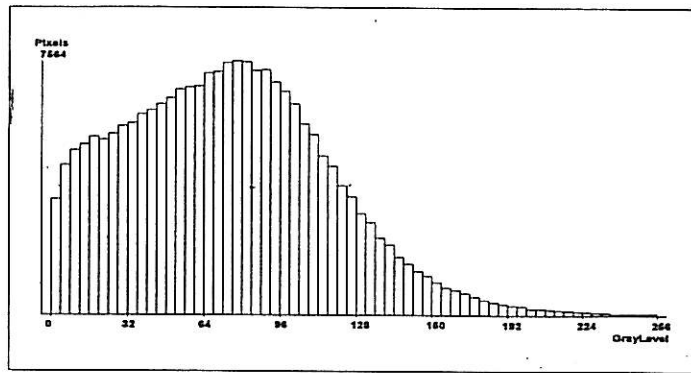


FIGURE 5 b. RLIA histograms for selected sandstone samples of increasing roughness. Pixel count corresponds to highest bar in the peak.

SS/BII (7347 pixels)



SS/BI (7564 pixels)



6. Conclusions

The main problem encountered in the evaluation of roughness of masonry materials is that their surfaces are uneven because of natural inhomogeneities and inconsistent application of surface finishes. This results in a wide spread of data, reflected in large standard deviations.

RLIA provides a more representative estimate of the surface texture than most techniques, since it can image a large area of the sample. Thus, uneven abrasion patterns introduced by non-uniform blasting are taken into account. Pixel counts can be used to estimate roughness in some cases, but because these do not follow changes in roughness in every case, a better indicator should be derived from the data provided by the image analysis. The technique also gives information on texture although interpretation of the histograms requires further study. It should also be noted that levelling and replication of illumination are critical for the RLIA technique, and, as discussed in the paper in Appendix VII, demand attention and care.

Given the roughness range encountered in masonry materials, stylus profilometry does not appear to be the most practical method for evaluating roughness. It can only measure a straight 2.5 cm line (with a 5 μ m tip radius), and to reproduce the area "seen" by RLIA would require about 275 scans!

Microdrop water absorption tests provide supportive information about microstructural changes induced by blasting. Since water is one of the key damaging factor for masonry materials this technique may aid in the selection of the most appropriate cleaning technique.

More research is needed to understand the effect of softer abrasive materials because differences in the microdrop water absorption time have been observed. This is of particular concern because of the present trend in the use of soft materials like sodium bicarbonate.

7. Summary

The experience gained from this study can be summarized as follows:

- abrasion systems can cause severe damage to the surface of masonry materials;
- damage depends on the abrasive, the nature of the material blasted, the pressure, the air/abrasive ratio, and the dwell-time;
- extrapolation should not be made between different materials and blasting methods;
- it is not easy to obtain evenly abraded surfaces. Hence, the evaluation of surface texture on a small area can be misleading;
- stylus profilometry may not provide representative measurements of overall surface roughness;
- micro-drop absorption rate can serve as an indicator of microstructural changes;
- reflectometry is a sensitive technique to evaluate changes of gloss on polished surfaces;
- visual examination and touch can be used to evaluate roughness provided adequate standard materials are available for comparison;
- LTP appeared to provide the most accurate roughness data;
- RLIA shows promise of being capable of evaluating both surface roughness and texture. However, further testing is required to establish this new technique as a practical, routine system for evaluating surface roughness;
- roughness changes do not unequivocally follow changes in the surface microstructure nor do they necessarily reflect the amount of stone loss;

IV. BIBLIOGRAPHY

- Aires-Barros, L., Mauricio, A. and Figueiredo, C. (1994)
"Profilometry and Image Analysis Applications to 'in situ' Study of Monuments Stone Decay Phenomena" in The Conservation of Monuments in the Mediterranean Basin, Proceedings of the 3rd International Symposium, V.Fassian, H.Ott & F.Zezza, Eds., Soprintendenza ai Beni Artistici e Storici di Venezia, Venice, pp.19-24
- ASTM D 4417-84 Standard Test Methods for Field Measurement of Surface Profile of Blast Cleaned Steel
- ASTM D 523-85 Standard Test Method for Specular Gloss
- Baer, N.S. and Berman, S.M. (1983) "Marble Tombstones in National Cemeteries as Indicators of Stone Damage: General Methods" 76th Annual Meeting Air Pollution Control Association, Atlanta, 83-5.7
- Baronio, G., Binda, L., Cantoni, F. and Rocca, P. (1992)
"Durability of Preservative Treatments of Masonry Surfaces: Experimental Study on Outdoor Physical Models" in *Proceedings of the 7th International Congress on Deterioration and Conservation of Stone*, Lisbon, pp. 1083-1092
- Bentz, D.P., Martin, J.W. and Batts, M.E. (1991)
"Characterization of Cylindrical Holes in Metallic Substrates via their Infrared Emission Patterns" *Wear* 143 255-266
- Berra, M., Faticcioni, A., Binda, L. and Squarcina, T. (1993)
"Laboratory and in-situ Measurement Procedure of the Decay of Masonry Surfaces" in *Durability of Building Materials and Components 6*, S.Nagataki, T.Nireki and F.Tomosawa, Eds., E & FN Spon, London, pp. 834-843
- Cann, J.H. "A field investigation into rock weathering and soil forming processes" *J.Geol Ed.* 1974)
- Cielo, P. (1988) "Optical Techniques for Industrial Inspection" Academic Press, New York, pp. 278-310

- Deck, L. & de Groot, P. (1994) "High-speed Noncontact Profiler based on Scanning White-Light Interferometry" *Applied Optics* 33 (31) 7334-7338
- Fairbrass, S. and Williams, D.R. (1995) "A New Surface Imaging Technique in Conservation" in From Marble to Chocolate, The Conservation of Modern Sculpture, Archetype, London, pp. 82-86
- Grimm, W.D. (1983) "Rauhigkeitsmessungen zur Kennzeichnung des Verwitterungsfortschrittes an Naturwerkstein-Oberflächen" *Int.Coll. Materials Science and Restoration*, Esslingen, F.H.Wittmann, Ed., Lack + Chemie, pp. 321-324
- Grimm, W.D. and Völkl, J. (1983) "Rauhigkeitmessungen zur Kennzeichnung der Naturwerksteinverwitterung" *Z. geol. Ges.* 134 pp. 387-411
- High, C. and Hanna, F.K. (1970) "A Method for the Direct Measurement of Erosion on Rock Surfaces" Technical Bulletin 5, British Geomorphological Research Group
- Hoffmann, M., Heuser, H. and Prickartz, R. (1992) "Beurteilungskriterien für die Reinigung von Natursteinfassaden aus Sandstein mit einem Trockenstrahlverfahren" in Jahresbericthe aus dem Forschungsprogramm Steinzerfall-Steinkonservierung, R.Snehthlage, Ed., Ernst & Sohn, Berlin, pp.147-155
- Hoffmann, M. and Heuser, H. (1993) "The Injector Jet Process for the Cleaning of Natural Facades" in Conservation of Stone and Other Materials, M.-J.Thiel, Ed., E & FN Spon, London, pp. 526-533
- Lauffenburger, J.A., Grissom, C.A. and Charola, A.E. (1992) "Changes in Gloss of Marble Surface as a Result of Methylcellulose Poulticing" *Studies in Conservation* 37 155-164
- Livingston, R.A. and Baer, N.S. (1985/86) "The Accuracy of Stone Weathering Rates Measured on Historic Structures" in *Wiener Berichte über Naturwissenschaft in der Kunst* 2/3 pp. 272-297
- Martin, J.W. and Bentz, D.P. (1987) "Fractal-Based Description of the Roughness of Blasted Steel Panels" *J. Coat. Technol.* 59 35-41

Mossotti, V.G. and Eldeeb, A.R. (1992) "Effect of Cleaning Techniques on Dimension Limestone. Case Study: Chicago Tribune Tower"

Oursler, D.A. and Wagner, J.W. (1994) "Microwave Speckle Contrast for Surface Roughness Measurements" in *Nondestructive Characterization of Materials V*, R.E.Green et al. Eds., Plenum Press, NY , pp. 599-606

Realini, M., Toniolo, L., Zanetta, P., Albrecht, D. and Facchini, M. (1994) "A Laser Method for the Study of Salt Crystallization on Stone Surfaces" in The Conservation of Monuments in the Mediterranean Basin, Proceedings of the 3rd International Symposium, V.Fassian, H.Ott & F.Zezza, Eds., Soprintendenza ai Beni Artistici e Storici di Venezia, Venice, pp. 73-76

Song, J.F. and Vorburger, T.V. (1992) "Surface Texture" in Metals Handbook Vol.18: Friction, Lubrication, and Wead Technology, ASM, Ohio, pp. 332-345

Stonecleaning in Scotland (1992) Vol.2 Research Report, Historic Scotland, Aberdeen, pp. 154

TAPPI (1988) Smoothness of Paper and Paperboard (Sheffield Method) T 538 om-88

TAPPI (1991) Smoothness of Paper (Bekk Method) T 179 om-91

Trudgill, S., High, C.J. and Hanna, F.K. (1981) "Improvements to the Micro Erosion Meter" Technical Bulletin 29, British Geomorphological Research Group, pp. 3-17

Veloz, N.F. (1994) "Practical Aspects of Using Walnut Shells for Cleaning Outdoor Sculpture" APT Bulletin Vol.XXV No.3-4 70-76

Winkler, E.M. (1986) "A Macrostereogrammetric Technique for Measuring Surface Erosion Losses on Stone" in Cleaning Stone and Masonry, J.R.Clifton, Ed., ASTM STP 935, pp, 153-161

APPENDIX I
THERMOGRAPHIC IMAGING



UNITED STATES DEPARTMENT OF COMMERCE
National Institute of Standards and Technology
Gaithersburg, Maryland 20899-0001

May 4, 1995

Carol Grissom
Conservation Analytical Laboratory
CAL/MSC
Smithsonian Institution
Washington, D.C. 20560

Dear Carol:

I have finally had a chance to spend a few hours looking at the samples that you left during your visit with the infrared thermography cameras. I am enclosing several images of the results obtained. It appears that the stone sample itself has a very high emissivity, as even lead pencil marks are overwhelmed by the emissions from the stone. You can see that for the smooth side of the stone, we basically see a homogeneous background image. Conversely, for the rough side, we see many dark spots in the image. However, it is difficult to match these with protrusions from the surface in any kind of a one-to-one fashion, so the dark spots may be due to emissivity differences due to different crystallography or mineralogy. For the stone, I have marked with lead pencil the area viewed on each side; with an upward pointing arrow indicating the top line of the rectangular border.

In the case of the replicate, we can indeed see the protrusions from the replica as a dark spots in the infrared image. I am enclosing one image obtained with our conventional infrared camera (lower resolution) and two photographs obtained with our very high resolution infrared camera. In the latter, the dark spots are quite large and could probably be easily quantified. With the conventional camera, the spots are visible, but are rather small for performing a quantitative analysis.

Based on these preliminary results, I would project that analysis of the replicates should be a more robust technique than viewing the stone samples directly. This would be partially due to the fact that the replicate material should be more controllable, whereas the mineralogy, etc. of the stone will vary from sample to sample, making calibration a more difficult task. On the other hand, it will be necessary to control the uniformity of the thickness of the replicate to avoid signal variations across the viewed area. In either case, a relatively high resolution infrared camera will be necessary to resolve the smaller irregularities in the surface roughness.

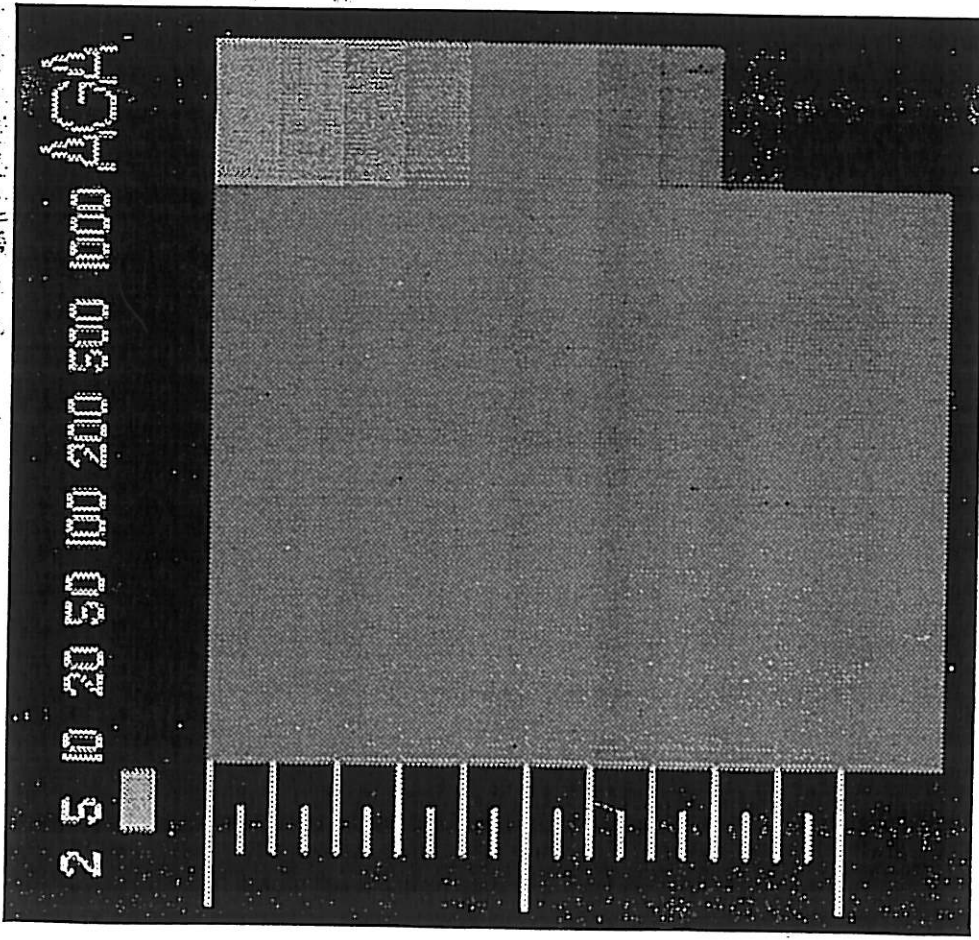
I hope that you find these results useful in your research effort. If I can be of further service, please do not hesitate to contact me directly.

Sincerely,

Dale P. Bentz

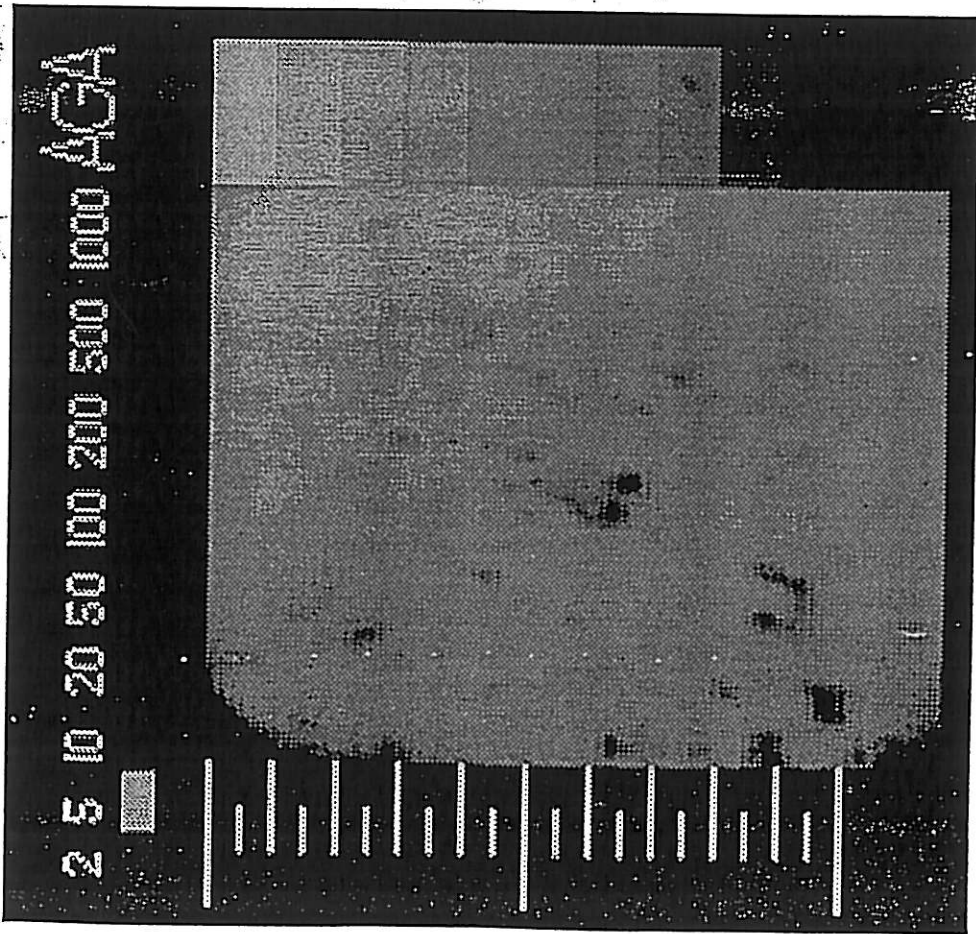
Dale P. Bentz
Chemical Engineer

Enclosures



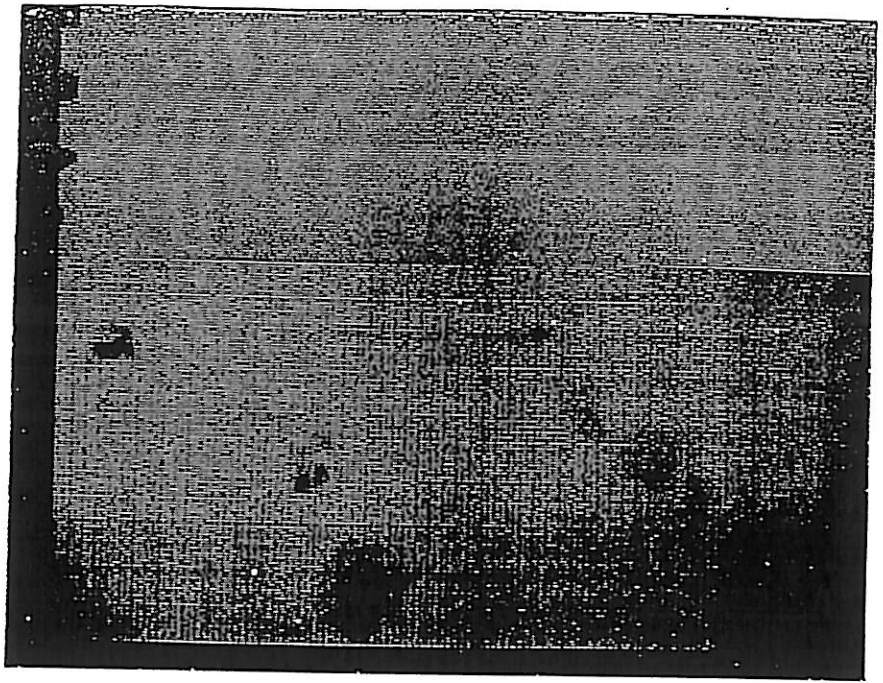
2 5 10 20 50 100 200 500 1000 4G4

Smooth Side of Stone

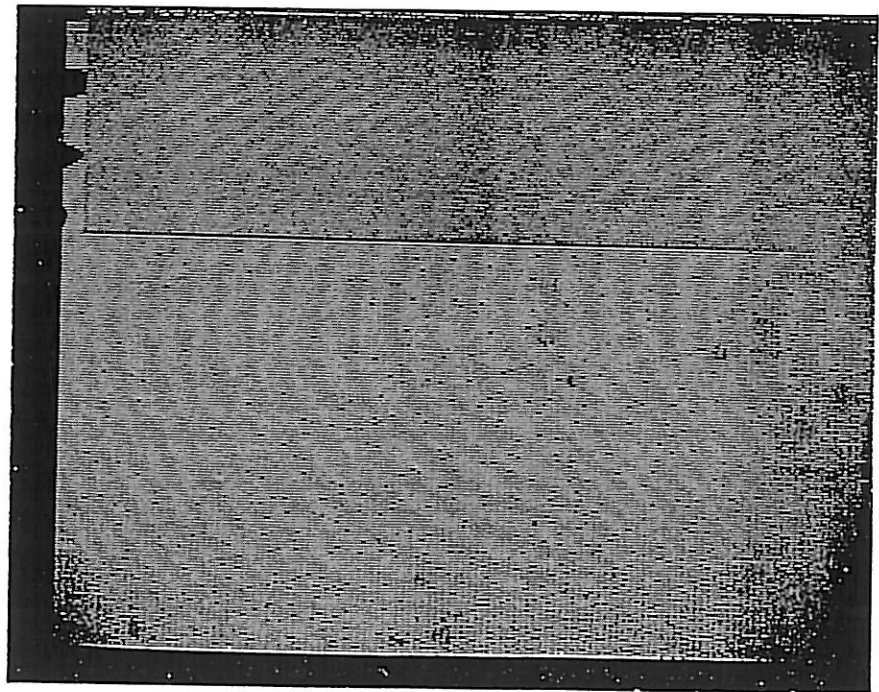


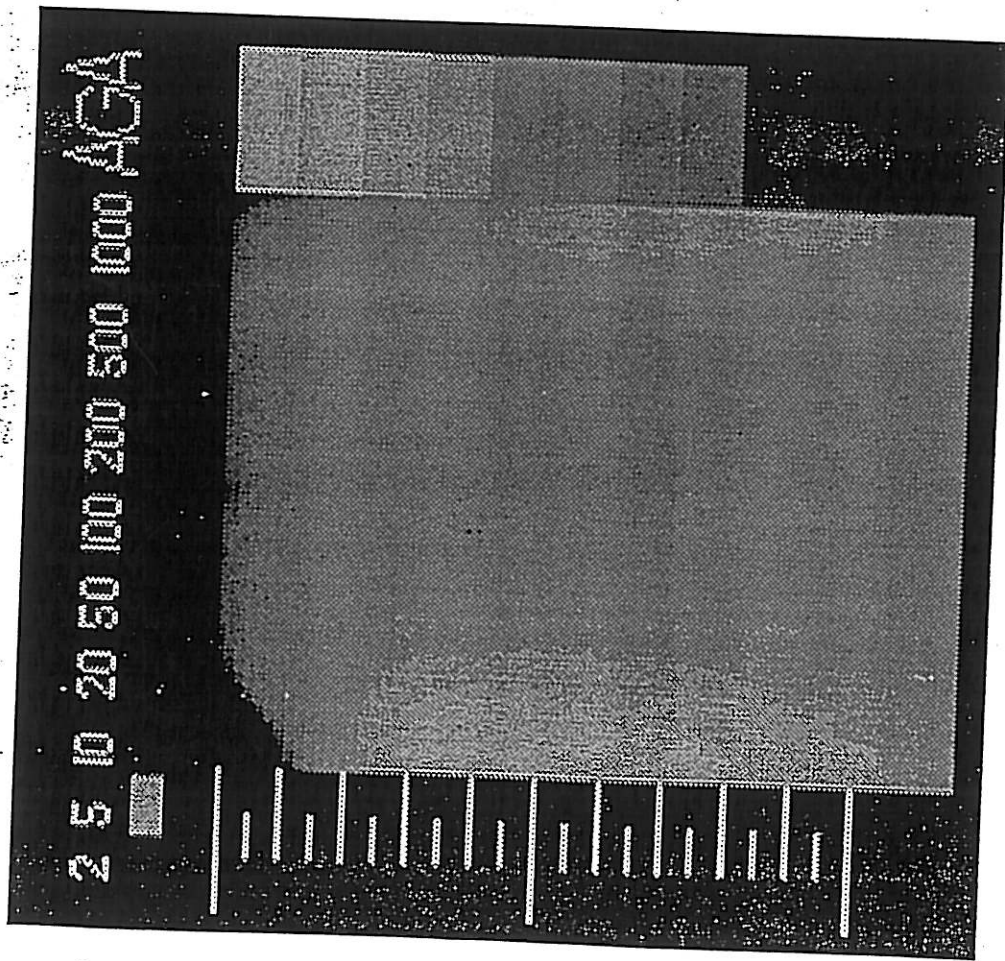
Rough Side of Stone

REPLICA - HIGH RES.



REPLICA - HIGH RES.





Replica Surface

APPENDIX II
SCANNING WHITE LIGHT INTERFEROMETRY

Silicon Rubber Replica

Submitted By

Smithsonian Institution

Samples Evaluated by:

John W. Roth
Applications Support Engineer

Zygo Corporation
Laurel Brook Road
Middlefield, CT 06455
(203) 347 - 8506, Ext. 205

June 8, 1995

Objective

Characterize the surface structure of silicone rubber replica submitted by the Smithsonian Institution. Emphasis will be placed on 3-D surface characterization and representation.

Equipment Used

The Zygo NewView 100 Non-Contact Surface Structure Analyzer was used to make the measurements on the samples provided. An HP 715 system controller running MetroPro™, Zygo's graphical user interface, controlled the process. Graphical results were output from the HP workstation to a HP PaintJet color printer.

To obtain the resolution necessary for meaningful measurements a 40X Mirau objective was used. The objective has the following specifications:

Objective	Field of View H x V (mm)	Lateral Resolution (μm)	Spatial Sampling (μm)
40X	0.18 mm x 0.13 mm	0.73	0.55

Theory of Operation

The NewView 100 is a precision microscope which uses Scanning White Light Interferometry (SWLI) to generate quantitative three-dimensional images. In the NewView 100, an interferometer objective is mounted in a precision piezo scanning device which moves vertically (in the Z direction) over the sample. Data is collected from a CCD camera and processed by a Hewlett Packard 700 series system controller. The phase relationships of individual components of the white light spectrum in the interferogram are analyzed by Zygo's patented Frequency Domain Analysis (FDA). The result is a surface map with ultra high Z resolution, independent of the objective's magnification. The NewView 100 has angstrom resolution over long vertical distances of up to 100 μm (standard), 5mm, or 10mm (optional) and large fields of view up to 23.8 mm^2 (2.5X objective with the Microscope Image Zoom Option).

The entire system is managed by Zygo's sophisticated but easy to use MetroPro™ Software. Using an interactive window display, MetroPro simultaneously presents on-screen instrument control, surface images, plots and data. Available data includes a high fidelity 3D image, 3D plots, multiple 2D profiles of 3D data, and a wide range of surface roughness parameters. The HP Color PaintJet printer is available to create high quality color copies of the graphic data. Data can be saved to disk or tape or transferred to another computer for use in process tracking or statistical analysis.

Some Key Features of MetroPro™

- High Resolution Graphics
- User configurable software and screens without using “macros”
- Built in Print Spooler
- All desired results displayed on one screen for easy analysis
- Built in SPC with run charts, controls charts and summary statistics
- Built in networking
- Mature software - Metropro™ was introduced in 1989 and we are currently shipping version 6.0. Each version has progressively added more capabilities, ease of use, and customer suggested enhancements

Test Conditions

The samples were tested as received. Room temperature was 72° F during the test. Humidity was maintained at 64%.

Explanation of Printouts

Printouts characterizing the samples at each magnification are appended to this report. The attributes box at the bottom identifies the sample and the objective used. The units used in the plots are metric, however, any commonly used english, metric or optical units can be set.

All of the printouts include a *Filled Contour* plot, an *Oblique Plot*, a *Profile Plot* and a *Solid Plot*. Various numerical results are listed below the Filled Contour and Profile Plot.

Plots

The **Filled Contour Plot** is a 2 dimensional plot which shows the surface heights as viewed along the instrument's z axis (a bird's eye view). Different heights are represented by different colors. Red shows high points and violet shows low points.

The **Oblique Plot** is a three dimensional display of the surface. All three axes have labeled scales. Similarly to the filled plot, red areas are high points and violet areas show low points.

The **Profile Plot** shows a two dimensional “slice” through the data, similar to what a stylus profiler system would measure. The location, orientation and length of the slice is completely user definable in the Filled Plot. For these measurements, the slice was placed horizontally, across the Filled Plot.

The **Solid Plot** is actually a 3D image of the surface. Surface slopes as viewed in the instruments Z axis are highlighted, allowing a more qualitative analysis of the surface.

Numerical Results

The **PV** number is the vertical distance between the highest point and lowest point in the measured area (Peak-to-Valley).

Ra is the arithmetic average deviation from the center plane of the data.

rms is the root mean square average deviation height. It is the square root of the mean of the sum of the squares of the distances of every point from the mean height.

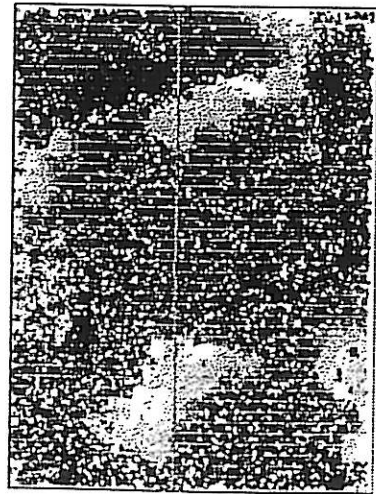
Conclusions

The New View 100 was able to quickly and easily obtain data on the surface characteristics of the samples provided using a 40X objective. However, it should be noted that to observe surface detail over a larger area requires an objective with a lower magnification. It was observed that these objectives were not able to resolve significant detail due to the extremely rough surface samples to be measured. The surface contained areas of high slope that exceeded the slope resolution (N.A.) of the objective. In cases where the slope exceeds the numerical aperture of the objective, light does not return to the objective and measurement data in those areas is not feasible.

Measurement Results

ZY90

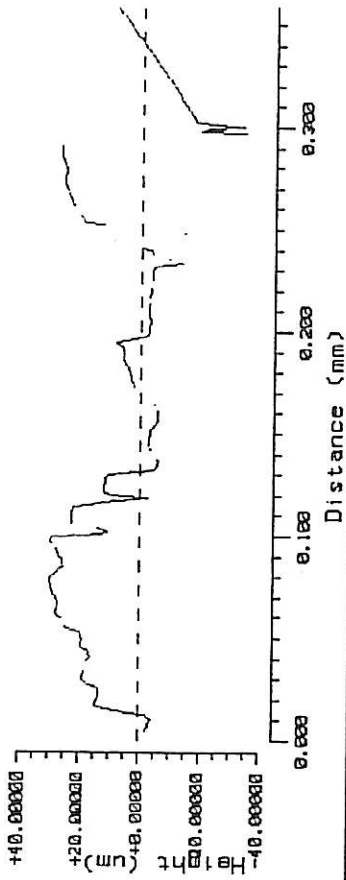
Surf Map



PV 184.973 um
 rms 18.597 um
 Ra 14.720 um

ZY90

Surface Profile



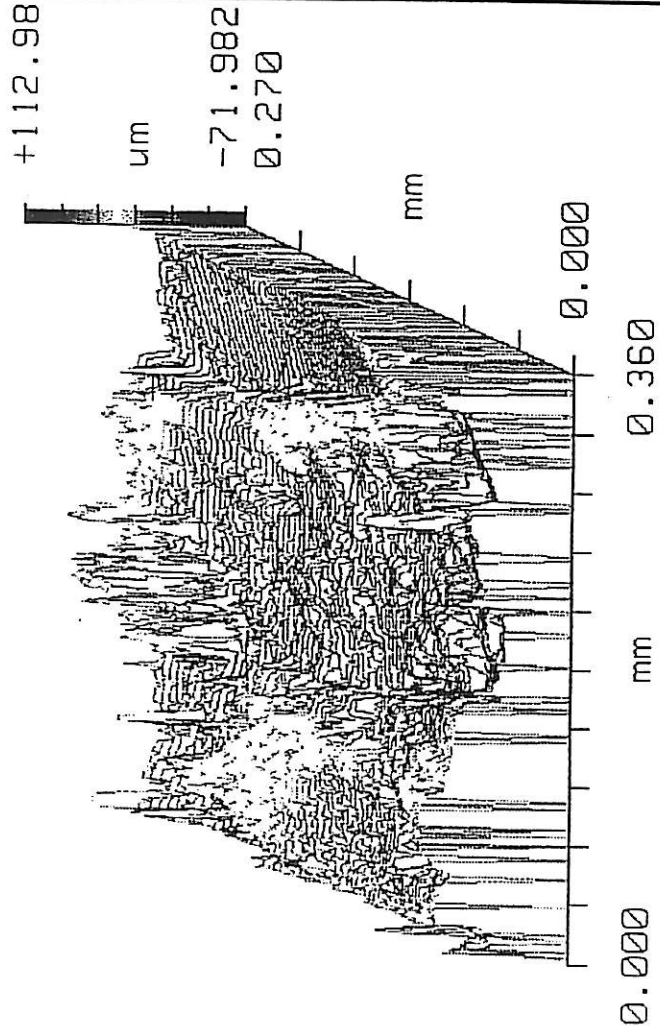
PV 64.360 um
 rms 14.273 um
 Ra 12.498 um

Profile Stats

Silicone Rubber Replica - Low Relief Area

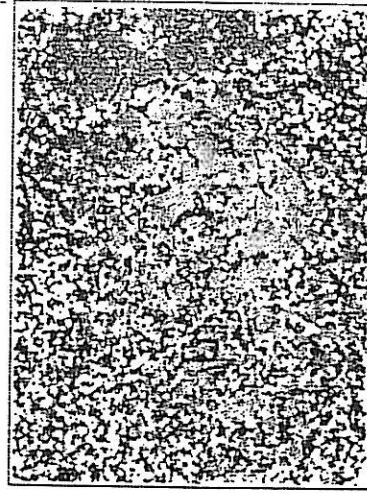
ZY90

Oblique Plot



ZY90

Solid Plot



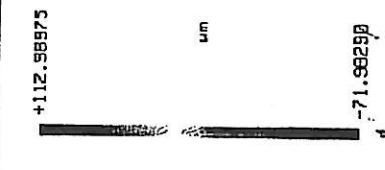
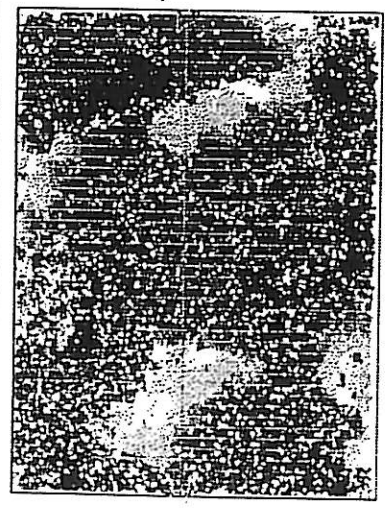
Measure Attributes

Wed Jun 7 08:13:44 1995

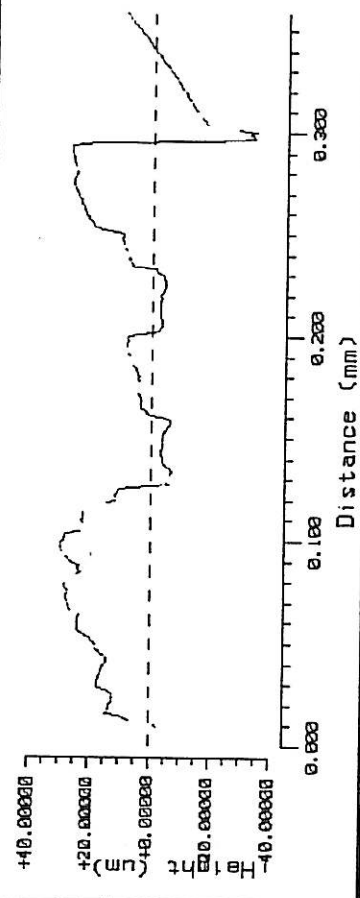
Objective: 40X Mirau

zygo

Surf Map



Surface Profile



PV 184.973 μm
 rms 18.597 μm
 Ra 14.720 μm

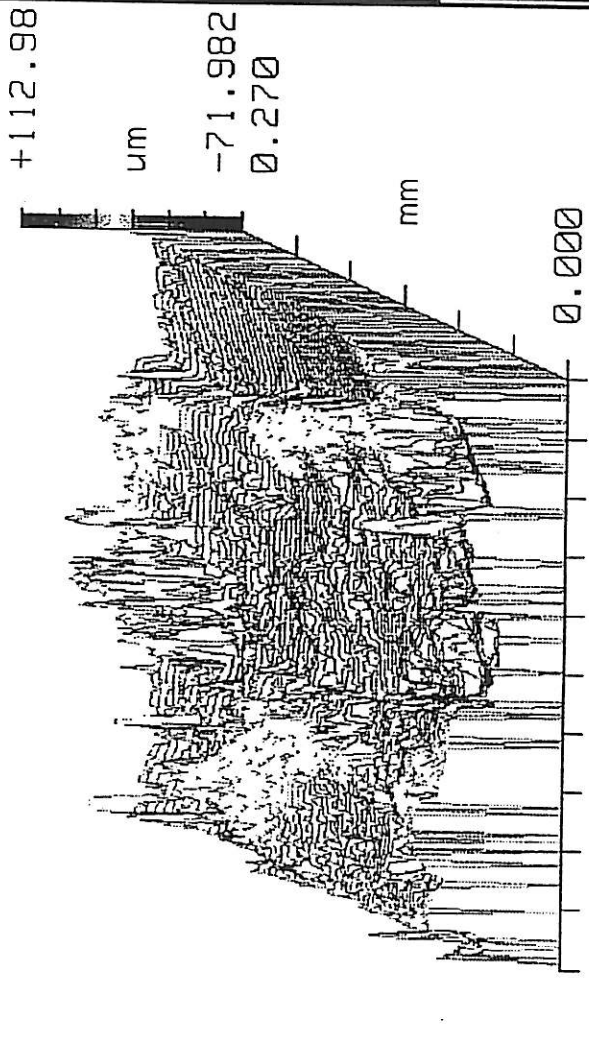
PV 64.125 μm
 rms 13.953 μm

Ra 11.828 μm
 Profile Stats

Silicone Rubber Replica - Low Relief Area

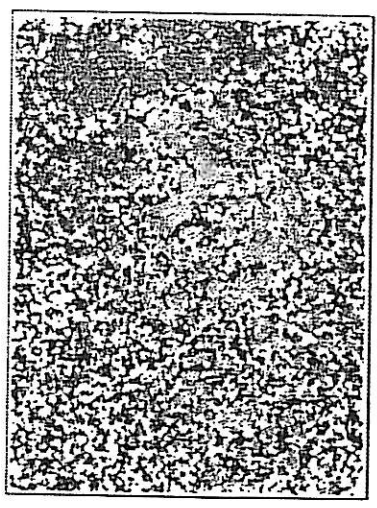
zygo

Oblique Plot



zygo

Solid Plot



Measure Attributes

Wed Jun 7 08:13:44 1995

Objective: 40X Mirau

ZY90

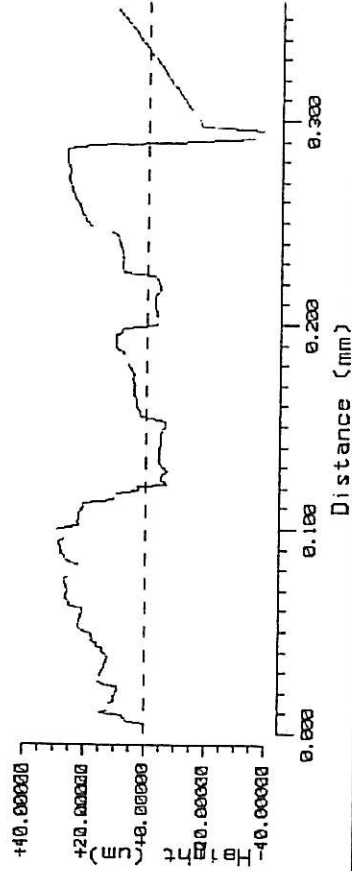
Surf Map



+169.37657 μm
-69.56569 μm

ZY90

Surface Profile



PV 178.962 μm
rms 18.797 μm
Ra 14.865 μm

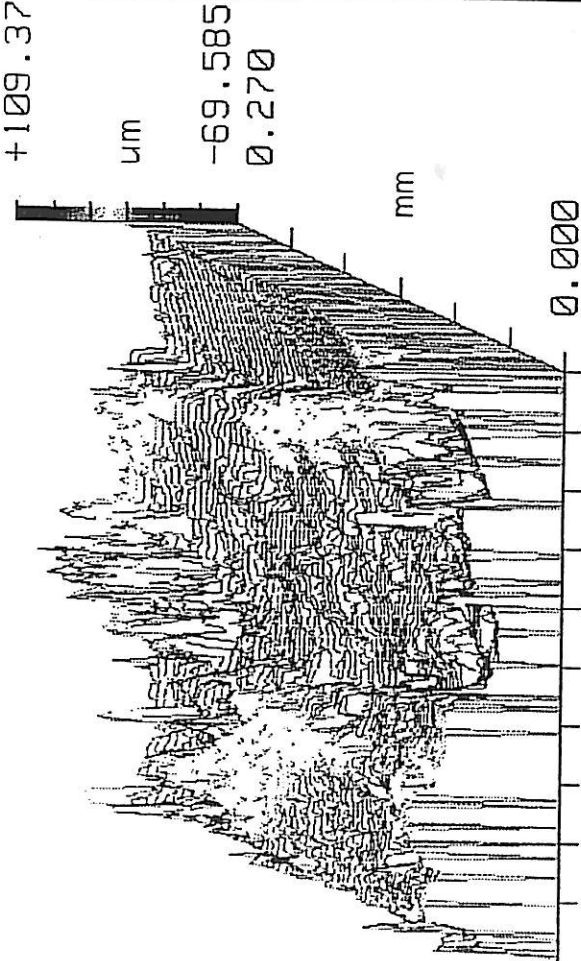
PV 67.182 μm
rms 13.181 μm

Ra 10.856 μm
Profile Stats

Silicone Rubber Replica - Low Relief Area

ZY90

Oblique Plot



+109.37 μm
-69.585 μm
0.270

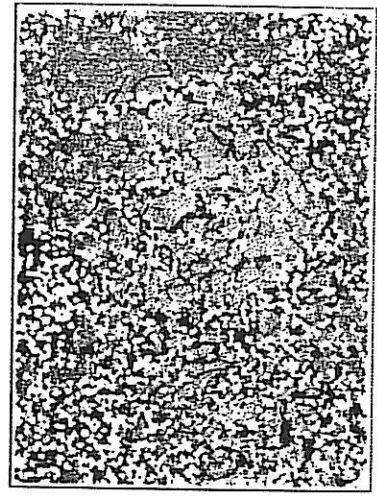
0.000

mm

0.360

ZY90

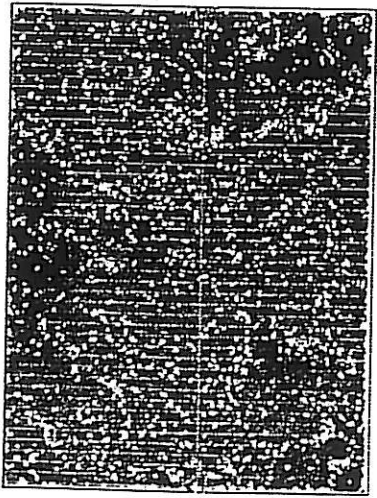
Solid Plot



Measure Attributes

Wed Jun 7 08:13:44 1995

Objective: 40X Mirau

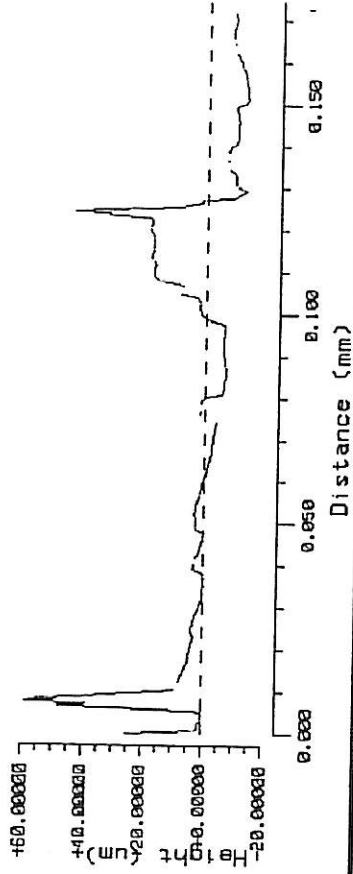


PV 154.729 um
 rms 9.798 um
 Ra 7.295 um

Oblique Plot

zygo

Surface Profile

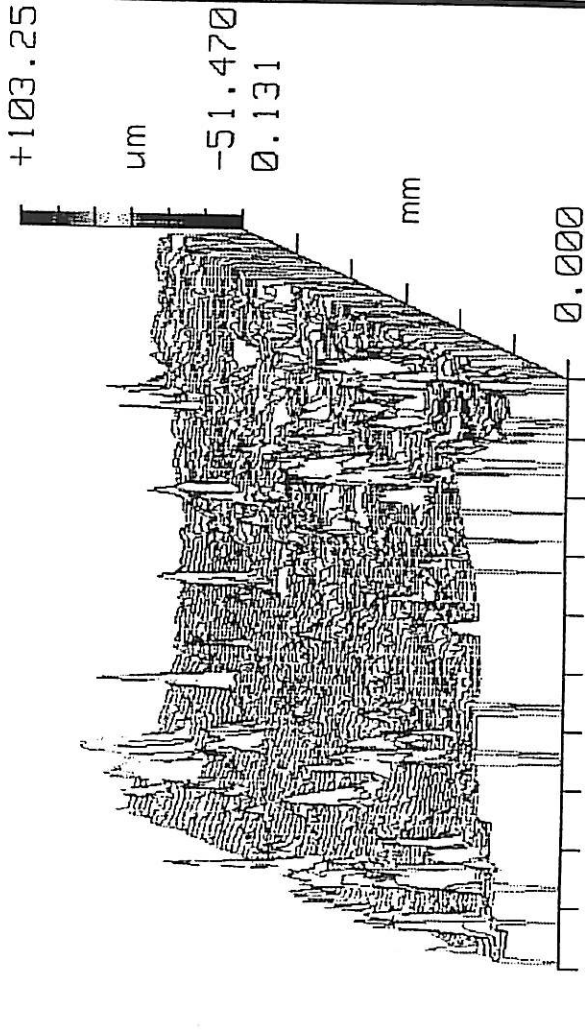


PV 72.070 um
 rms 11.337 um
 Ra 7.697 um

Profile Stats

Silicone Rubber Replica - High Relief Area

zygo Solid Plot



+103.25 um
 -51.470 um
 0.131

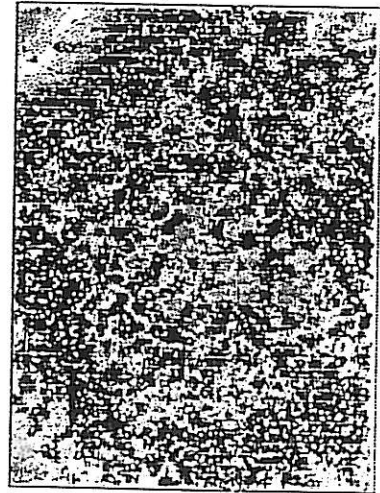
0.000 mm
 0.175 mm

Measure Attributes

Wed Jun 7 08:30:41 1995

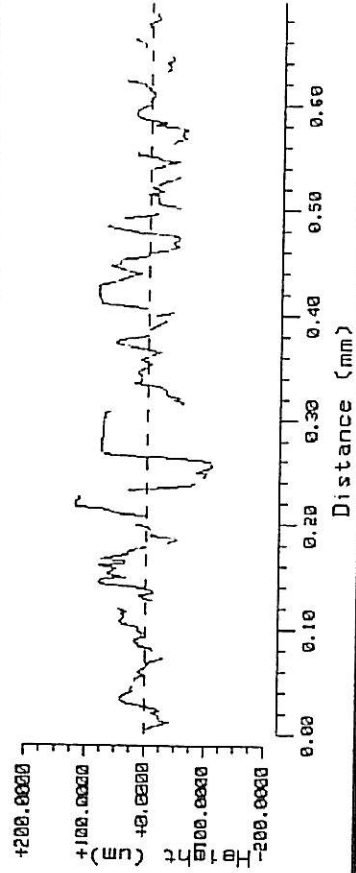
Objective: 40X Mirau

Image Zoom: 1X



PV 301.307 um
 rms 46.321 um
 Ra 36.615 um

Surface Profile



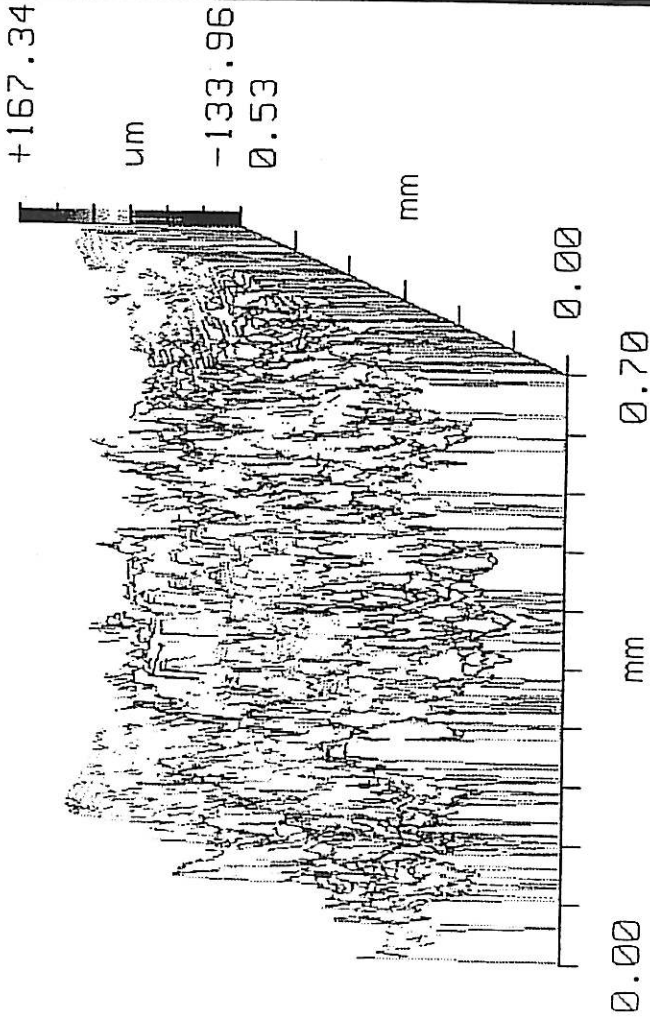
PV 227.812 um
 rms 44.669 um
 Ra 35.147 um

Profile Stats

Silicone Rubber Replica - High Relief Area

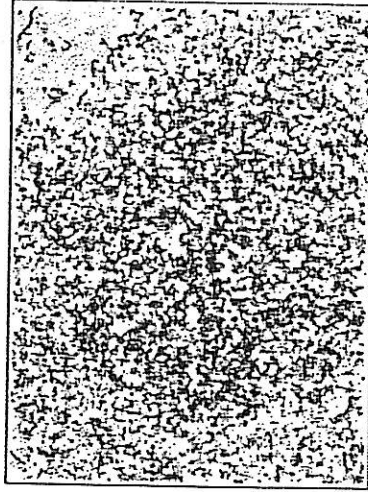
Oblique Plot

ZY90



Solid Plot

ZY90



Measure Attributes

Wed Jun 7 08:38:07 1995
 Objective: 10X Mirau
 Image Zoom: 1X

APPENDIX III
LASER TRIANGULATION PROFILOMETRY

APPENDIX III

Summary of average roughness Ra [μm] data from laser triangulation. Each number is the average of 50 blocks (each with 40 points), scanned in ten lines of 5 block each, over a 1 cm² area. Three areas were measured in duplicate on each sample. The measurements were carried out at Johns Hopkins University by D.Oursler and E.Erder.

	Carrara marble [# 14]	White replica [S-27]	Red replica [S-29]
C-1	49.78 \pm 11.48 50.27 \pm 11.40	2.42 \pm 0.54 2.38 \pm 0.40	5.63 \pm 1.40 5.97 \pm 1.13
C-2		2.38 \pm 0.44	5.47 \pm 0.96 5.52 \pm 1.03
C-3			5.39 \pm 0.97 5.38 \pm 0.97
Av.	50 \pm 11 μm	2.5 \pm 0.5 μm	5.5 \pm 1 μm
GB-1	42.44 \pm 11.37 42.45 \pm 11.38	5.39 \pm 1.31 5.34 \pm 1.40	7.50 \pm 1.70 7.12 \pm 1.56
GB-2	41.22 \pm 10.17 41.30 \pm 10.24	4.93 \pm 1.57 5.05 \pm 1.42	7.04 \pm 1.56 6.92 \pm 1.51
GB-3	42.98 \pm 8.72 42.93 \pm 9.09	4.89 \pm 1.30 4.88 \pm 1.34	6.67 \pm 1.55 6.76 \pm 1.59
Av.	42 \pm 10 μm	5.1 \pm 1.4 μm	7.1 \pm 1.5 μm
Al-1	37.46 \pm 9.24 37.36 \pm 9.12	3.27 \pm 0.78 3.30 \pm 0.78	6.30 \pm 1.40 6.02 \pm 1.13
Al-2	33.45 \pm 9.04 33.61 \pm 8.98	3.45 \pm 0.92 3.38 \pm 0.93	5.97 \pm 0.98 6.02 \pm 1.13
Al-2	35.21 \pm 7.37 35.09 \pm 7.44	3.67 \pm 0.87 3.62 \pm 0.85	6.43 \pm 1.30 6.46 \pm 1.35
Av.	35 \pm 8 μm	3.5 \pm 0.8 μm	6.2 \pm 1.2 μm

	Indiana limestone [# 12]	White replica [S-23]	Red replica [S-33]
C-1	17.94 ± 10.75 17.75 ± 10.78	13.18 ± 4.49 13.07 ± 4.55	24.28 ± 13.19 24.11 ± 13.29
C-2	19.34 ± 9.04 19.36 ± 8.97	13.97 ± 5.37 13.81 ± 5.38	23.77 ± 13.19 23.74 ± 13.31
C-3	16.87 ± 7.53 16.85 ± 7.54	11.52 ± 4.77 11.34 ± 4.68	25.25 ± 13.99 25.30 ± 14.23
Av.	18 ± 9 μm	13 ± 5 μm	24 ± 13 μm
GB-1	27.53 ± 11.56 27.61 ± 11.66	18.53 ± 8.21 18.57 ± 8.19	42.24 ± 21.89 41.91 ± 21.75
GB-2	28.19 ± 12.11 28.12 ± 12.17	20.21 ± 10.09 20.17 ± 9.86	45.14 ± 19.36 45.33 ± 19.17
GB-3	23.80 ± 10.36 23.81 ± 10.45	21.63 ± 11.78 21.81 ± 11.81	45.35 ± 24.68 45.35 ± 24.70
Av.	26.5 ± 11 μm	20 ± 10 μm	44 ± 20 μm
Al-1	31.08 ± 13.24 31.18 ± 13.25	19.92 ± 7.63 20.01 ± 7.80	48.79 ± 26.80 48.83 ± 26.96
Al-2	32.58 ± 13.78 32.78 ± 13.86	21.91 ± 9.90 22.98 ± 9.73	54.19 ± 25.67 53.96 ± 25.96
Al-2	27.01 ± 11.93 27.06 ± 11.94	20.02 ± 7.35 19.98 ± 7.17	48.25 ± 23.40 47.98 ± 22.71
Av.	30 ± 12 μm	21 ± 8 μm	50 ± 24 μm

	Brick paver [# 13]	White replica [S-24]	Red replica [S-31]
C-1	9.61 ± 3.62 9.59 ± 3.63	8.82 ± 3.55 8.81 ± 3.75	8.99 ± 3.37 9.02 ± 3.41
C-2	9.14 ± 3.92 9.24 ± 3.94	6.96 ± 3.13 6.83 ± 3.10	8.79 ± 3.27 8.71 ± 3.31
C-3	8.34 ± 1.86 8.30 ± 1.83	6.68 ± 2.05 6.60 ± 2.06	9.16 ± 3.99 9.13 ± 4.03
Av.	9 ± 3 μm	7.5 ± 3 μm	9 ± 3 μm
GB-1	8.27 ± 4.05 8.23 ± 4.05	5.65 ± 1.79 5.71 ± 1.76	11.70 ± 7.81 11.80 ± 7.75
GB-2	11.79 ± 4.02 11.86 ± 4.09	8.92 ± 4.14 8.91 ± 4.06	14.44 ± 7.21 14.51 ± 7.22
GB-3	13.30 ± 8.37 13.43 ± 8.44	8.35 ± 4.20 8.38 ± 4.11	11.22 ± 3.62 11.18 ± 3.66
Av.	11 ± 5 μm	7.6 ± 4 μm	12 ± 7 μm
Al-1	10.11 ± 5.23 10.25 ± 5.26	8.07 ± 2.60 8.11 ± 2.66	12.68 ± 3.30 12.64 ± 3.28
Al-2	12.37 ± 6.43 12.34 ± 6.51	9.03 ± 2.50 8.83 ± 2.47	12.46 ± 4.33 12.57 ± 4.40
Al-3	13.71 ± 7.27 13.75 ± 7.36	9.04 ± 3.25 9.21 ± 3.23	10.23 ± 3.70 10.24 ± 3.64
Av.	12 ± 6 μm	9 ± 3 μm	12 ± 4 μm

Analysis of Variance. Example for red replica of limestone

Table of Ra [μm] for limestone red replica of limestone area C-1

Mean 24.28 standard deviation 13.19

37.273	10.360	19.420	45.521	26.473
15.965	26.238	15.979	30.084	22.030
25.563	8.980	17.681	17.934	11.366
17.026	29.596	24.786	19.093	50.521
12.662	39.536	7.937	13.779	13.655
30.844	8.080	26.446	12.792	23.467
15.469	16.876	17.286	25.220	14.647
15.362	18.064	25.177	36.761	40.080
70.125	26.859	18.727	47.352	26.186
28.907	8.937	10.189	57.097	33.505

Table of Ra [μm] for limestone red replica of limestone area GB-1

Mean 42.24 standard deviation 21.89

75.172	32.091	27.755	70.553	49.415
26.167	36.781	102.475	28.918	61.941
41.778	110.912	33.226	28.071	39.162
45.169	26.663	25.800	39.255	26.033
33.962	39.076	92.845	38.255	13.061
11.369	29.289	77.530	50.181	20.479
46.559	31.274	11.845	35.426	34.225
25.284	27.479	54.065	54.738	37.950
39.759	36.631	70.948	57.014	18.740
51.206	23.025	65.103	34.098	23.198

Table of Ra [μm] for limestone red replica of limestone area A1-1

Mean 48.79 standard deviation 26.80

25.621	44.003	60.532	19.894	63.841
32.613	23.802	52.685	72.639	74.127
24.472	21.737	37.600	53.369	83.857
22.483	36.968	20.126	83.994	158.903
23.944	33.663	33.861	23.235	68.152
40.067	25.428	30.366	64.076	47.953
45.752	30.770	33.234	73.958	70.053
16.695	27.381	76.635	60.724	106.810
61.687	41.590	32.830	35.412	90.910
61.778	56.258	18.194	48.979	46.024

Analysis of variance table for control, glass-bead abraded and alumina abraded areas of a limestone surface. Data from a red silicone replica.

Source of variation	Degrees of freedom	Sum of squares	Mean square
Between Treatments	2	S_T 16,103	s_T^2 8051.5
Within Treatments	147	S_R 68,575.53	s_R^2 466.50
Total about the Grand Average	149	S_D 84,678.53	s_D^2 568.31

The difference between the mean squares (s^2), which are an estimate of the variance σ^2 , calculated between treatments, i.e., considering each area separate, and within treatments, i.e., pooling all the data obtained from the three areas, is sufficiently different so suppose that the differences observed are real.

The differences arise because the mean square between treatments, s_T^2 , reflecting variations among the abrasion treatments as well as the intrinsic error variance, will be larger than the mean square within treatments, s_R^2 .

The ratio of the mean squares between treatments and within treatments is F :

$$F = s_T^2 / s_R^2 = 17.26 (2, 147)$$

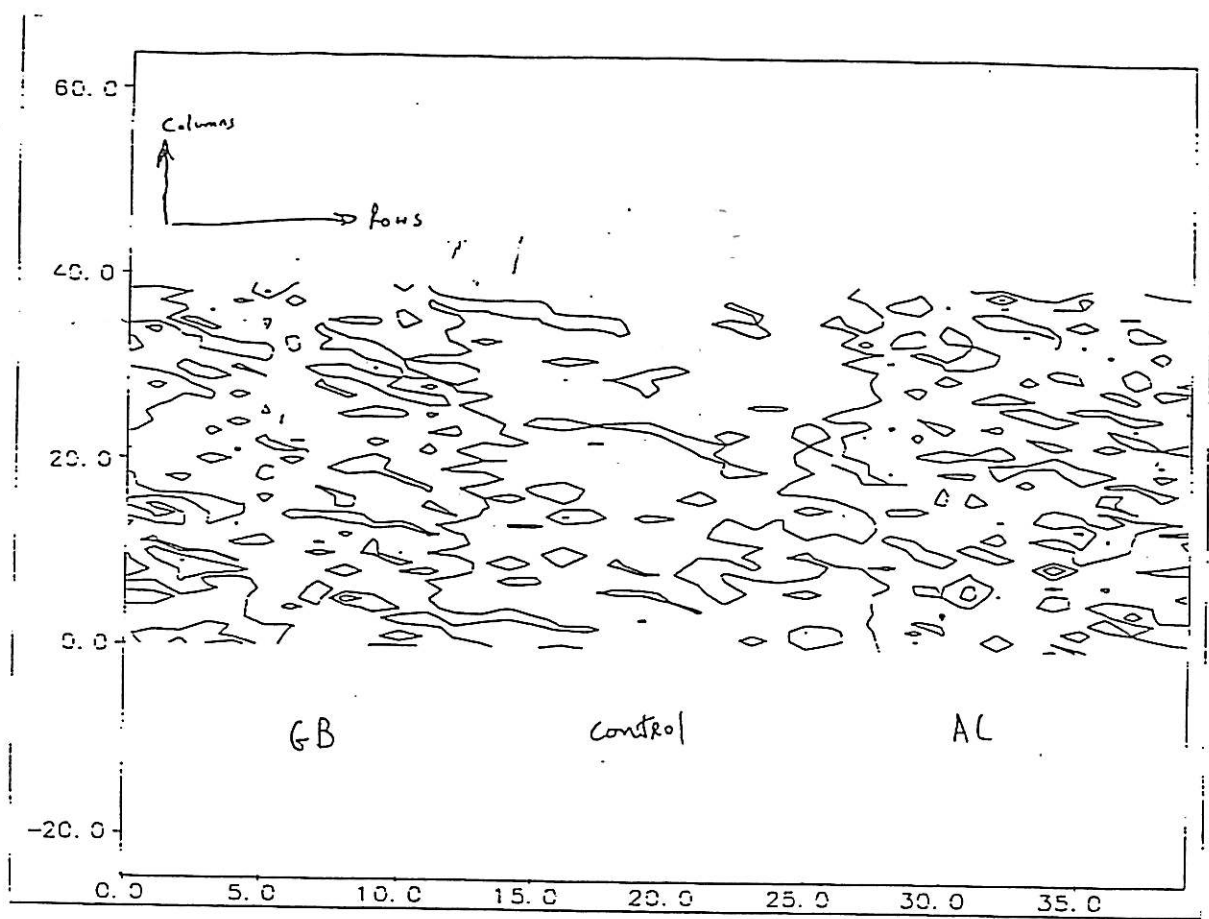
From tables $F_{1\%} (2, \infty) = 6.91$

The values are sufficiently different to discredit the null hypothesis. Therefore real differences exist among the treatments.

References

Box, G.E.P., Hunter, W. and Hunter, J.S. (1978) Statistics for Experimenters, John Wiley & Sons, Inc., New York, pp. 165-188 and Table D, p.640

Brookes, C.J., Betteley, I.G. and Loxston, S.M. (1979) Fundamentals of Mathematics and Statistics. John Wiles & Sons, Inc., New York, pp. 398-425



Limestone

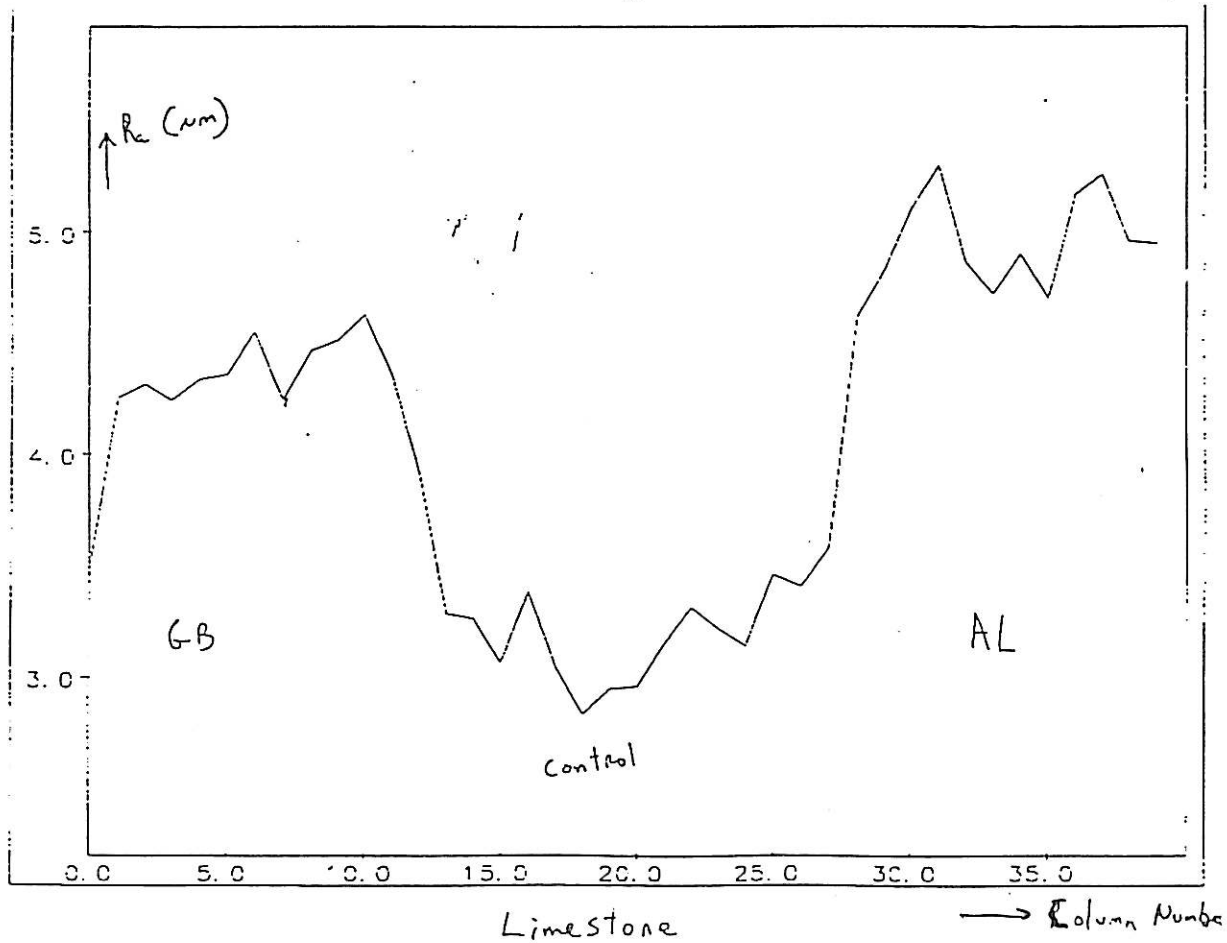


FIG. I. Contour map and line graph for the limestone sample.

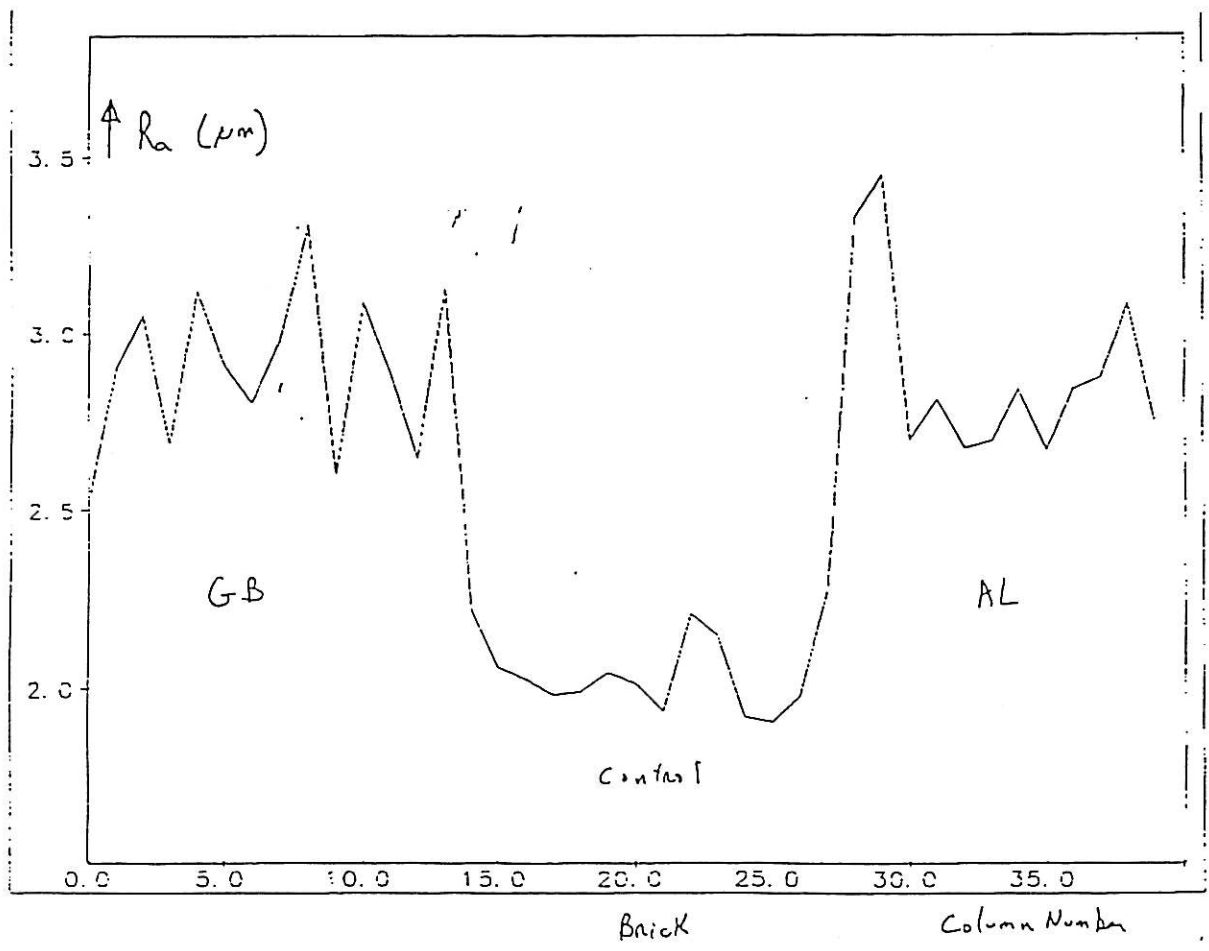
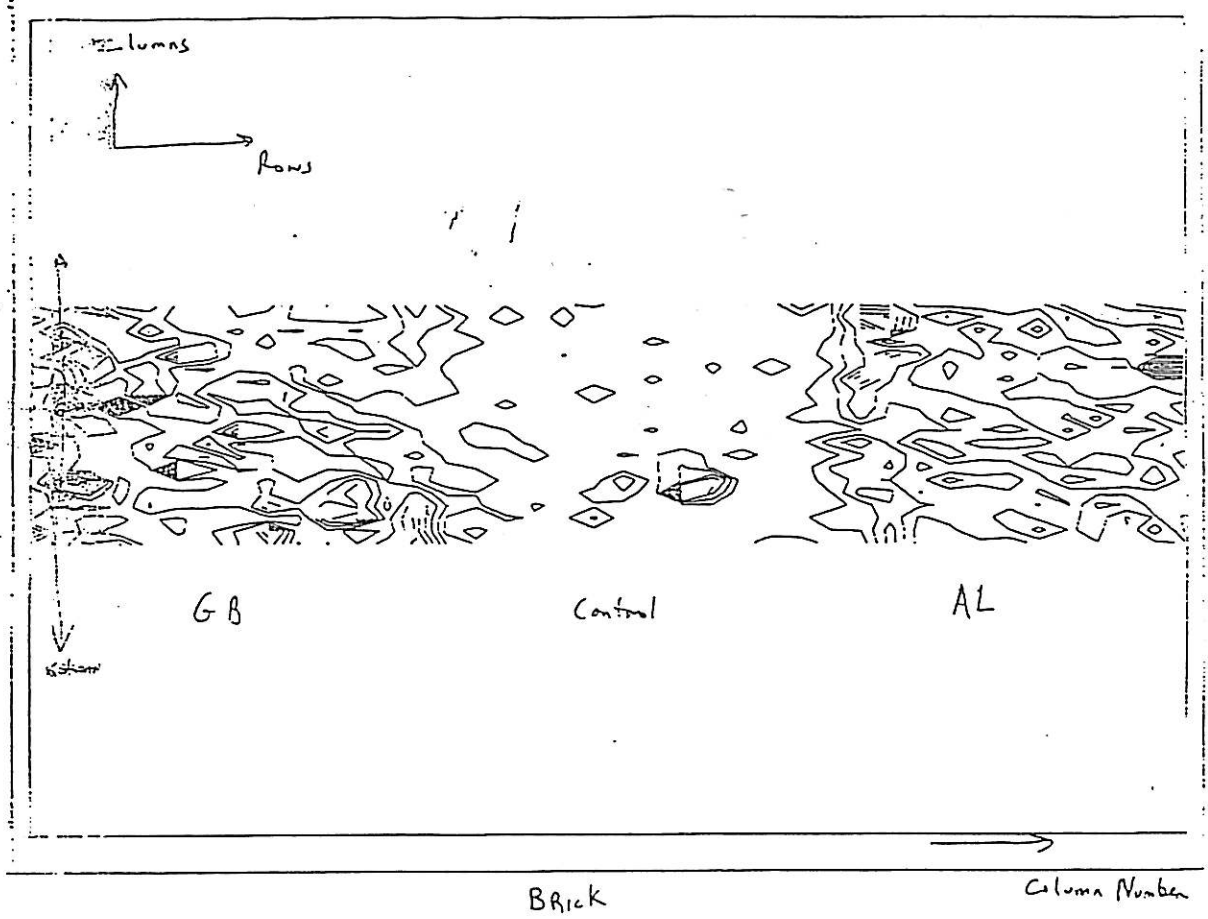


FIG. II. Contour map and line graph for the brick sample.

APPENDIX IV
GLOSS MEASUREMENTS - PHASE I

APPENDIX IV

Gloss measurements of the marble [#14] made on the polished and abraded sections. Measurements were taken with a Lange Labor-Reflektometer at 20°. Values between brackets were obtained with a calculator to check on the instrument.

First set of measurements

Control		Glass beads		Alumina	
77.6	82.1	1.6	1.6	1.5	1.4
85.2	72.4	1.6	1.5	1.4	1.3
77.5	79.9	1.6	1.6	1.5	1.5
70.6	74.7	1.6	1.6	1.5	1.1
81.3	76.0	1.6	1.6	1.3	1.5
75.1	78.1	1.6	1.6	1.5	1.4
81.2	83.7	1.6	1.5	1.4	1.4
86.6	82.8	1.6	1.6	1.5	1.4
80.7	73.1	1.6	1.6	1.4	1.4
76.3	52.0	1.6	1.6	1.1	1.4
79.4	83.9				
82.2					
Av	[77.93]	1.6	[1.59]	1.4	[1.39]
s	[7.06]	0.5	[0.03]	0.1	[0.11]

Second set of data

	Control	Glass beads		Alumina
	81.9	1.4	1.6 1.6	1.6
	79.6	1.6	1.4 1.6	1.2
	81.7	1.7	1.4 1.6	1.6
	82.3	1.6	4.3 1.6	1.1
	83.6	1.6	1.6 1.5	1.3
		1.6	1.1 1.6	1.4
		1.6	1.6 1.6	1.2
		1.6	1.6 1.6	
		1.6	1.6 1.5	
		1.6	1.6 1.6	
		1.6	1.6 1.2	
		1.6	1.6 1.6	
		1.6	1.4 1.6	
		1.6	1.4	
Av	81.8 [81.82]	1.6	[1.69]	1.3 [1.34]
s	1.4 [1.44]	0.6	[0.65]	0.1 [0.198]

APPENDIX V
STYLUS PROFILOMETRY - PHASE I

APPENDIX V

Roughness measurements carried out with the Surtronic 3+ [Rank Taylor Hobson] instrument. The evaluation length [Ln] was of 4.00 mm, the sampling or cut-off length [Lc] was 0.80 mm and the gauge range 100 μm . The results are given in average roughness Ra [μm].

Polished Marble [#14]	Glass Beads	Alumina
0.08	3.60	3.86
1.24	4.00	2.88
0.90	3.40	2.64
0.42	4.20	3.42
0.04	4.00	2.60
0.48	4.20	5.20
1.44	3.88	2.80
	4.00	4.44
	4.20	3.80
		2.88
		3.76
Average 0.6 (\pm 0.5) μm	4.3 (\pm 1.0) μm	3.5 (\pm 0.8) μm
Limestone [#12]	Glass Beads	Alumina
18.4	29.0	38.8
13.6	25.4	47.2
20.0	27.4	41.8
11.8	31.4	43.2
21.8	31.0	46.8
18.9	37.0	35.0
14.2		41.8
16.0		
Average 16.9 (\pm 3.5) μm	30 (\pm 4) μm	42 (\pm 4) μm
Brick Paver [#13]	Glass Beads	Alumina
6.6	13.4	20.0
8.0	10.2	11.0
5.8	7.2	8.8
6.0	16.4	9.4
8.0	13.6	12.8
		13.2
		16.2
		11.2
Average 6.9 (\pm 1) μm	12.2 (\pm 3.5) μm	12.8 (\pm 3.7) μm

Roughness measurements were also carried out with an evaluation length [Ln] of 25 mm, a sampling or cut-off length [Lc] of 2.5 mm and a gauge range of 500 μm . The results are given in average roughness Ra [μm] and are recalculated for an Lc of 8 mm.

	Ra [μm]	
	@ Ln 2.5 mm	@ Ln 8.0 mm
Polished Marble [#14]	0.30	0.36
	0.95	1.02
	0.98	1.16
Average	0.74 (\pm 0.38)	0.85 (\pm 0.43)
PM/Glass beads	6.30	6.96
	7.41	8.40
	7.33	8.18
Average	7.01 (\pm 0.62)	7.85 (\pm 0.78)
PM/Alumina	6.50	9.56
	4.68	6.90
	5.18	6.95
Average	5.45 (\pm 0.94)	7.8 (\pm 1.5)
Limestone [#12]	35.89	42.83
	28.00	32.63
	28.27	33.95
	29.47	35.83
Average	30.4 (\pm 3.7)	36.3 (\pm 4.5)
LS/Glass beads	39.22	45.91
	40.21	48.09
	35.33	41.66
	39.62	48.42
Average	38.6 (\pm 2.2)*	46.0 (\pm 3.1)*
LS/Alumina	34.91	41.77
	41.53	49.77
	39.03	50.01
	35.82	46.27
	35.86	42.61
	41.39	51.35
Average	38.1 (\pm 2.9)*	46.8 (\pm 4.0)*

Note:

Averages with (*) signify that instrument failed to read some areas because roughness was too high.

	Ra [μm]	
	@ Ln 2.5 mm	@ Ln 8.0 mm
Brick Paver [#13]	11.57	22.82
	13.66	22.28
	11.20	20.17
Average	12.1 (\pm 1.3)	21.8 (\pm 1.4)
BP/Glass beads	15.56	25.56
	18.55	34.36
	15.15	19.86
Average	16.4 (\pm 1.8)	21.8 (\pm 1.4)
BP/Alumina	23.32	34.99
	14.82	21.83
	15.43	22.61
Average	17.9 (\pm 4.7)	26.5 (\pm 7.4)

APPENDIX VI
REFLECTED LIGHT IMAGE ANALYSIS - PHASE I

APPENDIX VI

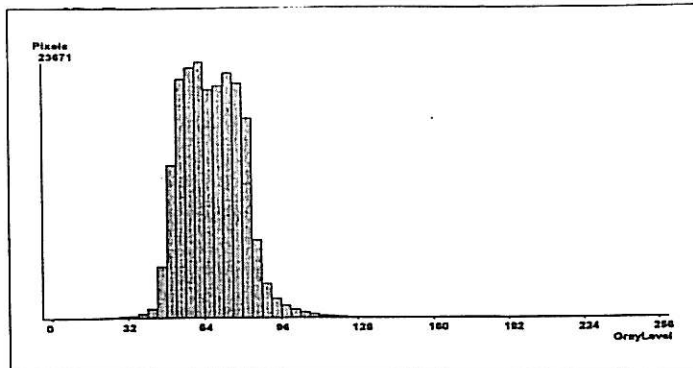
Data from representative runs obtained with RLIA on the red silicone replicas of the surfaces of the marble, limestone and brick samples, and after abrasion with glass beads or with alumina. The histograms are presented in the following pages.

Sample	Sum of Gray	Mean Gray	Std. Dev.	Median	Mode
PM [#29]	14,552,117	68.65	12.59	68	62
	14,255,738	67.25	13.27	67	62
	14,939,424	70.48	14.61	70	62
PM/GB	17,735,693	83.67	17.32	83	84
	19,008,040	89.67	18.07	89	89
	18,211,822	85.92	17.49	86	83
PM/Al	19,103,173	90.12	14.57	90	80
	19,575,363	92.36	13.58	92	97
	20,143,530	95.03	14.37	94	97
LS [#33]	14,719,179	69.44	41.47	70	0
	15,151,505	71.48	42.50	71	0
	14,620,264	68.97	41.45	69	0
LS/GB	12,851,176	60.63	47.89	54	0
	12,826,192	60.51	48.32	53	0
	13,250,832	62.51	46.96	57	0
LS/Al	12,283,329	57.95	50.03	48	0
	11,990,018	56.56	50.34	46	0
	11,913,811	56.20	47.75	47	0
BP [#31]	18,409,410	86.88	17.66	86	84
	15,635,881	73.76	18.98	74	75
	17,140,382	80.86	20.08	80	80
BP/GB	16,473,665	77.72	24.64	79	80
	15,868,619	74.86	24.40	77	80
	16,424,145	77.48	24.81	78	80
BP/Al	15,728,256	74.20	27.54	76	80
	13,675,577	64.52	28.02	65	72
	13,896,868	65.56	30.21	67	75

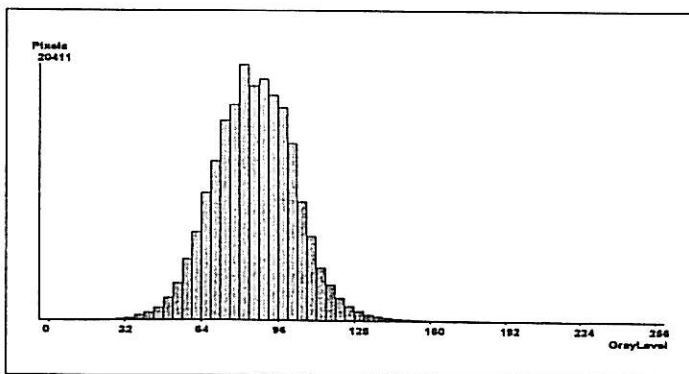
Marble 29 -

RLIA histograms for red silicone replicas of the marble surface, polished and abraded with glass beads and alumina. Pixel count corresponds to highest bar in the peak.

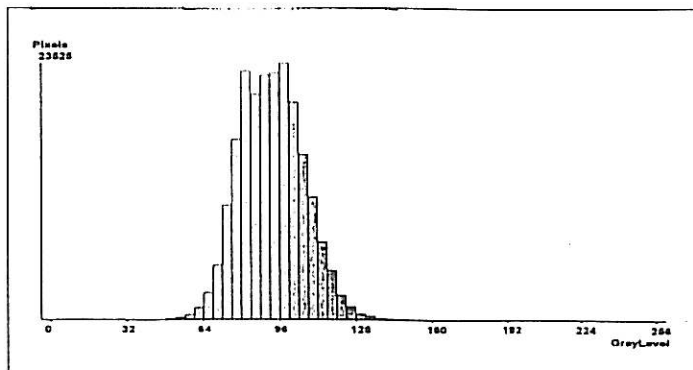
Polished surface (23671 pixels)



Abraded w/glass beads (20411 pixels)

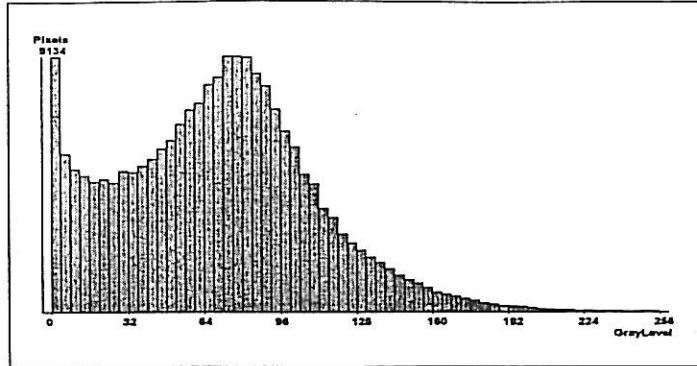


Abraded w/alumina (23525 pixels)

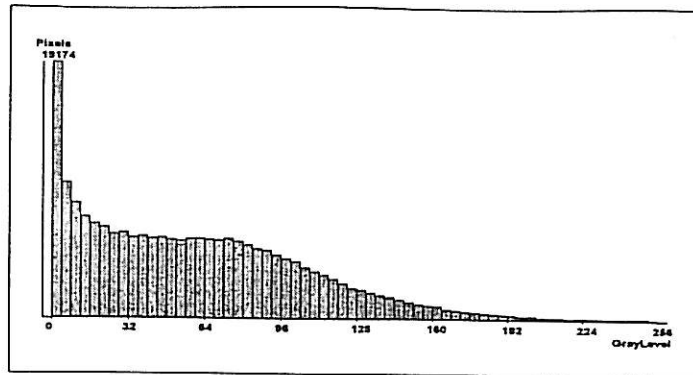


Limestone 33 - RLIA histograms for red silicone replicas of the limestone surface, sawn and abraded with glass beads and alumina. Pixel count corresponds to highest bar in the peak.

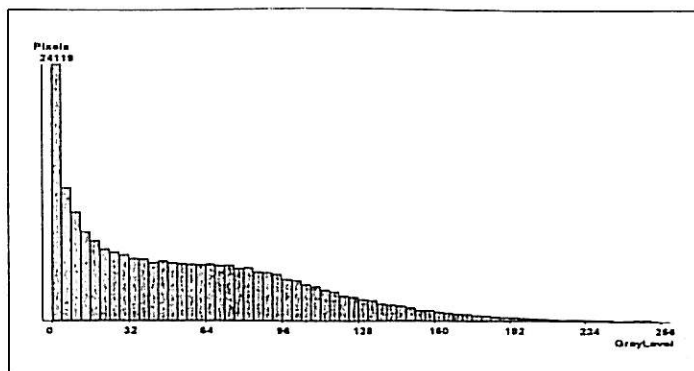
Sawn surface (9134 pixels)



Abraded w/glass beads (5973 pixels)



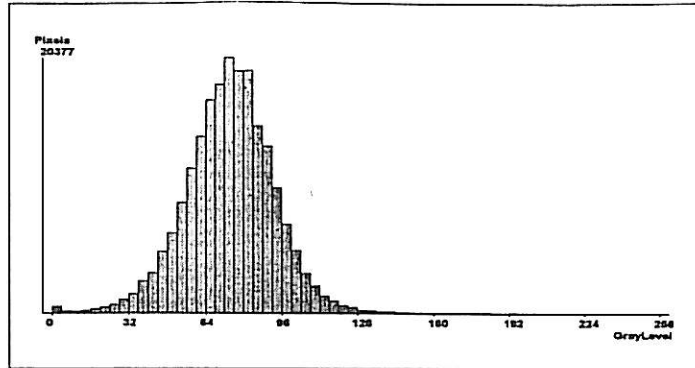
Abraded w/alumina (5332 pixels)



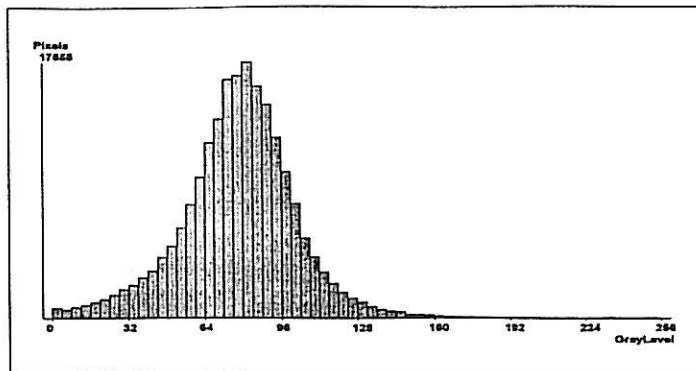
Brick Paver 31 -

RLIA histograms for red silicone replicas of the brick surface, before and after abrasion with glass beads and alumina. Pixel count corresponds to highest bar in the peak.

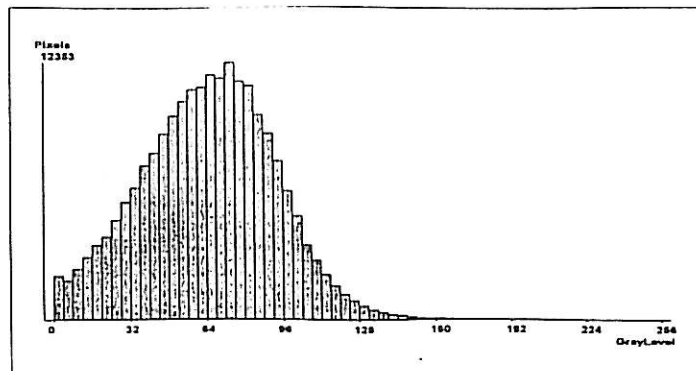
Control surface (20377 pixels)



Abraded w/glass beads (17658 pixels)



Abraded w/alumina (12353 pixels)



APPENDIX VII

MEASURING SURFACE ROUGHNESS: THREE TECHNIQUES

*Paper submitted to the 8th International Congress
on the Deterioration and Conservation of Stone
Berlin, September 30th to October 4th, 1996*

MEASURING SURFACE ROUGHNESS: THREE TECHNIQUES

A. Elena Charola*, Carol A. Grissom, Evin Erder**, Melvin J. Wachowiak, and Douglas Oursler***

Conservation Analytical Laboratory, Museum Support Center,
Smithsonian Institution, Washington, DC 20560, USA

* 8 Barstow Road #7B, Great Neck, NY 11021, USA

** c/o The Graduate Program in Historic Preservation, Graduate
School of Fine Arts, University of Pennsylvania, 115 Meyerson
Hall, Philadelphia, PA 19104, USA

*** Center for Nondestructive Evaluation, Johns Hopkins
University, 102 Maryland Hall, Baltimore, MD 21218, USA

SUMMARY

This preliminary study compared three techniques to determine their range of applicability for measurement of surface roughness of stone: stylus profilometry; laser triangulation profilometry; and reflected light image analysis, a technique new to stone conservation. Samples of three materials were measured, representing a range of finishes from high polish (marble) to medium roughness (brick paver) to rough (sawn limestone). To measure changes in roughness from cleaning, one third of each sample was blasted with glass beads and another third with aluminum oxide. Laser triangulation profilometry and reflected light image analysis required that replicas of the surface be made for accurate measurement. Red silicone rubber replicas gave the best results, allowing comparison of roughness between materials with differently colored surfaces. The paper analyzes data, compares the results of the different techniques, and discusses their limits of applicability.

1 INTRODUCTION

The present study stems from an earlier experiment in which changes in surface roughness after cleaning polished marble were successfully measured using reflectometry [1]. The question then arose as to what methods could effectively be used to measure cleaning changes on masonry materials having rougher surfaces, which cannot be measured with reflectometry. A secondary consideration was to find a method that could be used in the

field. A survey of the stone conservation literature found only one text that considered the accuracy and applicability of available methods, but focussed principally on physical measurement instruments like stylus profilometers and depth gauges [2]. Most articles described use of a single technique to measure damage during cleaning or artificial aging experiments.

For this preliminary study, three techniques were selected for comparison. Stylus profilometry, developed and widely used for measuring surface roughness of metals, has been most frequently used in measuring roughness of stone [3-5], but little information is given in the stone conservation literature beyond the name of the instrument used. Recently laser triangulation profilometry has been used for measuring damage to brick, even in the field [6]. Also referred to as laser profilography or laser surface profilometry, the technique has begun to be applied to measure minute changes resulting from cleaning of other artist's materials [7]. Reflected light image analysis is new to stone conservation, although image analysis has a long history of use for measuring texture [8]. It had been hoped that a line profilometer in conjunction with a stereomicroscope [9,10] could be used for our experiments but the equipment and software were not commercially available.

2 EXPERIMENTAL

Stylus profilometry, laser triangulation profilometry, and reflected light image analysis were used to measure roughness of polished marble, sawn limestone, and a brick paver. Each sample was divided into three sections: one served as a control, the second was blasted with glass beads, and the third, with alumina powder. Silicone rubber replicas were also made of all the samples.

2.1 Sample Materials

The Carrara marble sample (15cm x 15cm square, approximately 1cm thick) was cut from a commercial tile. The Indiana limestone sample was a 5cm thick prism with a 6cm x 23cm top sawn surface. The red brick paver was approximately 20cm x 10cm x 5cm. Both the narrow and wide (bedding) faces of the brick were blasted, but because the wide face had deep pits, measurements were made on the narrow face.

2.2 Sample Preparation

The blasting of the samples was carried out in the laboratory using a pencil micro-abrader (S.S. White Airbrasive Unit Model-K). The glass beads were S.S. White abrasive powder #9 (44 μ m in average diameter), and the alumina powder was S.S. White abrasive powder #3 (50 μ m in average diameter). Unblasted areas were

protected with plastic tape during blasting. The tip of the nozzle ($\phi = 0.018$ ") was held about 3/4" from the surface, with a flow rate of the abrasive powder approximately 10g/min at 60psi. The blasting was carried out by scanning first in horizontal and then vertical rows using a circular motion, attempting to achieve an even-looking surface. Blasting the polished marble with glass beads required extra passes to produce this surface.

2.3 Replica Preparation

Silicone rubber replicas of the masonry materials were made for laser triangulation profilometry and reflected light image analysis because color variations of the masonry would bias results for those techniques. Initial measurements on white silicone rubber replicas showed the white color to be too reflective for good results. Red silicone rubber replicas were subsequently prepared and used successfully.

Surfaces to be replicated were first brush-coated with a 5% w/v solution of Acryloid B-72 (Röhm & Haas) in acetone to avoid adherence of the silicone rubber to the stone, as well as staining. The replicas were made with Dow Corning silicone rubber (3110 RTV for the white and 3120 RTV for the red) with standard cure catalyst #1 in a 10:1 w/w ratio. The silicone rubber was poured onto the stone surface, which had been framed with a plasticine "dam" to hold the liquid, and a vacuum was drawn on the silicone rubber. The vacuum was drawn approximately ten times. The silicone rubber cured for 24 hours and was removed from the surface of the stone. Small amounts of silicone rubber could be seen afterwards at low magnification in the interstices of the limestone, but replication of all the surfaces was generally excellent.

The replica of the marble tile even reproduced brushstrokes of the Acryloid B-72, particularly for the polished control. Hence the surface was cleaned with toluene to remove the acrylic coating, and a second replica was made. Subsequent experimentation showed that a more dilute solution (2%), which would reduce the possibility of brush strokes, effectively prevented staining. If staining were not an issue, successful replication of a number of uncoated stone materials later showed coating to be unnecessary for release in most cases; however, silicone rubber did adhere tenaciously to sandstone.

The set-up for reflected light image analysis required replicas of uniform thickness. These proved difficult to realize for the relatively viscous 3120 silicone rubber using the standard dilution. Better levelling was achieved by using a 20:1 w/w ratio, but differences in thickness could still be measured. These were finally eliminated by applying silicone rubber caulk to the reverses of the replicas and placing them between heavy Plexiglas sheets clamped together with 3/16" spacers in between.

Experiments were also made with a methylmethacrylate reproduction material (Facsimile made by Flexbar), recommended by metrologists for field replication of materials to be measured with a laboratory stylus profilometer. However, replication of the masonry surfaces appeared poor compared to the silicone rubber. Moreover, variable coloration of the replica, visible at low magnification, precluded use of the material for laser triangulation profilometry and reflected light image analysis. Producing a hard positive cast of the silicone rubber replica remains a possibility.

3 RESULTS

3.1 Stylus profilometry

The samples were measured with a relatively inexpensive field model Surtronic 3+ profilometer (Rank Taylor Hobson Ltd). It has a diamond stylus with a $5\mu\text{m}$ tip radius and a 6mm radius red ruby skid. The maximum traverse length is 25mm, and the maximum gauge (vertical) range is $500\mu\text{m}$. The resolution is $1\mu\text{m}$ for horizontal measurements and 10nm for vertical. The instrument is calibrated against a standard by the operator. It is computer operated, and data were analyzed through the ST3PLUS program.

Roughness average (R_a) is the primary statistical parameter of several used by metrologists to describe surface texture. It is defined as the arithmetic average of the absolute values of the profile height deviations recorded within the evaluation length and measured from the mean line:

$$R_a = (1/L) \int_0^L |y(x)| dx$$

where $y(x)$ is the surface profile, sampled by a set of N points y_i over the length L .

The R_a may change significantly depending on the cut-off or sampling length (L_c). The upper limit for L_c on the Surtronic 3+ is 2.5mm. However, the software can recalculate the R_a using an L_c of 8mm. This longer sampling length is recommended for surfaces with an R_a over $10\mu\text{m}$ [11,12].

Table I shows average roughnesses obtained at the 2.5mm sampling length and recalculated for an 8mm sampling length. Data were averaged from at least five measurements but in most instances 10 or 15 were used. The apparatus was unable to "read" the rougher surfaces; in these cases, the average presented in the table is artificially low. Furthermore, even when the machine gave a roughness measurement, it is likely that the tip "skidded" over the surface without measuring deeper pits.

3.2 Laser triangulation profilometry (LTP)

A custom-made laser triangulation profilometer was used to measure the surface profile of the samples as well as both white and red silicone rubber replicas. This consisted of an Aromat laser distance sensor (LM200 RAC) mounted on an X-Y translation stage. A computer with an analog to digital board was used to digitize the laser distance sensor's signal, control the stage positioning, and process the surface profile.

The laser distance sensor projects a beam of light perpendicularly to the specimen surface. Its light source is a low power (<1.9mW) laser diode (red, 670nm). The sensor triangulates the surface position by imaging the laser spot with an adjacent lens to a position sensitive detector. The device calibration is tested by translating it towards a stationary surface using a precision stage.

The results are expressed in R_a (μm), averaged for three areas on each sample (Table II). Each area (1 cm^2) was scanned in ten lines which contained 5 blocks of 40 reading points each, thus totalling 2000 reading points per cm^2 . Each point is equivalent to $50\mu\text{m}^2$. The reproducibility of each area was excellent. Since the standard deviations calculated for the average roughness of each area overlapped, results were subjected to an analysis of variance which confirmed that real differences existed between the means of each area.

Even a cursory examination of the data shows some wide variations in results between the masonry surfaces and their replicas. In the case of marble, artificially high measurements can be attributed to the relative transparency of the stone. Light returning to the displacement sensor from below the surface of the marble exaggerated the signal. The LTP signal accuracy is also adversely affected when measuring highly reflective surfaces, such as polished marble. Mirror-like surfaces scatter very little light in directions other than the direct reflection; therefore, a small amount of light is collected by the sensor's lens, resulting in a noisier signal. In the case of the limestone, measurements would have been affected by the occasional presence of quartz grains and traces of iron oxides. By contrast, similar results for the red replica of the brick and the brick surface reflect the fact that they are similar in color and confirm that the silicone rubber reproduces the brick surface accurately.

Comparison of measurements for the white and red silicone rubber replicas of the same surface shows that the white replicas "appear" smoother. This erroneous result is because the area around the laser spot on the white silicone rubber tended to glow (the laser spot "bloomed"). The sensor's effective footprint was resultantly much larger and therefore averaged or smoothed the

surface features. The red silicone rubber demonstrated none of this effect.

3.3 Reflected light image analysis (RLIA)

Reflected light image analysis reduces three-dimensional information to two-dimensional representation, measuring texture indirectly. It was carried out on the white and red silicone rubber replicas with a video microscope, assembled with a 55 mm Micro-Nikkor lens (set at f4) and a single 1/2" RGB chip camera (World Video Automaticam). These were mounted on a fixed stand with its optical axis perpendicular to the sample surface. The light source was a Fostec fiber optic 21V 150 W tungsten halogen EJA lamp, controlled by rheostat (set at 60%) and with the iris diaphragm open, distributed through two 2" fiber optic line generators. These were set at a fixed angle (24°), illuminating the sample with even raking light. Shutter speed was 1/1000 sec. The image analysis workstation was a Leica Quantimet 500.

An area of 5.43cm² was captured in monochrome in a frame of 538 x 394 pixels (211,972 total); each pixel corresponded to 2500μm². The distribution of pixels on a grey scale which ranged from 0 (black) to 256 (white) was presented in a histogram. The value of the highest bar was indicated on the pixel (y) axis. At least three different areas were randomly selected and measured on each sample. The values for the three areas measured on each sample were similar.

Reproducibility of results proved to be predicated on a fixed set-up and the use of replicas of the same substance and uniform thickness. When the lighting conditions, color of the sample, its reflectivity, or degree of tilt from the optical axis was changed, the shape and position of the peak in the histogram changed. Figure 1 shows the difference in the peak's shape and position between a white and red silicone rubber replica of the same surface (note that the y axes of all the histograms are on different scales, indicated by the number of pixels for the highest bar). Figure 2 shows differences for the same red replica examined at two different light intensities. Figure 3 shows the effect that changes in tilt can introduce, representing measurements made on a slightly wedge-shaped replica that was rotated.

The shape and position of peaks in the histograms provide qualitative measures of surface texture, although uncertainties remain regarding interpretation. For the polished marble surface, the peak of the histogram appears as a high block of reflected light (Figure 4a). As the surface roughens, the block becomes a relatively symmetrical bell-shaped peak (Figure 4b,c). With increasing roughness, the peak broadens while losing height, illustrated by the brick sample (Figure 5). On the limestone, a spike is present at the dark end of the grey scale, which can be

attributed to deep shadows cast by its rough surface; this spike increases and the central peak flattens after blasting (Figure 6).

The intention was to find a single parameter for surface texture with which comparisons could be made between samples. The number of pixels of the highest bar in the peak towards the center of the histogram, averaged from at least three different areas on each sample, can be inversely correlated with roughness, giving a quantitative measure (Table III). However, this measure does not encompass all the information provided by RLIA, and several parameters may be necessary for good characterization. More experimental work is required.

4 DISCUSSION

In reviewing results for the different techniques, distinctions can be made between control and blasted areas, which were clearly rougher for all samples. By contrast, little difference was apparent between surfaces of the same samples blasted with glass beads and with alumina.

Average roughnesses obtained with the stylus profilometer and LTP can be compared in Table IV. Polished surfaces, exemplified by the polished marble sample, are better characterized by the stylus profilometer, given the difficulties described above for LTP. These are reflected in an order of magnitude difference in the values. However, from a practical standpoint, one rarely finds outdoor stonework which requires cleaning and has any degree of polish, with the possible exception of granite.

The stylus profilometer produced less satisfactory results for rougher surfaces, such as those of blasted limestone. It requires a longer cut-off length to approach values obtained with LTP, and a longer gauge length is required to measure deep pits. Only an expensive laboratory model profilometer could measure these types of surfaces, and field measurement would then require use of hard replicas or removal of a core. Finally, stylus profilometers were developed for measuring the roughness of metals, which are not porous, i.e., not having deep holes. Therefore, computation of the average roughness parameter (Ra) may not adequately characterize the surface roughness of masonry materials. Other parameters such as skewness, a measure of the asymmetry of the profile about the mean line, may be necessary for making this relevant to stone.

LTP appeared to be more reliable than the stylus profilometer for rougher surfaces. Although data have a wide spread, the average is taken from far more points. LTP, through appropriate image analysis systems, can also produce line profiles and three-dimensional representations of the surface.

RLIA is a promising technique, particularly because it can rapidly measure large surface areas, but the full potential and limits of applicability have yet to be determined. Results cannot be compared directly with the two other methods in the absence of an Ra for the RLIA, although an Ra might be calculated from a line profile that the computer software can produce. Calibration of the system would be required, which would contribute as well to comparison between laboratories. RLIA can also produce an image of the surface, and the image analysis system can easily process data, e.g., subtracting a control from a blasted sample.

The purpose of this study was to compare measurement techniques, not to compare damage from different cleaning techniques. Nevertheless, preliminary evidence suggests that roughness measurements are not sufficient to evaluate damage induced through cleaning. Similar roughnesses, as those produced by blasting with glass beads and alumina, do not necessarily reflect equal damage done to the surface at a microscopic level. Nor do roughness measurements indicate the amount of material removed.

5 CONCLUSION

In this preliminary study none of the three techniques was found to be entirely satisfactory for measuring roughness of the three masonry materials. In nearly all cases the techniques require use of replicas or destructive sampling if field measurement is desired. All require expensive instrumentation and skilled operators for good results. However, the newest technique for measurement of stone, reflected light image analysis, shows promise and will be explored further.

6 ACKNOWLEDGMENTS

This paper summarizes results for the first phase of a research project carried out at the Conservation Analytical Laboratory (CAL) of the Smithsonian Institution through a Cooperative Agreement (1443CA000194036) with the National Park Service. The authors wish to acknowledge E. Blaine Cliver, Anne Grimmer, and Judy Jacobs of the National Park Service for their stimulation and support of the research.

7 REFERENCES

1. LAUFFENBURGER, J.A., GRISSOM, C.A. and CHAROLA, A.E. - Changes in Gloss of Marble Surfaces as a Result of Methylcellulose Poulticing. *Studies in Conservation*, Vol. 37, 1992, 155-164
2. LIVINGSTON, R.A. and BAER, N.S. - The Accuracy of Stone

- Weathering Rates Measured on Historic Structures. Wiener Berichte über Naturwissenschaft in der Kunst, 2/3, 1985/1986, 272-298
3. GRIMM, W-D. - Rauigkeitsmessungen zur Kennzeichnung des Verwitterungsfortschrittes an Naturwerkstein-Oberflächen. International Colloquium on Materials Science and Restoration, Esslingen, F.H. Wittmann, Ed., 1983, pp. 321-324
 4. YOUNG, M. and URQUHART, D. - Abrasive Cleaning of Sandstone Buildings and Monuments: An Experimental Investigation. Stone Cleaning and the Nature, Soiling and Decay Mechanisms of Stone, Donhead, Wimbledon, 1992, pp. 128-140
 5. Stone Cleaning in Scotland. Research Summary, Historic Scotland, Edinburgh, 1992, pp. 47-56
 6. BERRA, M., FATTICCIONI, A., BINDA, L., and SQUARCINA, T. - Laboratory and In-situ Measurement Procedure of the Decay of Masonry Surfaces. Durability of Building Materials and Components 6, S. Nagataki et al., Eds., E & FN Spon, London, 1993, pp. 834-843
 7. FAIRBRASS, S. and WILLIAMS, DARYL R. A New Surface Imaging Technique in Conservation. From Marble to Chocolate, J. Heuman, Ed., Archetype, London, 1995, pp. 82-86
 8. RUSS, J.C. - The Image Analysis Handbook. CRC Press, Boca Raton, Florida, 1994
 9. AIRES-BARROS, L., MAURICIO, A., and FIGUEIREDO, C. - Profilometry and Image Analysis Applications to "In Situ" Study of Monuments Stone Decay Phenomena. III International Symposium on the Conservation of Monuments in the Mediterranean Basin, V. Fassina et al., Eds., Venice, 1994, pp. 19-24
 10. AIRES-BARROS, L., MAURICIO, A.M., and FIGUEIREDO, C. - Line Profilometer and Surface Weathering Characterization of Carbonate Ornamental Rocks, Proceedings of the 4th Portuguese Conference on Pattern Recognition, Coimbra, Portugal, 1992, pp. 373-384
 11. VORBURGER, T. - Surface Texture (Surface Roughness, Waviness, and Lay), New York, The American Society of Mechanical Engineers, 1995, ASME B46.1, Section 3.20.2
 12. SONG, J.F. and VORBURGER, T.V. - Surface Texture, Metals Handbook, Vol 18: Friction, Lubrication, and Wear Technology, ASM International, Materials Park, Ohio, 1992, pp. 334-345.

Table I. Average roughness measured with a stylus profilometer at an evaluation length of 25mm and cut-off length of 2.5mm, also given as recalculated at a cut-off length of 8mm. Standard deviations are given in parentheses.

Sample	Roughness Ra (μm)	
	@ Lc 2.5mm	@ Lc 8mm
Marble/polished	0.74 (± 0.38)	0.85 (± 0.43)
Marble/glass beads	7.01 (± 0.62)	7.85 (± 0.78)
Marble/alumina	5.45 (± 0.94)	7.8 (± 1.5)
Limestone/sawn	30.4 (± 3.7)	36.3 (± 4.5)
Limestone/glass beads	38.6 (± 2.2)*	46.0 (± 3.1)
Limestone/alumina	38.1 (± 2.9)*	46.8 (± 4.0)
Brick	12.1 (± 1.3)	21.8 (± 1.4)
Brick/glass beads	16.4 (± 1.8)	26.6 (± 7.3)
Brick/alumina	17.9 (± 4.7)	26.5 (± 7.4)

* Instrument failed to read some points because of roughness.

Table II Average roughness measured with LTP on masonry surfaces, white and red silicone rubber replicas. Standard deviations are given in parentheses.

Sample	Roughness Ra (μm)		
	Masonry	White replica	Red replica
Marble/polished	50 (± 11)	2.5 (± 0.5)	5.5 (± 1.0)
Marble/glass beads	42 (± 10)	5.1 (± 1.4)	7.1 (± 1.5)
Marble/alumina	35 (± 8)	3.5 (± 0.8)	6.2 (± 1.2)
Limestone/sawn	18 (± 9)	13 (± 5)	24 (± 13)
Limestone/gl. beads	26 (± 11)	20 (± 10)	44 (± 20)
Limestone/alumina	30 (± 12)	21 (± 8)	50 (± 24)
Brick	9 (± 3)	7 (± 3)	9 (± 3)
Brick/glass beads	11 (± 5)	8 (± 4)	12 (± 7)
Brick/alumina	12 (± 6)	9 (± 3)	12 (± 4)

Table III Total pixels for the highest bar towards the center of the histogram, measured by RLIA on the red silicone rubber replicas. Standard deviations are given in parentheses.

Sample	total pixels (in thousands)	
Marble/polished	25	(±1)
Marble/glass beads	21	(±10)
Marble/alumina	23	(±8)
Limestone/sawn	8.7	(±0.4)
Limestone/glass beads	6.0	(±0.2)*
Limestone/alumina	5.3	(±0.2)*
Brick	20	(±1)
Brick/glass beads	18	(±7)
Brick/alumina	13	(±11)

* Indicates a spike at the black end of the histogram.

Table IV Average roughness measured with the stylus profilometer and LTP on red silicone rubber replicas of the same surfaces. Standard deviations are given in parentheses.

Sample	Roughness Ra [μm]		LTP
	Stylus @ Lc 2.5mm	Stylus @ Lc 8mm	
Marble/polished	0.74 (±0.38)	0.85 (±0.43)	5.5 (±1.1)
Marble/glass beads	7.01 (±0.62)	7.85 (±0.78)	7.1 (±1.5)
Marble/alumina	5.45 (±0.94)	7.8 (±1.5)	6.2 (±1.2)
Limestone/sawn	30.4 (±3.7)	36.3 (±4.5)	24 (±13)
Limestone/glass beads	38.6 (±2.2)*	46.0 (±3.1)	44 (±20)
Limestone/alumina	38.1 (±2.9)*	46.8 (±4.0)	50 (±24)
Brick	12.1 (±1.3)	21.8 (±1.4)	9 (±3)
Brick/glass beads	16.4 (±1.8)	26.6 (±7.3)	12 (±7)
Brick/alumina	17.9 (±4.7)	26.5 (±7.4)	12 (±4)

* Instrument failed to read some points because of roughness.

Figure 1. RLIA histograms for replicas of a marble surface blasted with glass beads, made of (a) white silicone rubber and (b) red silicone rubber. Note that the y axes are not on the same scale.

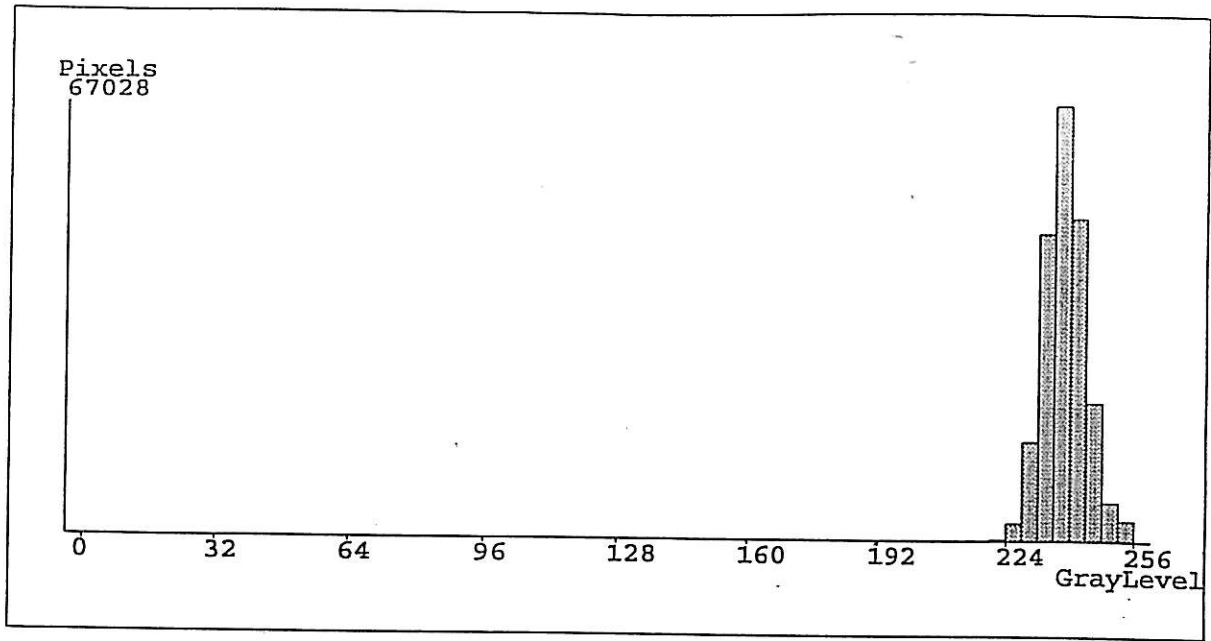
Figure 2. RLIA histograms for red silicone rubber replicas of a polished marble surface measured at different light intensities: (a) higher and (b) lower. Note that the y axes are not on the same scale.

Figure 3. RLIA histograms for red silicone rubber replicas of limestone blasted with alumina powder measured at slightly different tilts. Note that the y axes are not on the same scale.

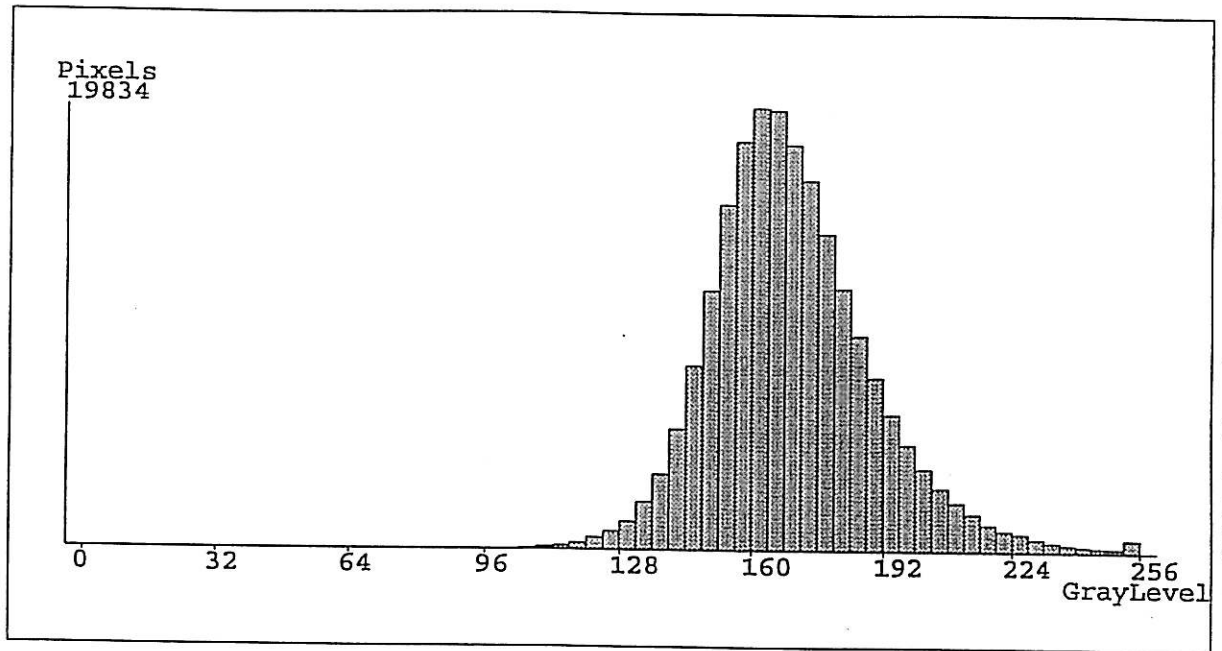
Figure 4. RLIA histograms for red silicone rubber replicas of polished marble: (a) control, (b) glass bead-blasted area, and (c) alumina powder-blasted area. Note that the y axes are not on the same scale.

Figure 5. RLIA histograms for red silicone rubber replicas of a brick paver: (a) control, (b) glass bead-blasted area, and (c) alumina powder-blasted area. Note that the y axes are not on the same scale.

Figure 6. RLIA histograms for red silicone rubber replicas of sawn limestone: (a) control, (b) glass bead-blasted area, and (c) alumina powder-blasted area. Note that the y axes are not on the same scale.

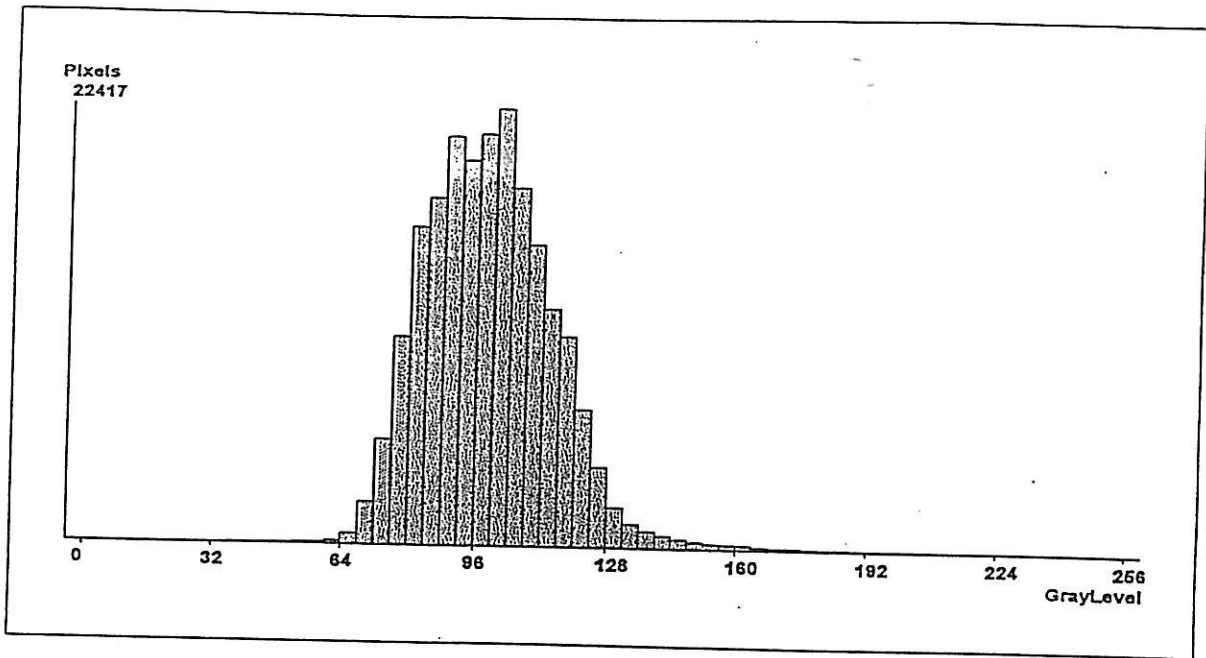


(a)

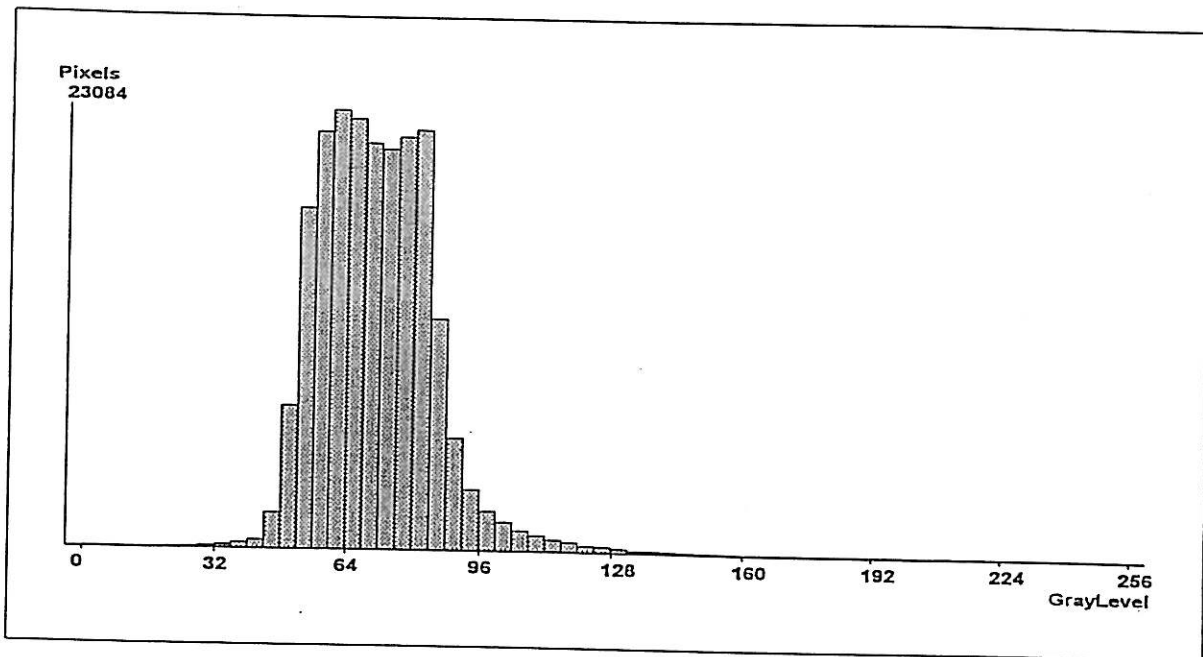


(b)

Figure 1. RLIA histograms for replicas of a marble surface blasted with glass beads, made of (a) white silicone rubber and (b) red silicone rubber

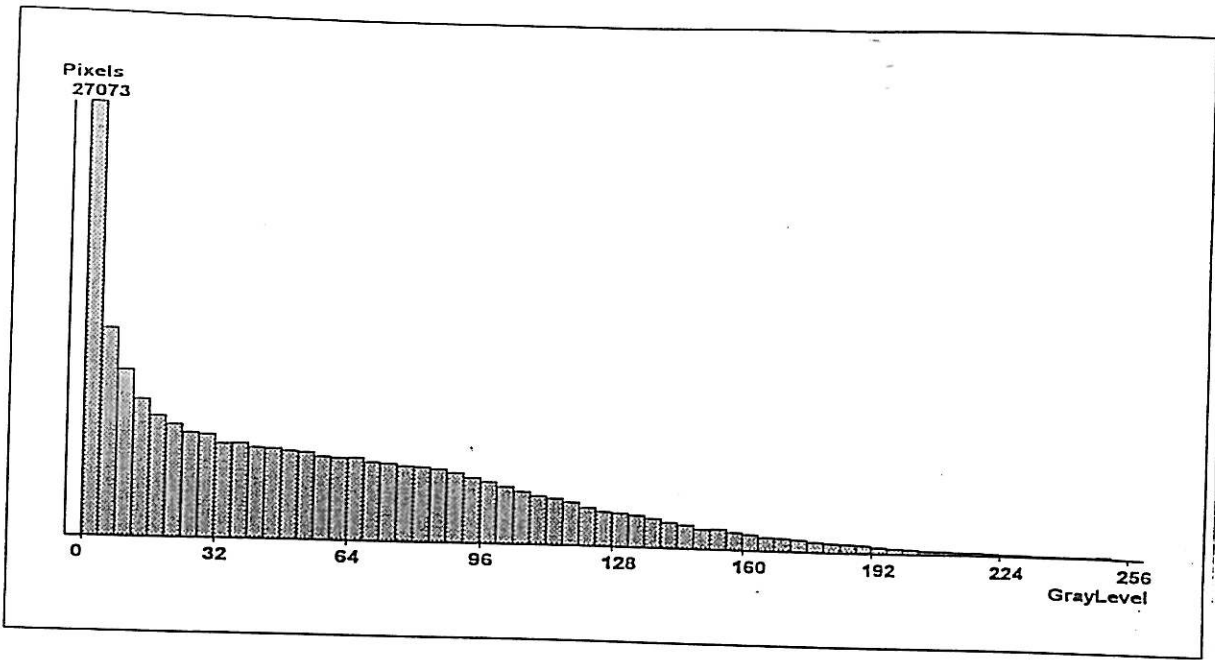


(a)

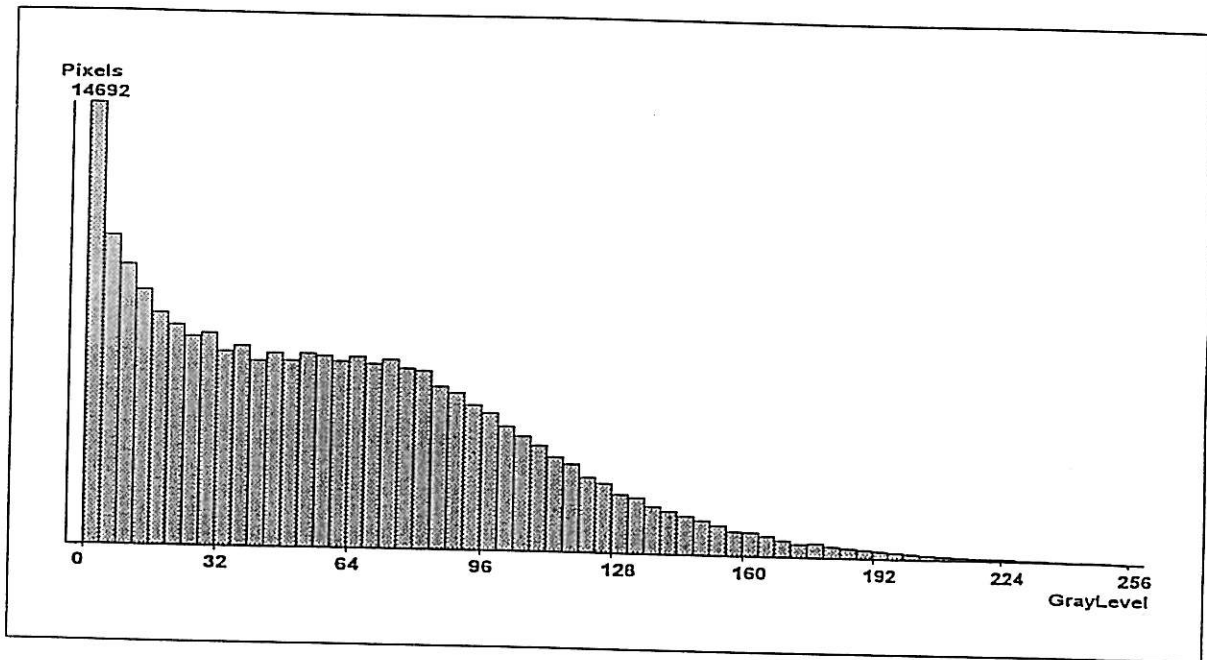


(b)

Figure 2. RLIA histograms for red silicone rubber replicas of a polished marble surface measured at different light intensities: (a) higher and (b) lower

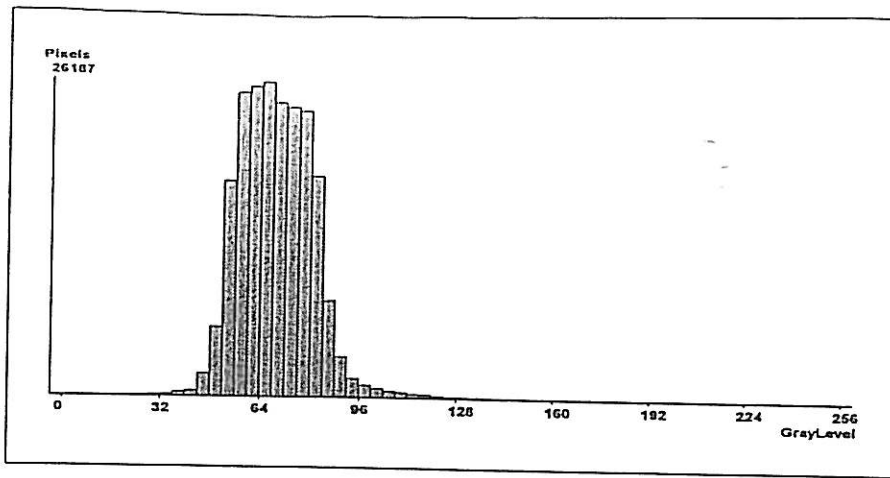


(a)

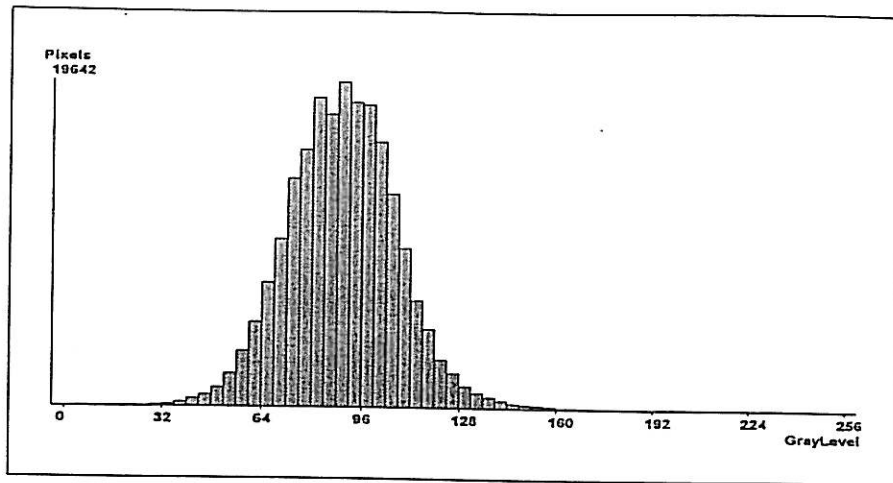


(b)

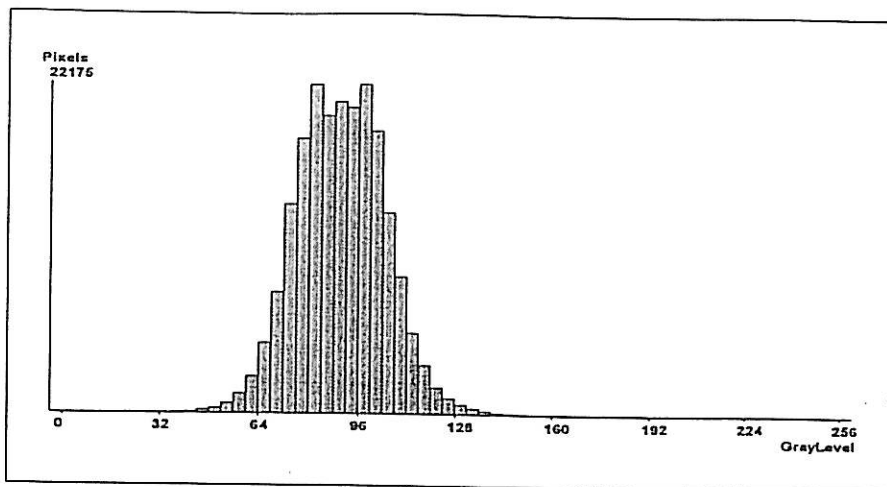
Figure 3. RLIA histograms for red silicone rubber replicas of limestone blasted with alumina powder measured at slightly different tilts



(a)

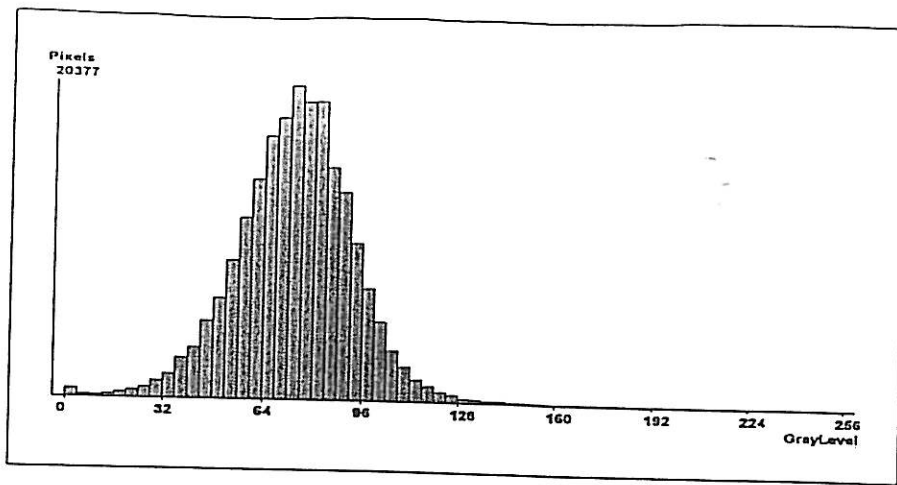


(b)

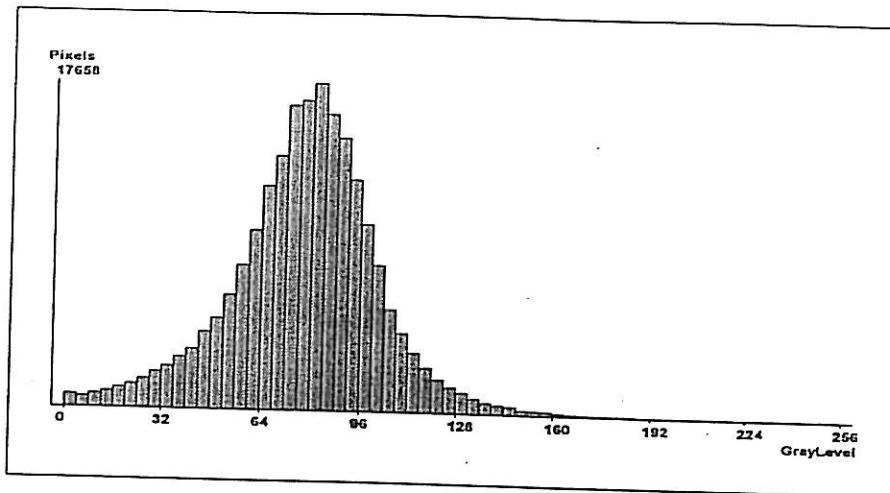


(c)

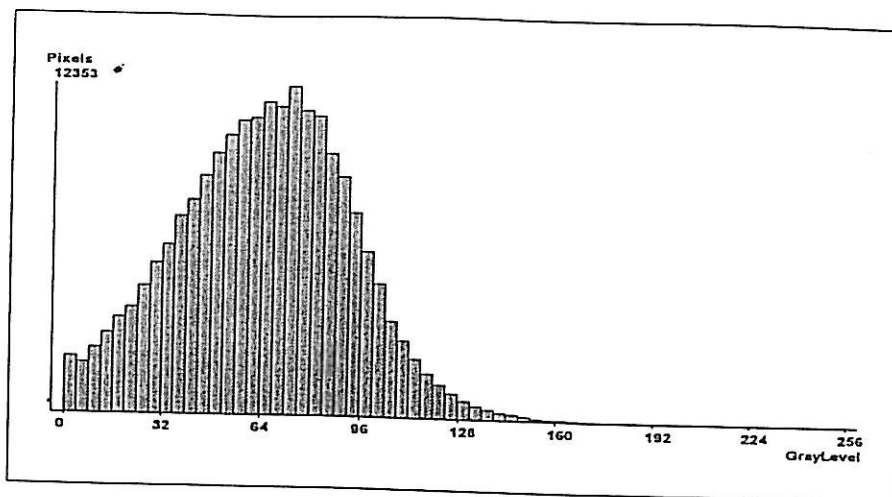
Figure 4. RLIA histograms for red silicone rubber replicas of polished marble: (a) control, (b) glass bead-blasted area, and (c) alumina powder-blasted area



(a)

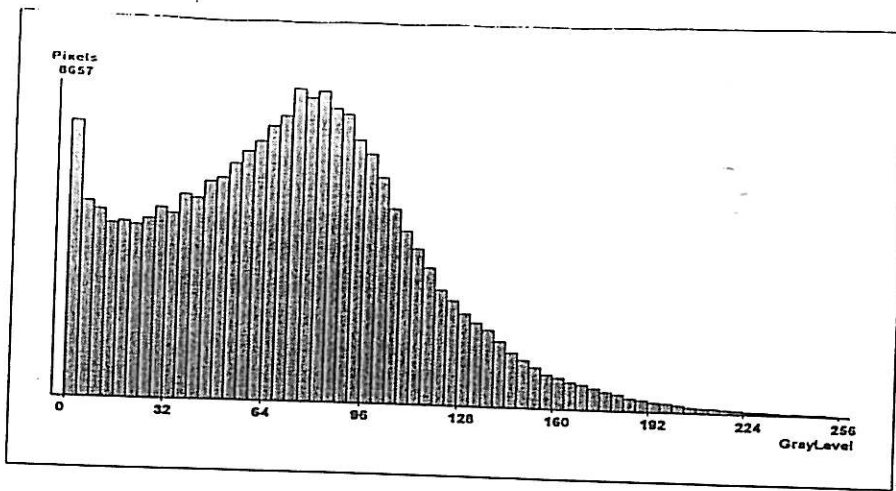


(b)

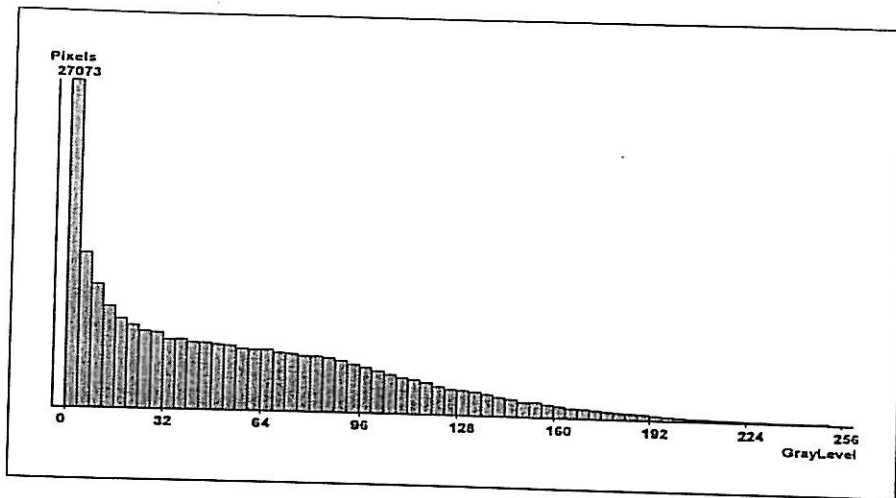


(c)

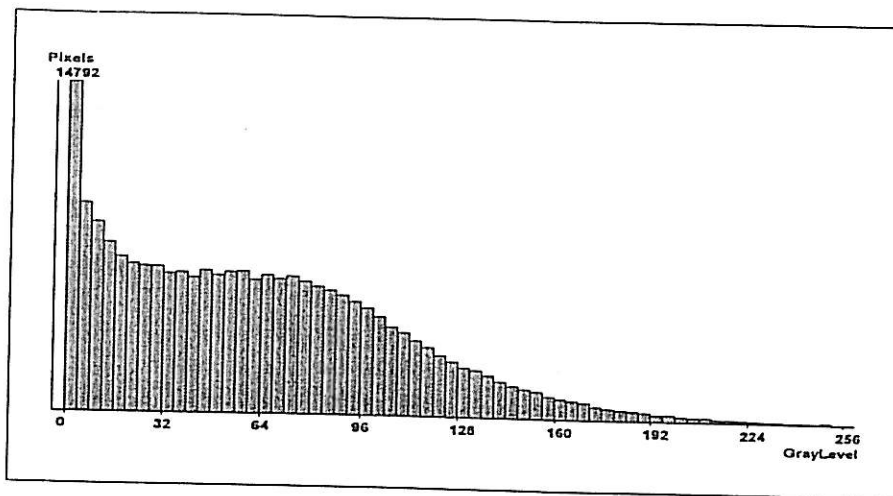
Figure 5. RLIA histograms for red silicone rubber replicas of a brick paver: (a) control, (b) glass bead-blasted area, and (c) alumina powder-blasted area



(a)



(b)



(c)

Figure 6. RLIA histograms for red silicone rubber replicas of
sawn limestone: (a) control, (b) glass bead-blasted area,
and (c) alumina powder-blasted area

APPENDIX VIII
GLOSS MEASUREMENTS - PHASE II

Appendix VIII

Average gloss values obtained from different runs—at least five individual measurements—taken on polished surfaces: polished marble, polished granite and glazed tile, and on some of the blasted surfaces. Measurements were taken with a Lange Labor-Reflektometer at 20°.

Data for Polished Marble tiles

Control areas		Abraded areas	
PM - 2.3 - C	71.0 ± 0.9 61.5 ± 3.3 66.3 ± 2.4	PM - 2.3 - WI	59.4 ± 1.5 60.6 ± 1.3 60.0 ± 1.4
PM - 2.4 - C	72.4 ± 2.1 71.5 ± 3.2 71.95 ± 2.7	PM - 2.4 - WII	58.1 ± 1.6 69.6 ± 2.3 63.8 ± 2.0
PM - 1.1 - C	70.2 ± 2.4 61.1 ± 4.5 65.65 ± 3.6	PM - 1.1 - NI	58.6 ± 1.4
PM - 1.2 - C	69.1 ± 4.6 71.9 ± 4.6 75.2 ± 5.2 72.1 ± 3.8	PM - 1.2 - NII	79.7 ± 1.3
PM - 1.3 - C	62.8 ± 2.9 58.3 ± 4.5 60.6 ± 3.8	PM - 1.3 - GI	68.7 ± 0.8
PM - 1.4 - C	76.6 ± 2.0 69.3 ± 2.7 72.9 ± 2.4	PM - 1.4 - GII	6.2 ± 3.4
PM - 2.1 - C	60.4 ± 3.5 62.4 ± 3.0 61.4 ± 3.4	PM - 2.1 - BI	1.4 ± 0.0
PM - 2.2 - C	70.3 ± 1.2 68.7 ± 4.7 64.1 ± 4.1	PM - 2.2 - BII	1.5 ± 0.0
PM - 3.1	57.8 ± 4.8		
PM - 3.2	70.4 ± 3.3 67.4 ± 3.55		
Control mean	67.3 ± 3.5		

Data for Polished Granite tiles
Control areas

PG - 7 - C	72.7 ± 1.1 72.7 ± 7.6 71.7 ± 8.1
PG - 8 - C	69.9 ± 4.5 74.6 ± 3.4
PG - 1 - C	72.4 ± 6.2 89.6 ± 6.6 75.1 ± 3.0
PG - 2 - C	69.8 ± 1.5 72.5 ± 3.9
PG - 3 - C	77.4 ± 3.3 74.2 ± 4.5
PG - 4 - C	75.0 ± 3.3 76.3 ± 4.0
PG - 5 - C	70.3 ± 4.1 74.5 ± 2.3
PG - 6 - C	72.0 ± 5.6 71.5 ± 6.3 72.5 ± 5.6
PG - 9	72.2 ± 3.3
PG - 10	72.9 ± 3.0
Control mean	73.8 ± 4.7

Abraded areas

PG - 7 - WI	69.4 ± 2.5
PG - 8 - WII	68.8 ± 3.3
PG - 1 - NI	68.3 ± 5.8
PG - 2 - NII	70.8 ± 3.5
PG - 3 - GI	68.4 ± 6.8
PG - 4 - GII	70.1 ± 2.2
PG - 5 - BI	1.3 ± 0.4
PG - 6 - BII	15.4 ± 4.0

Data for Glazed Tiles

Control areas

GT - 7 - C	80.7 ± 1.4
GT - 8 - C	82.4 ± 1.2
GT - 1 - C	75.8 ± 4.8
GT - 2 - C	78.9 ± 0.8
GT - 3 - C	83.2 ± 0.5
GT - 4 - C	83.3 ± 1.5
GT - 5 - C	83.3 ± 1.3
GT - 6 - C	82.5 ± 0.5
Control mean	81.3 ± 2.0

Abraded areas

GT - 7 - WI	78.5 ± 1.4
GT - 8 - WII	78.3 ± 2.2
GT - 1 - NI	66.0 ± 4.1
GT - 2 - NII	78.2 ± 2.0
GT - 3 - GI	83.6 ± 0.5
GT - 4 - GII	75.4 ± 0.8
GT - 5 - BI	3.8 ± 0.4
GT - 6 - BII	29.1 ± 0.6

APPENDIX IX

STYLUS PROFILOMETRY - PHASE II

Appendix IX

Roughness averages, of at least five individual measurements, carried out with the Surtronic 3+ [Rank Taylor Hobson] instrument. The evaluation length [Ln] was of 4.00 mm, the sampling or cut-off length [Lc] was 0.80 mm and the gauge range 100 μm . The results are given in average roughness Ra [μm].

The surface of the flame finished granite was too rough to obtain any measurements.

Representative profiles for each material and finish are presented at the end of this Appendix. Note that all profiles are represented on the same scale (Vv x 1000, Vh x 20) except for the sawn limestone samples which had to be represented at half the scale (Vv x 500, Vh x 20), and the glazed tile for which the scale is five times larger (Vv x 5000, Vh x 20) since this material was very resistant to damage.

Polished Granite

Control areas		Abraded areas	
PG-7-C	0.11 \pm 0.06	PG-7-WI	0.32 \pm 0.4
PG-8-C	0.3 \pm 0.3	PG-8-WII	0.15 \pm 0.06
PG-1-C	0.13 \pm 0.02	PG-1-NI	0.11 \pm 0.09
PG-2-C	0.4 \pm 0.3	PG-2-NII	0.2 \pm 0.2
PG-3-C	0.12 \pm 0.02	PG-3-GI	0.6 \pm 0.8
PG-4-C	0.22 \pm 0.26	PG-4-GII	0.31 \pm 0.3
PG-5-C	0.11 \pm 0.03	PG-5-BI	8.66 \pm 3.1
PG-6-C	0.4 \pm 0.3	PG-6-BII	2.0 \pm 0.8
Control Mean	0.22 \pm 0.21		

Polished Marble

Control areas		Abraded areas	
PM-2.3-C	0.18 ± 0.08	PM-2.3-WI	0.23 ± 0.2
PM-2.4-C	0.36 ± 0.10	PM-2.4-WII	0.18 ± 0.08
PM-1.1-C	0.14 ± 0.02	PM-1.1-NI	0.24 ± 0.08
PM-1.2-C	0.13 ± 0.03	PM-1.2-NII	0.21 ± 0.2
PM-1.3-C	0.32 ± 0.3	PM-1.3-GI	0.36 ± 0.2
PM-1.4-C	0.29 ± 0.3	PM-1.4-GII	6.44 ± 1.2
PM-2.1-C	0.15 ± 0.06	PM-2.1-BI	11.7 ± 0.9
PM-2.2-C	0.15 ± 0.09	PM-2.2-BII	9.98 ± 0.9
Control Mean	0.22 ± 0.16		

Sawn Marble

Control areas		Abraded areas	
SM-4.3-C	4.5 ± 0.4	SM-4.3-WI	4.9 ± 0.4
SM-4.4-C	4.1 ± 0.3	SM-4.4-WII	4.8 ± 0.9
SM-3.1-C	9.5 ± 1.3	SM-3.1-NI	6.5 ± 1.2
SM-3.2-C	5.7 ± 0.5	SM-3.2-NII	5.7 ± 0.7
SM-3.3-C	7.9 ± 0.8	SM-3.3-GI	6.5 ± 1.1
SM-3.4-C	5.5 ± 0.7	SM-3.4-GII	9.9 ± 1.1
SM-4.1-C	7.5 ± 0.7	SM-4.1-BI	13.3 ± 2.6
SM-4.2-C	6.4 ± 1.2	SM-4.2-BII	10.9 ± 1.7
Control Mean	5.9 ± 0.8		

Sawn Limestone

Control areas		Abraded areas	
SL-7-C	15.0 ± 3.7	SL-7-WI	20.5 ± 3.7
SL-8-C	14.0 ± 7.1	SL-8-WII	13.3 ± 1.9
SL-1-C	11.3 ± 0.6	SL-1-NI	18.0 ± 2.9
SL-2-C	11.9 ± 1.2	SL-2-NII	13.3 ± 1.5
SL-3-C	15.1 ± 1.9	SL-3-GI	14.5 ± 1.4
SL-4-C	13.6 ± 4.4	SL-4-GII	19.8 ± 5.7
SL-5-C	13.4 ± 3.0	SL-5-BI	OVERRANGE
SL-6-C	10.7 ± 1.1	SL-6-BII	17.2 ± 3.5
Control Mean	13.1 ± 3.5		

Sawn Sandstone

Control areas		Abraded areas	
SS-7-C	19.8 ± 1.5	SS-7-WI	21.7 ± 1.3
SS-8-C	19.2 ± 4.6	SS-8-WII	19.2 ± 2.5
SS-1-C	16.6 ± 2.7	SS-1-NI	23.5 ± 1.8
SS-2-C	19.8 ± 2.1	SS-2-NII	21.1 ± 3.6
SS-3-C	17.4 ± 1.8	SS-3-GI	19.9 ± 2.0
SS-4-C	19.7 ± 2.3	SS-4-GII	21.8 ± 2.9
SS-5-C	21.3 ± 1.8	SS-5-BI	19.0 ± 1.5
SS-6-C	17.0 ± 2.5	SS-6-BII	22.1 ± 2.3
Control Mean	18.8 ± 2.6		

Glazed Tile

Control areas		Abraded areas	
GT-7-C	0.15 ± 0.12	GT-7-WI	0.47 ± 0.55
GT-8-C	0.12 ± 0.07	GT-8-WII	0.07 ± 0.03
GT-1-C	0.11 ± 0.04	GT-1-NI	0.07 ± 0.02
GT-2-C	0.07 ± 0.01	GT-2-NII	0.09 ± 0.05
GT-3-C	0.06 ± 0.02	GT-3-GI	0.12 ± 0.07
GT-4-C	0.12 ± 0.10	GT-4-GII	0.10 ± 0.05
GT-5-C	0.09 ± 0.05	GT-5-BI	2.8 ± 1.2
GT-6-C	0.10 ± 0.08	GT-6-BII	1.1 ± 0.4
Control Mean 0.10 ± 0.07			

Quarry Tile

Control areas		Abraded areas	
QT-7-C	4.4 ± 1.1	QT-7-WI	4.8 ± 0.4
QT-8-C	4.2 ± 0.4	QT-8-WII	4.7 ± 1.3
QT-1-C	3.1 ± 0.5	QT-1-NI	3.5 ± 0.6
QT-2-C	3.6 ± 0.4	QT-2-NII	3.9 ± 0.5
QT-3-C	4.6 ± 1.1	QT-3-GI	3.6 ± 0.6
QT-4-C	3.4 ± 0.5	QT-4-GII	4.0 ± 0.6
QT-5-C	4.0 ± 0.3	QT-5-BI	12.9 ± 2.9
QT-6-C	3.1 ± 0.9	QT-6-BII	9.3 ± 0.9
Control Mean 3.8 ± 0.7			

Roughness Parameters

The roughness parameters corresponding to the profiles shown in the following pages are listed on the following table. When the skew (Rsk) of the profile exceeds ± 1.5 , Ra loses its usefulness and for strict measurements this parameter should be complemented with other surface parameters.

Polished Granite		Ra [μm]	Rq [μm]	Rsk
PG-C	(PG7WIC3)	0.18	0.58	- 8.1
PG-W	LP (PG8WII4)	0.19	0.45	- 3.0
PG-N	LP (PG2NII3)	0.26	0.51	- 1.6
PG-G	LP (PG4GII3)	0.29	1.21	- 7.9
PG-B	LP (PG6BII4)	3.01	5.19	0.1
PG-W	HP (PG7WI3)	0.95	2.05	- 2.0
PG-N	HP (PG1NI3)	0.24	0.49	- 6.0
PG-G	HP (PG3GI4)	0.18	0.45	- 8.0
PG-B	HP (PG5BI2)	8.04	10.57	0.1
Polished Marble				
PM-C	(PM23WIC3)	0.10	0.28	- 6.7
PM-W	LP (PM24WII4)	0.18	0.51	- 8.1
PM-N	LP (PM12NII1)	0.21	0.44	- 4.3
PM-G	LP (PM14GII2)	6.63	8.60	- 0.4
PM-B	LP (PM2BII4)	9.10	11.44	- 0.2
PM-W	HP (PM23WI3)	0.29	0.48	- 2.2
PM-N	HP (PM11NI2)	0.32	0.72	- 4.9
PM-G	HP (PM13GI2)	0.17	0.45	- 5.6
PM-B	HP (PM21BI1C)	12.74	15.77	0.3
Sawn Marble				
SM-C	(SM43WIC3)	4.11	5.22	- 0.4
SM-W	LP (SM44WII2)	4.76	6.11	- 0.3
SM-N	LP (SM32NII3)	5.71	7.33	- 0.5
SM-G	LP (SM34GII2)	10.39	13.08	- 0.4
SM-B	LP (SM42BII3)	10.41	12.94	- 0.1
SM-W	HP (SM43WI2)	4.76	6.04	- 0.2
SM-N	HP (SM31NI3)	5.13	6.46	- 0.6
SM-G	HP (SM33GI3)	6.98	9.53	0.8
SM-B	HP (SM41BI4)	16.90	20.61	- 0.1

Sawn Limestone

SL-C	(SL7WIC1)	15.60	19.12	- 0.1
SL-W	LP (SL8WII3)	15.28	19.93	0.0
SL-N	LP (SL2NII3)	12.95	15.79	0.3
SL-G	LP (SL4GII4)	17.83	23.11	- 0.1
SL-B	LP (SL6BII3)	19.95	25.70	0.1
SL-W	HP (SL7WI1)	24.23	30.02	- 0.1
SL-N	HP (SL1NI3)	17.54	23.30	- 0.3
SL-G	HP (SL3GI1)	13.91	17.91	0.0
SL-B	HP	not measurable with the instrument		

Sawn Sandstone

SS-C	(SS7WIC1)	20.25	24.48	- 0.1
SS-W	LP (SS8WII3)	16.99	21.26	0.1
SS-N	LP (SS2NII1)	16.41	20.26	- 0.1
SS-G	LP (SS4GII4)	25.69	30.18	- 0.2
SS-B	LP (SS6BII4)	21.96	26.40	0.0
SS-W	HP (SS7WI3)	21.29	27.02	- 0.4
SS-N	HP (SS1NI3)	25.29	30.73	- 0.4
SS-G	HP (SS3GI4)	20.93	24.92	0.1
SS-B	HP (SS5BI3)	17.37	22.01	- 0.3

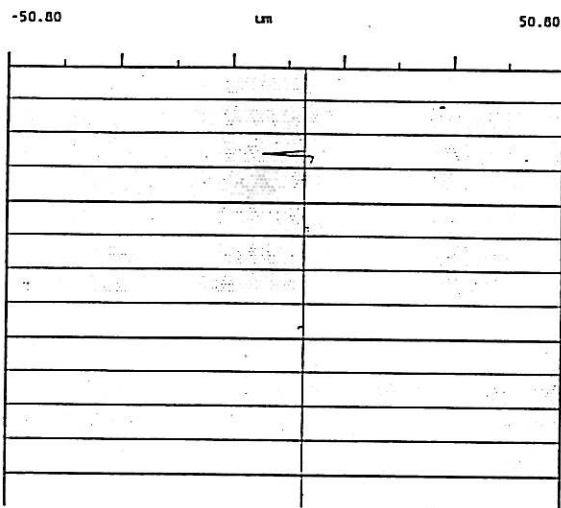
Glazed Tile

GT-C	(GT7WIC1)	0.07	0.09	0.5
GT-W	LP (GT8WII1)	0.08	0.16	3.6
GT-N	LP (GT2NII1)	0.08	0.16	3.5
GT-G	LP (GT4GII1)	0.08	0.17	3.6
GT-B	LP (GT6BII1)	1.33	2.50	- 1.6
GT-W	HP (GT7WI6)	0.15	0.22	2.3
GT-N	HP (GT1NI1)	0.10	0.21	0.2
GT-G	HP (GT3GI1)	0.08	0.16	3.7
GT-B	HP (GT5BI1)	2.66	4.12	- 0.2

Quarry Tile

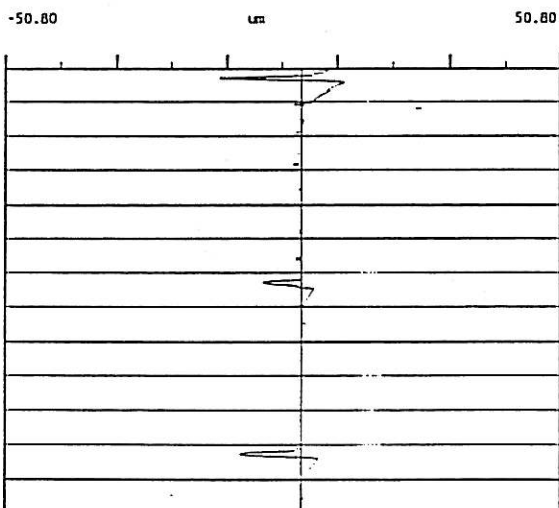
QT-C	(QT7WIC3)	3.12	3.97	- 0.2
QT-W	LP (QT8WII2)	3.77	4.65	- 0.3
QT-N	LP (QT2NII3)	3.55	4.59	- 0.6
QT-G	LP (QT4GII2)	4.73	5.73	0.0
QT-B	LP (QT6BII1)	9.35	12.42	- 0.2
QT-W	HP (QT7WI2)	4.63	5.44	0.0
QT-N	HP (QT1NI2)	3.17	3.97	0.0
QT-G	HP (QT3GI1)	3.77	4.77	0.1
QT-B	HP (QT5BI3)	11.47	14.34	0.2

Polished Granite - Roughness profiles for control and areas blasted at high pressures (100 psi for powdered materials, 2000 psi for water).
Vv x 1000 Vh x 20

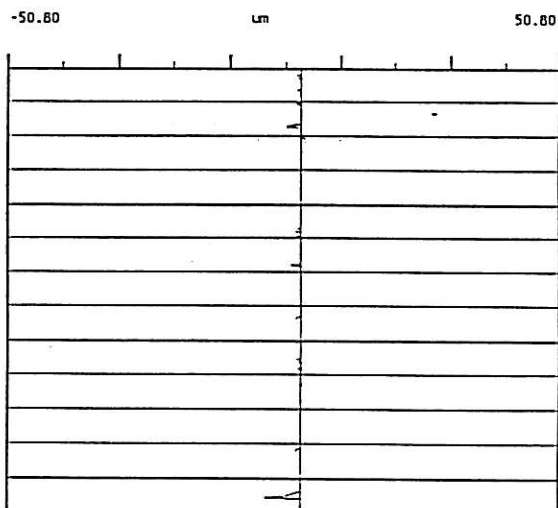


Control

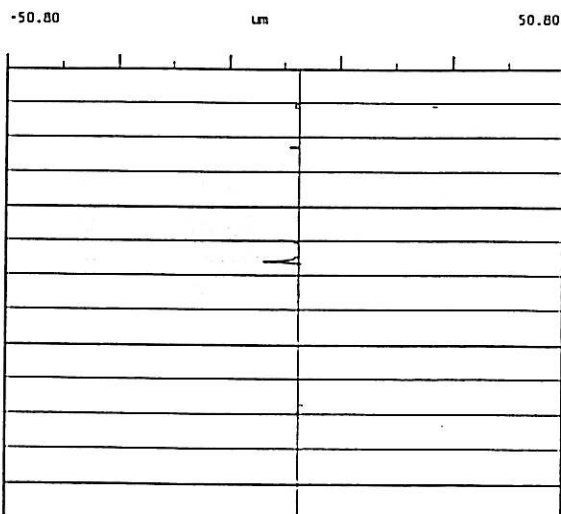
Water



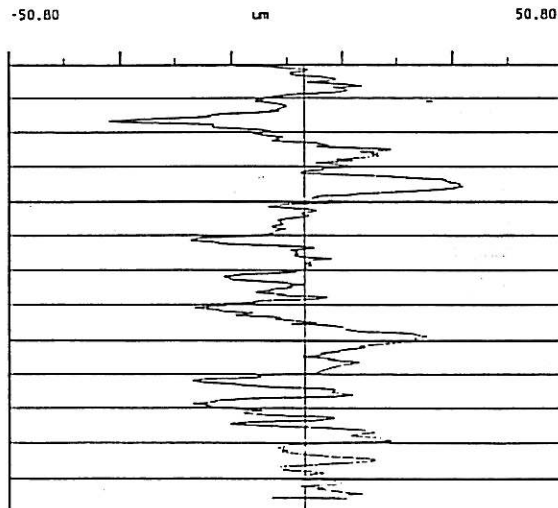
Nut Shells



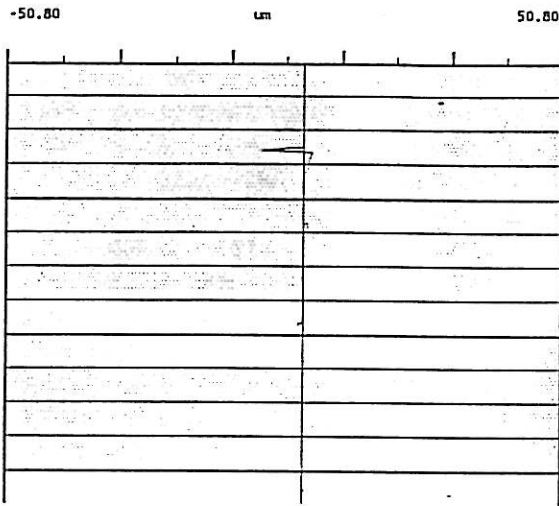
Glass Beads



Black Beauty

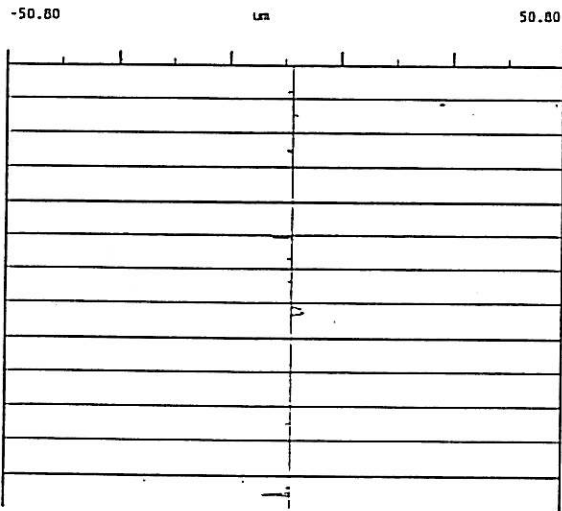


Polished Granite - Roughness profiles for control and areas blasted at low pressures (50 psi for powdered materials, 1000 psi for water).
Vv x 1000 Vh x 20

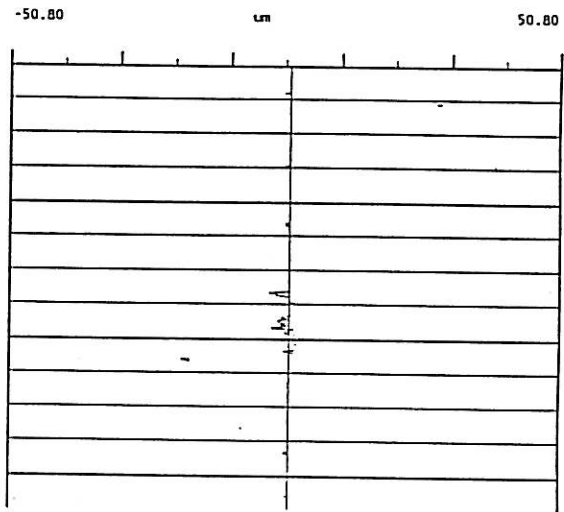


Control

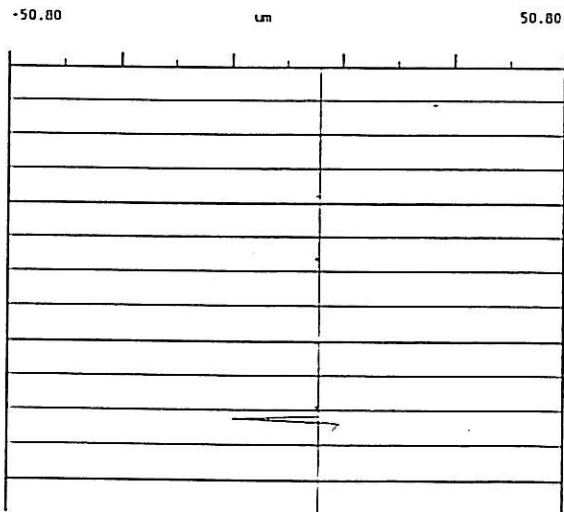
Water



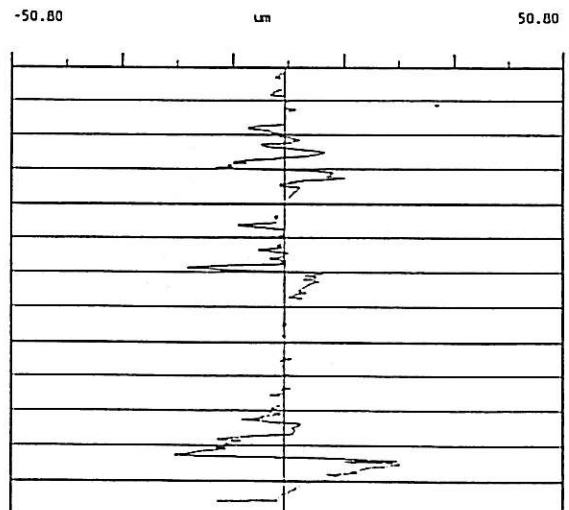
Nut Shells



Glass Beads

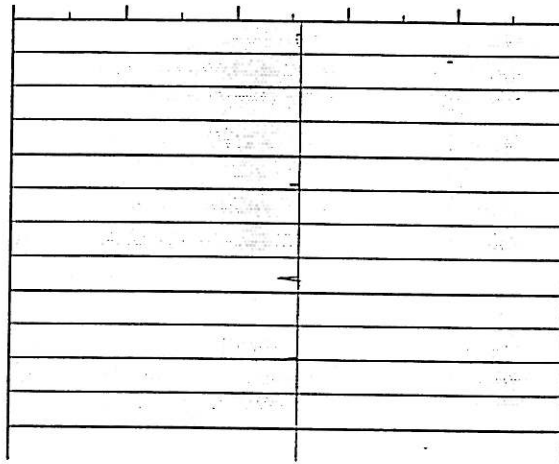


Black Beauty



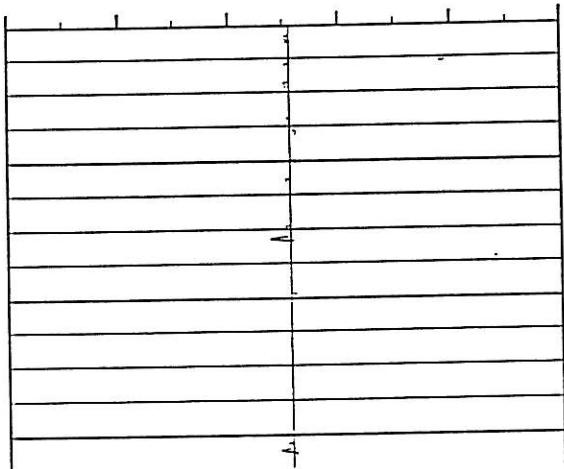
Polished Marble - Roughness profiles for control and areas blasted at high pressures (100 psi for powdered materials, 2000 psi for water).
Vv x 1000 Vh x 20

-50.80 μm 50.80 Control



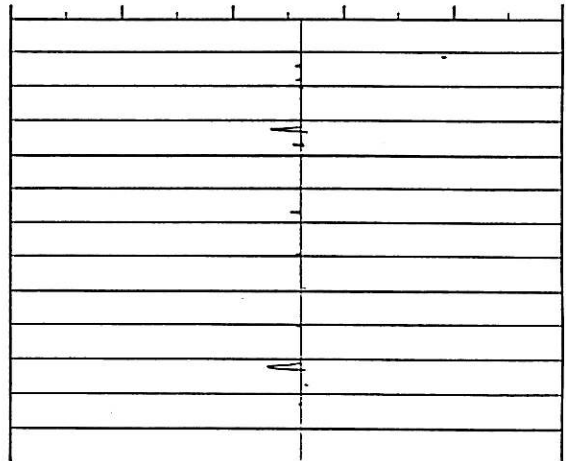
Water

-50.80 μm 50.80



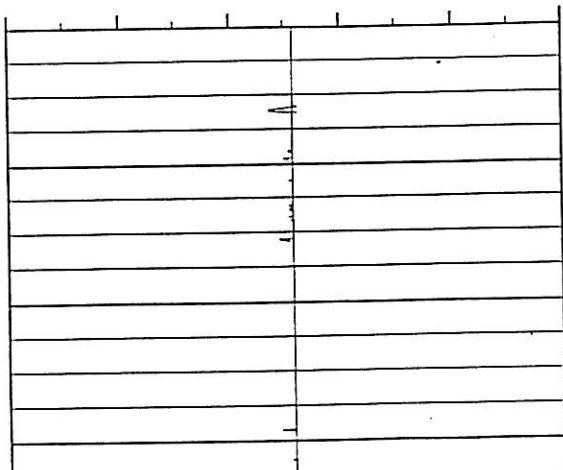
Nut Shells

-50.80 μm 50.80



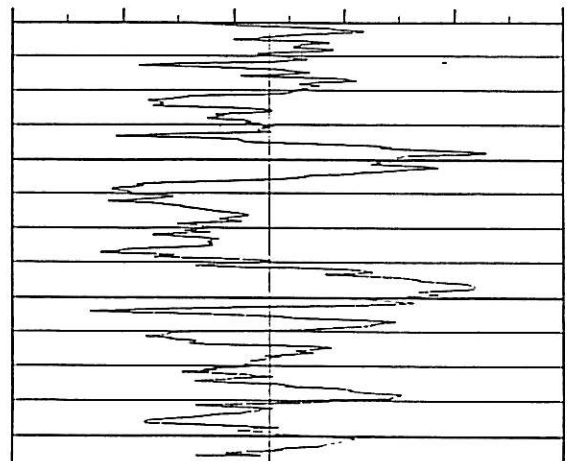
Glass Beads

-50.80 μm 50.80



Black Beauty

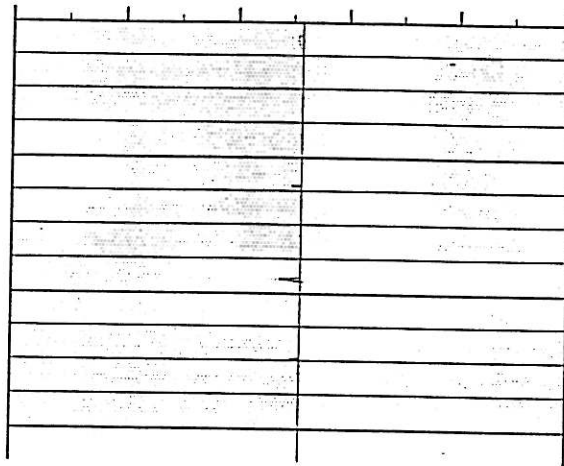
-50.80 μm 50.80



Polished Marble - Roughness profiles for control and areas blasted at low pressures (50 psi for powdered materials, 1000 psi for water).
Vv x 1000 Vh x 20

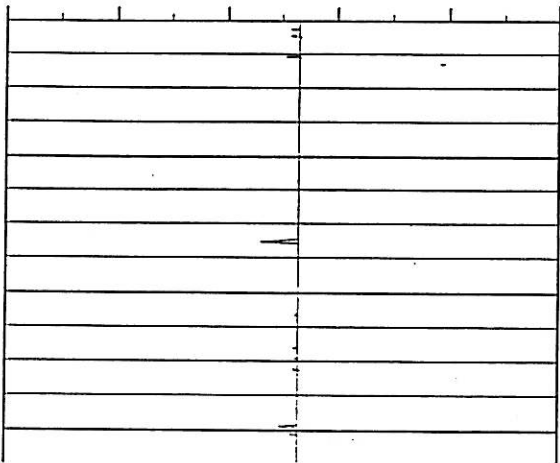
-50.80 μm 50.80

Control



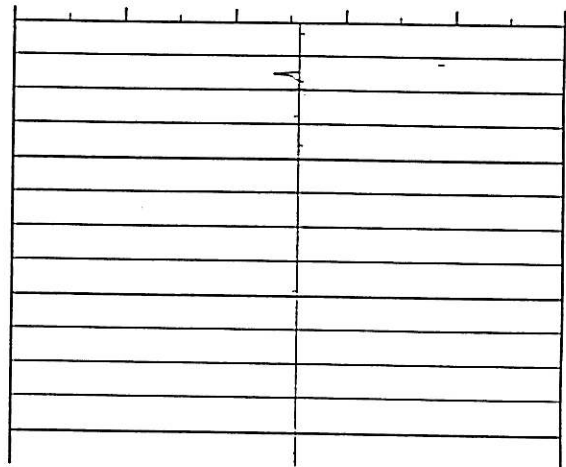
Water

-50.80 μm 50.80



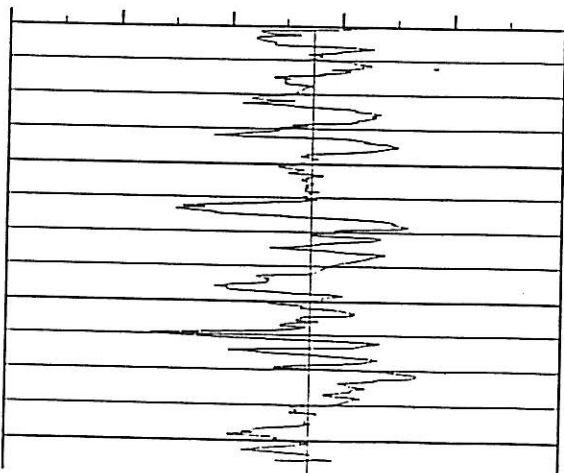
Nut Shells

-50.80 μm 50.80



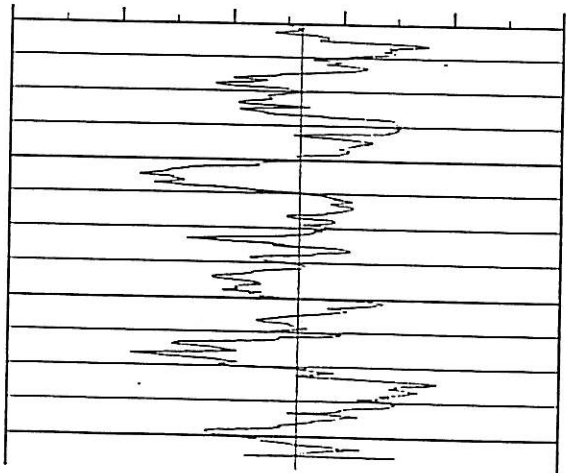
Glass Beads

-50.80 μm 50.80



Black Beauty

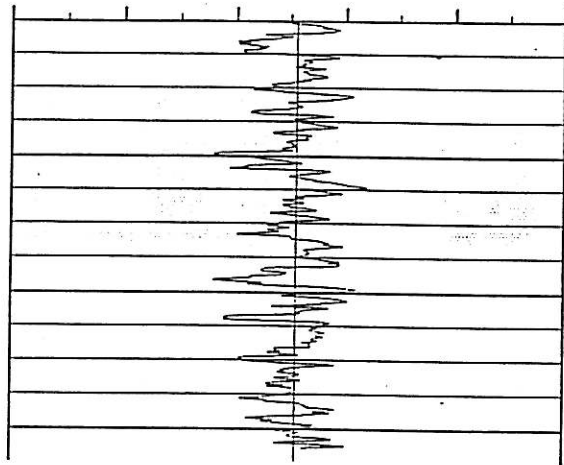
-50.80 μm 50.80



Sawn Marble - Roughness profiles for control and areas blasted at low pressures (50 psi for powdered materials, 1000 psi for water).
Vv x 1000 Vh x 20

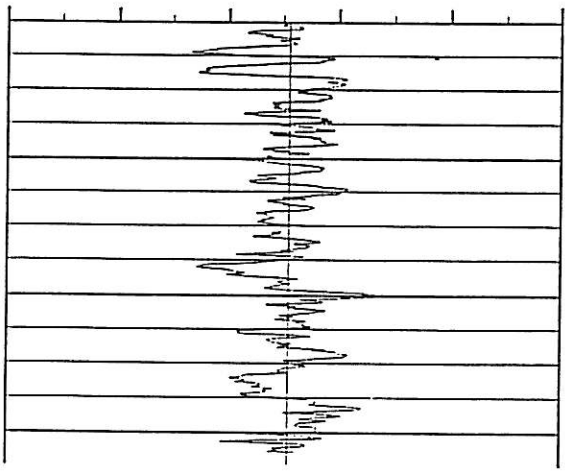
-50.80 50.80

Control



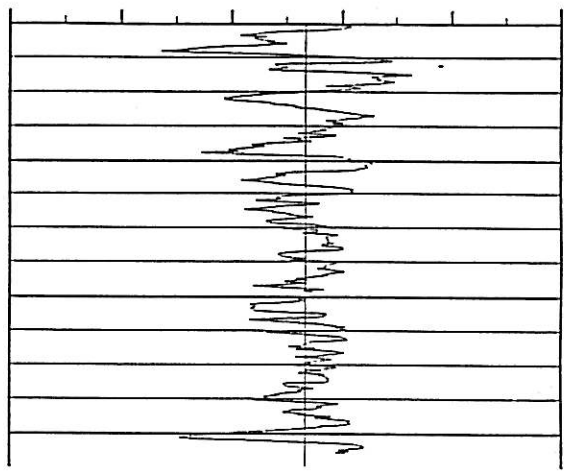
Water

-50.80 50.80



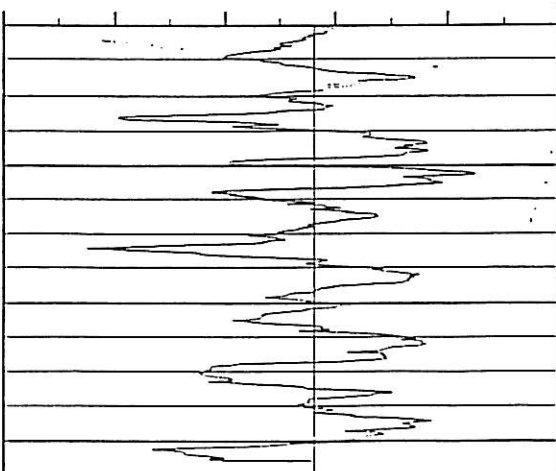
Nut Shells

-50.80 50.80



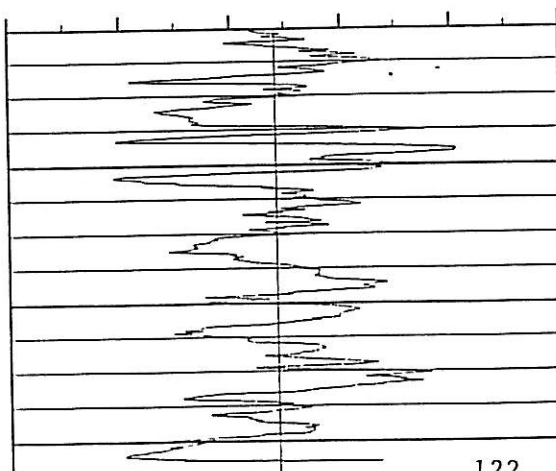
Glass Beads

-50.80 50.80

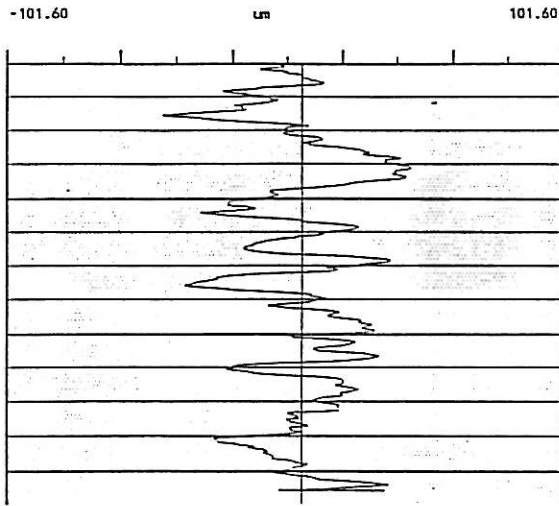


Black Beauty

-50.80 50.80

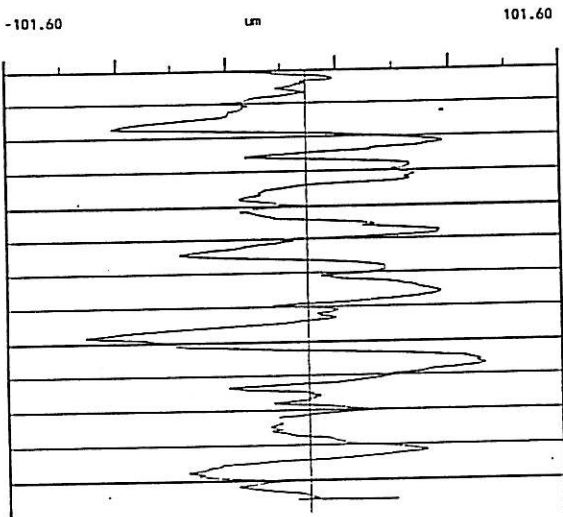


Sawn Limestone - Roughness profiles for control and areas blasted at high pressures (100 psi for powdered materials, 2000 psi for water).
Vv x 500 Vh x 20

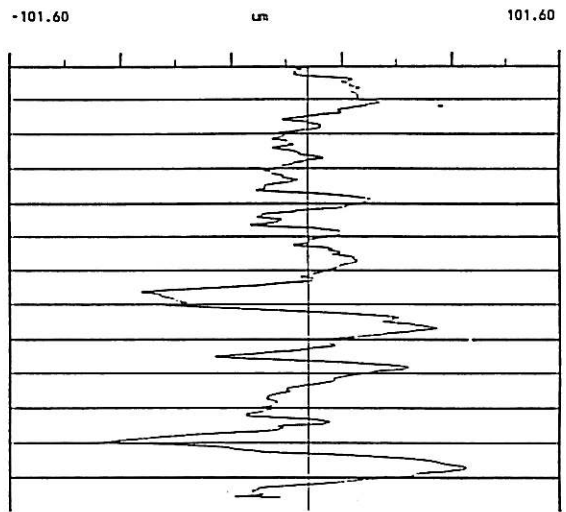


Control

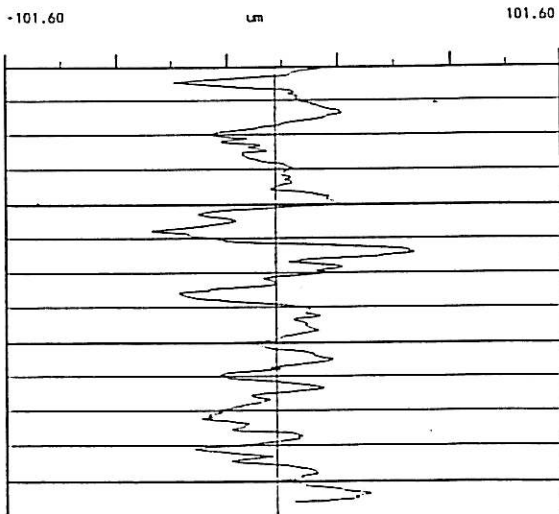
Water



Nut Shells

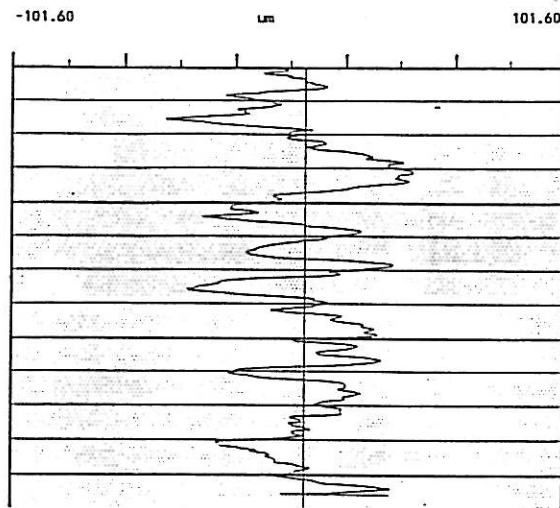


Glass Beads



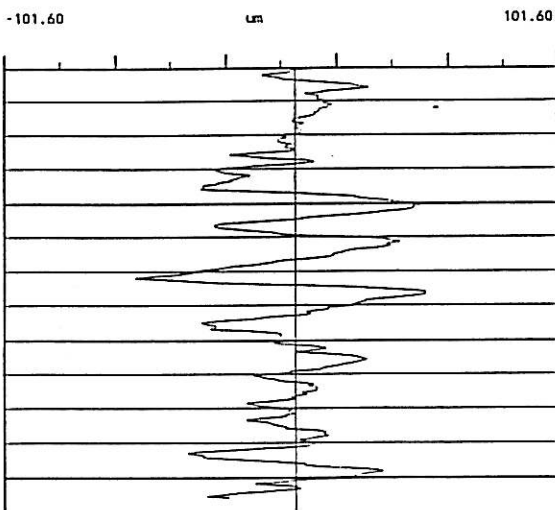
Black Beauty

Sawn Limestone - Roughness profiles for control and areas blasted at low pressures (50 psi for powdered materials, 1000 psi for water).
Vv x 500 Vh x 20

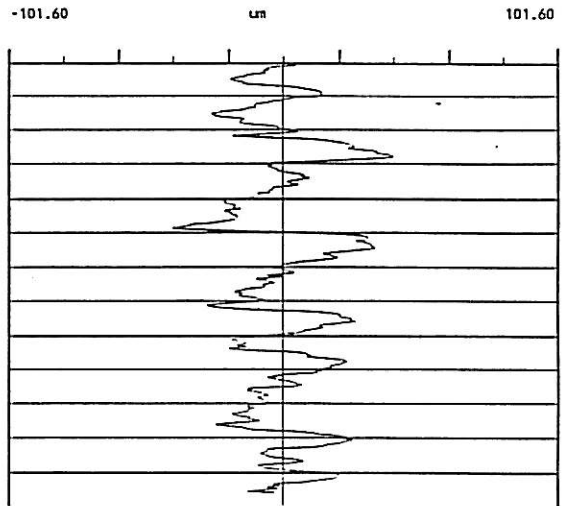


Control

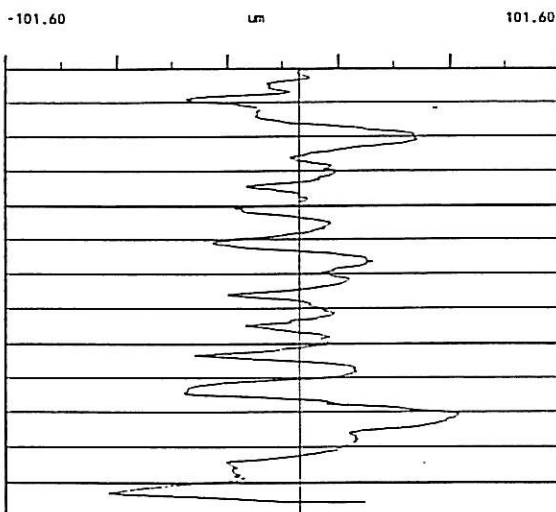
Water



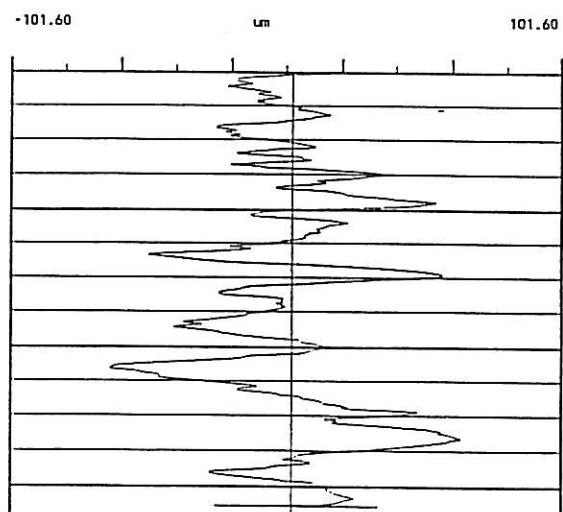
Nut Shells



Glass Beads



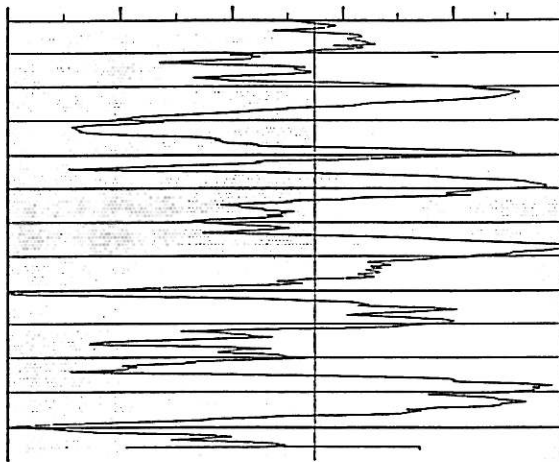
Black Beauty



Sawn Sandstone - Roughness profiles for control and areas blasted at high pressures (100 psi for powdered materials, 2000 psi for water).
Vv x 1000 Vh x 20

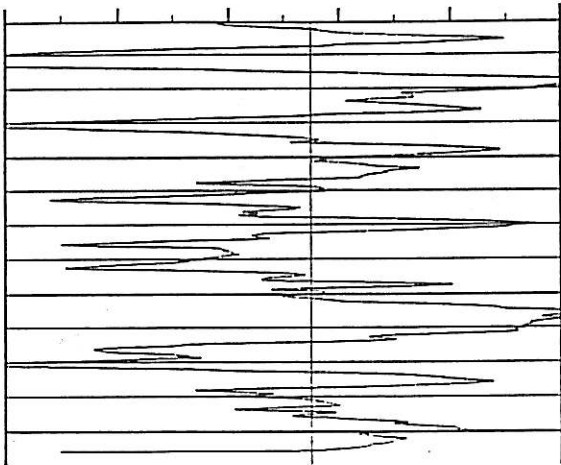
-50.80 um 50.80

Control



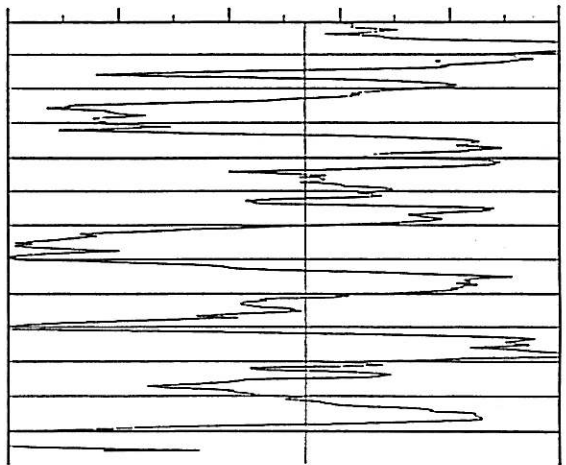
Water

-50.80 um 50.80



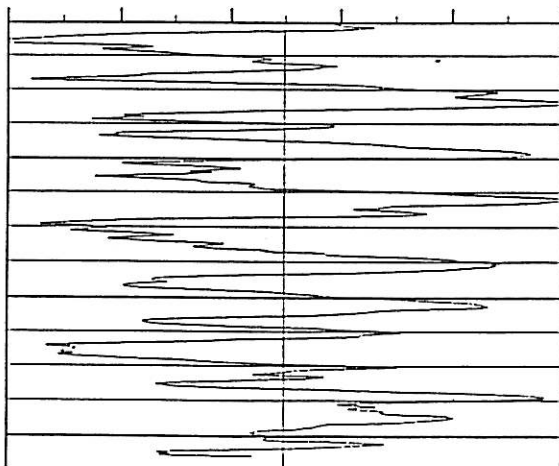
Nut Shells

-50.80 um 50.80



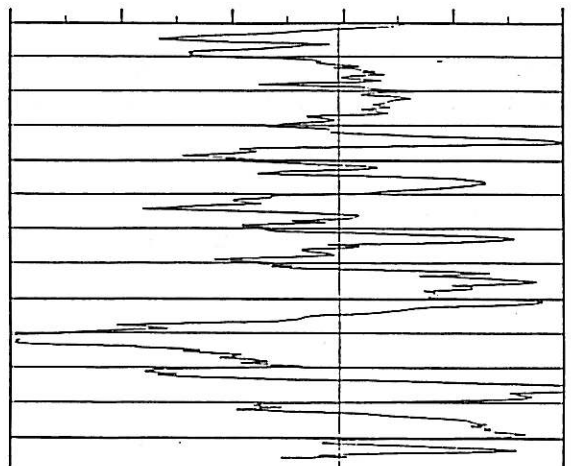
Glass Beads

-50.80 um 50.80



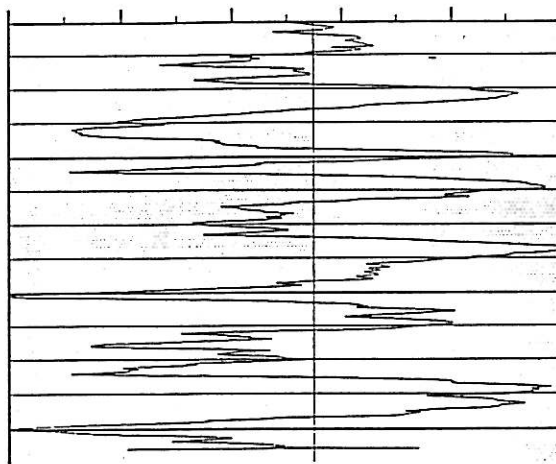
Black Beauty

-50.80 um 50.80



Sawn Sandstone - Roughness profiles for control and areas blasted at low pressures (50 psi for powdered materials, 1000 psi for water).
Vv x 1000 Vh x 20

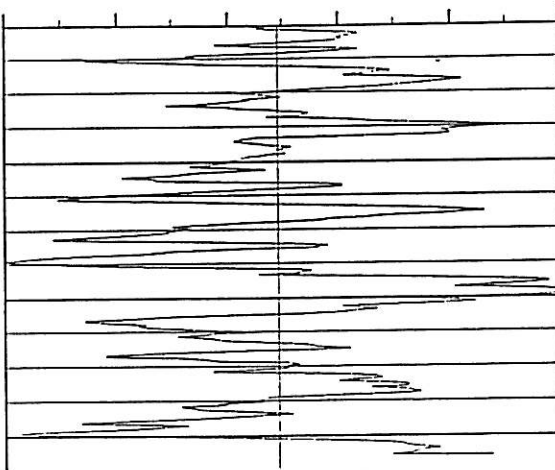
-50.80 μm 50.80



Control

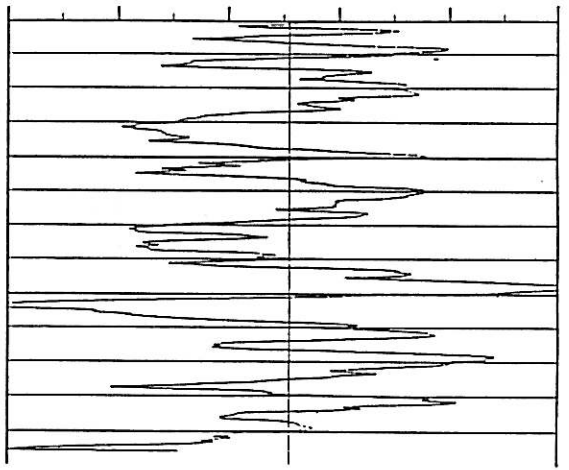
Water

-50.80 μm 50.80



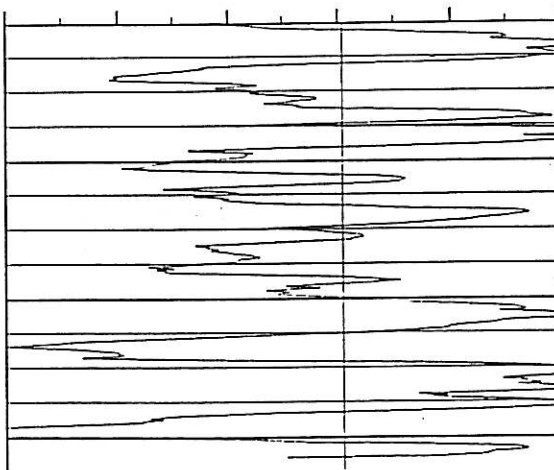
Nut Shells

-50.80 μm 50.80



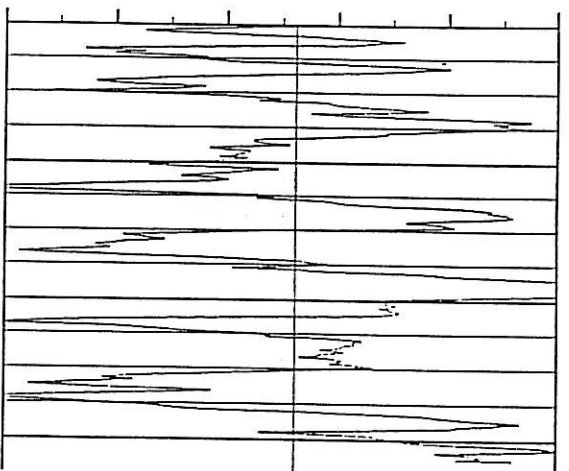
Glass Beads

-50.80 μm 50.80

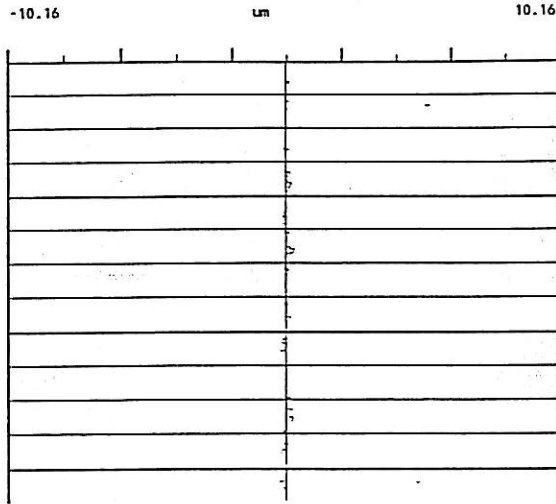


Black Beauty

-50.80 μm 50.80

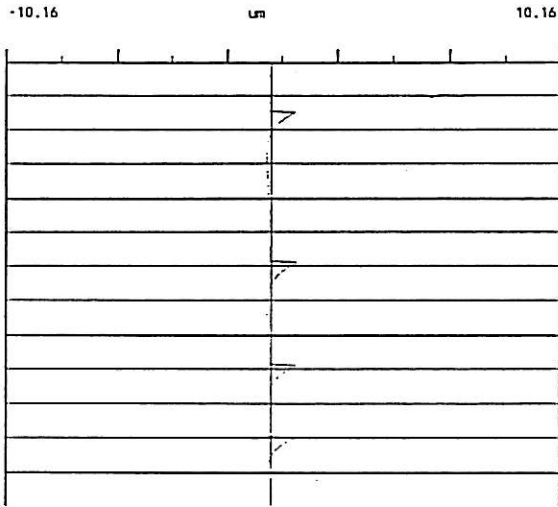


Glazed Tile - Roughness profiles for control and areas blasted at high pressures (100 psi for powdered materials, 2000 psi for water).
Vv x 5000 - Vh x 20

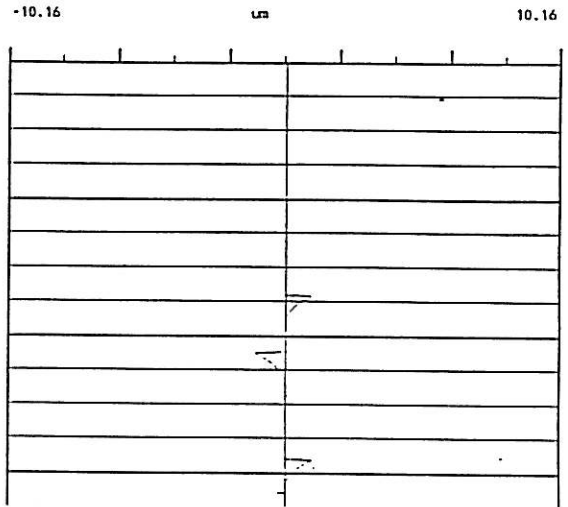


Control

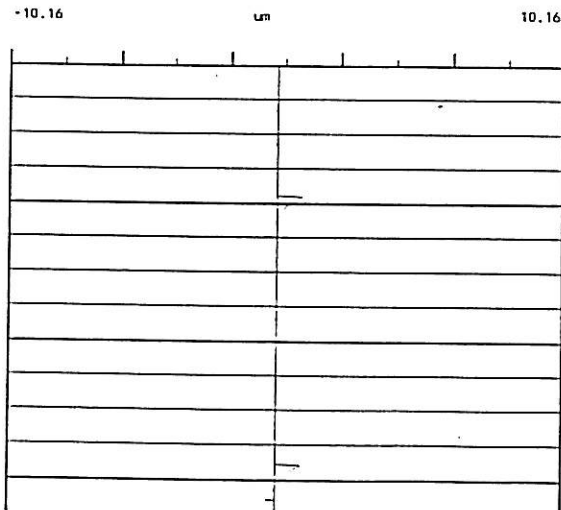
Water



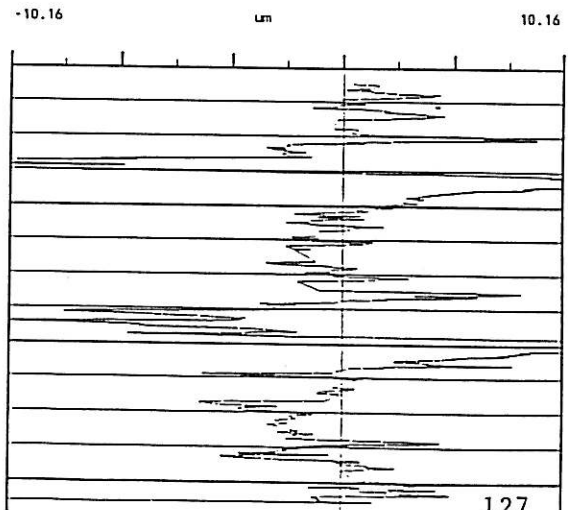
Nut Shells



Glass Beads



Black Beauty

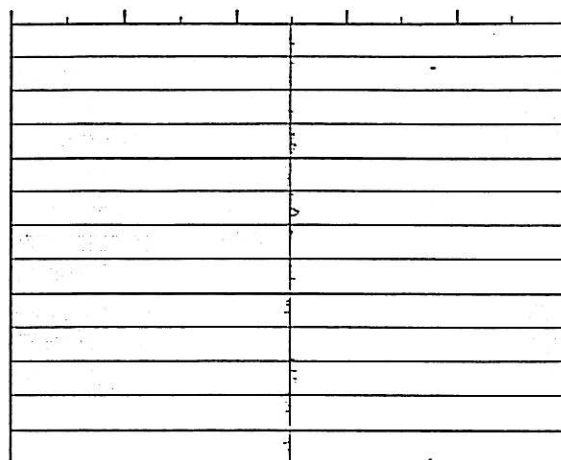


Glazed Tile - Roughness profiles for control and areas blasted at low pressures (50 psi for powdered materials, 1000 psi for water).

Vv x 5000

Vh x 20

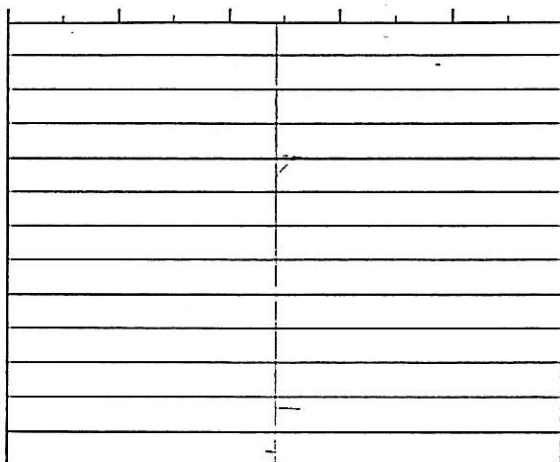
-10.16 um 10.16



Control.

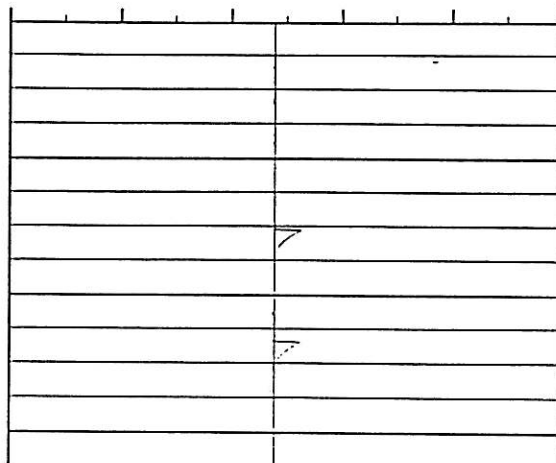
Water

-10.16 um 10.16



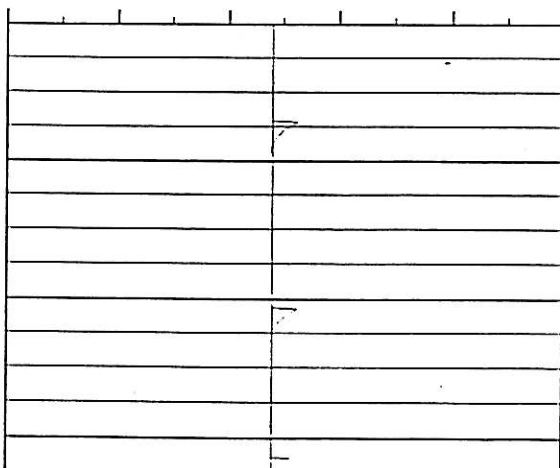
Nut Shells

-10.16 um 10.16



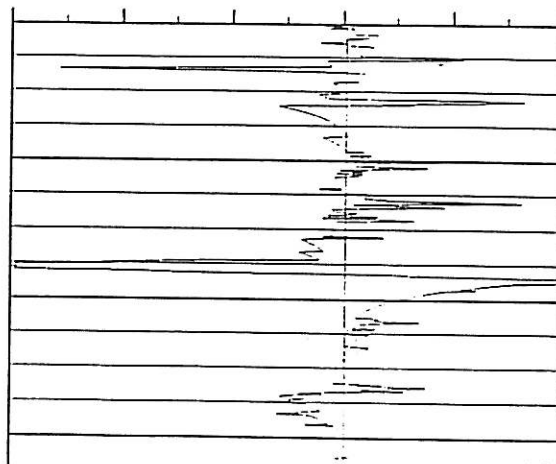
Glass Beads

-10.16 um 10.16

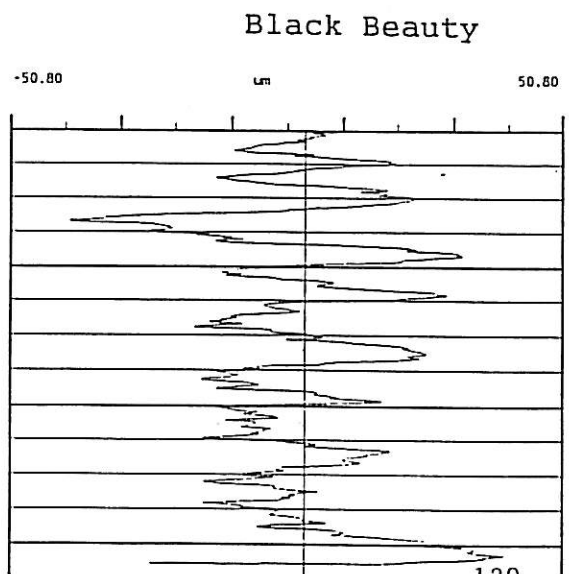
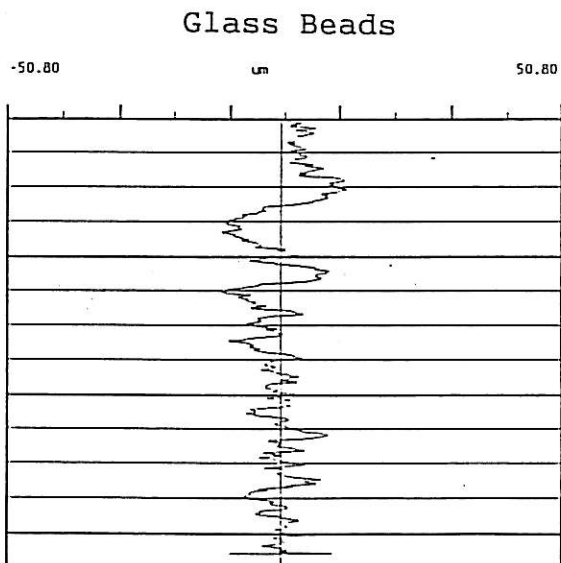
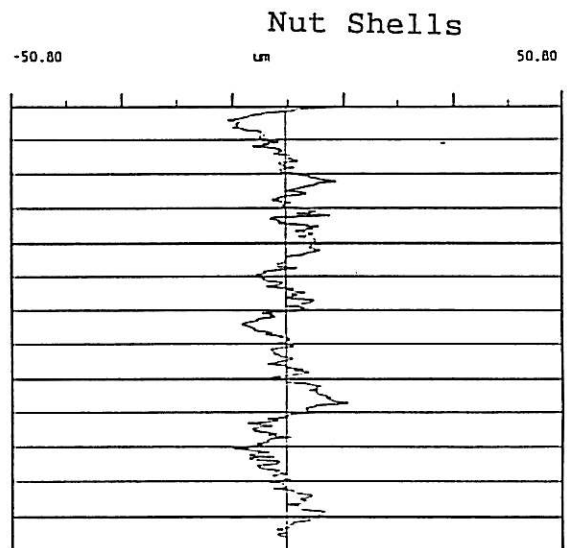
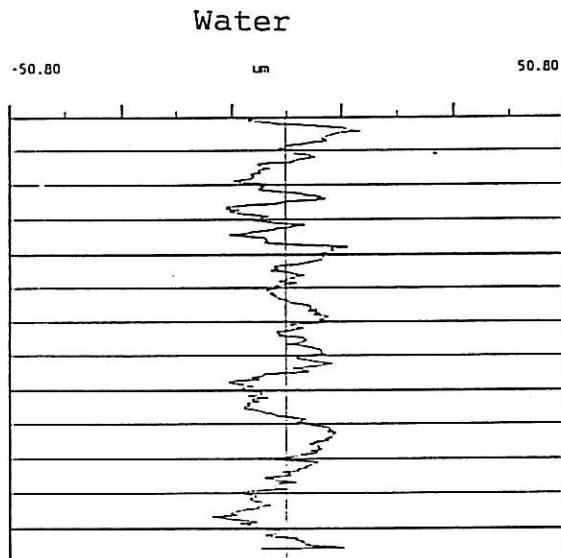
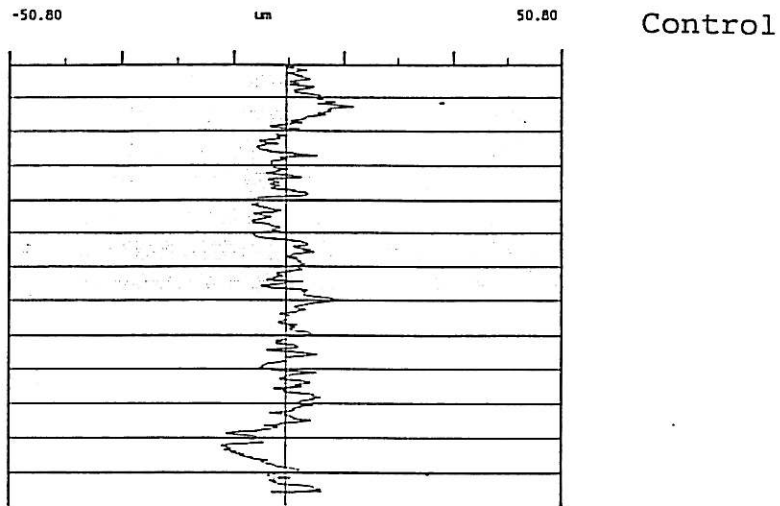


Black Beauty

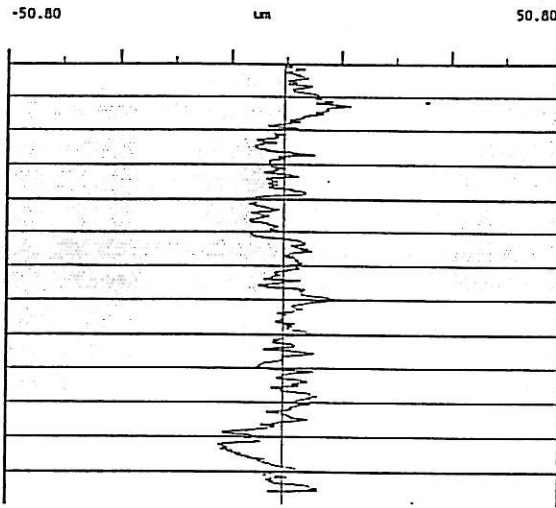
-10.16 um 10.16



Quarry Tile - Roughness profiles for control and areas blasted at high pressures (100 psi for powdered materials, 2000 psi for water).
Vv x 1000 Vh x 20

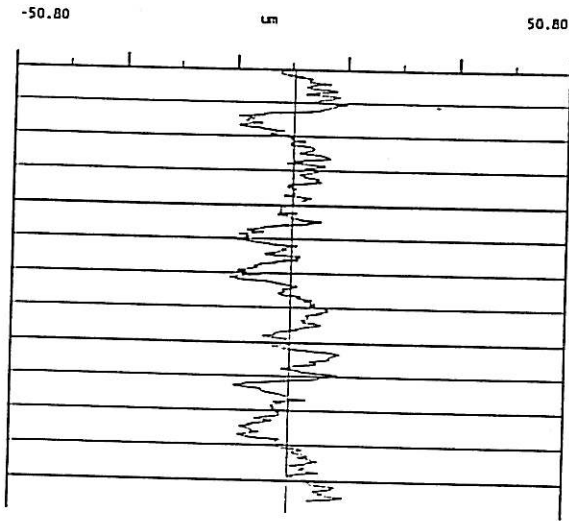


Quarry Tile - Roughness profiles for control and areas blasted at low pressures (50 psi for powdered materials, 1000 psi for water).
Vv x 1000 Vh x 20

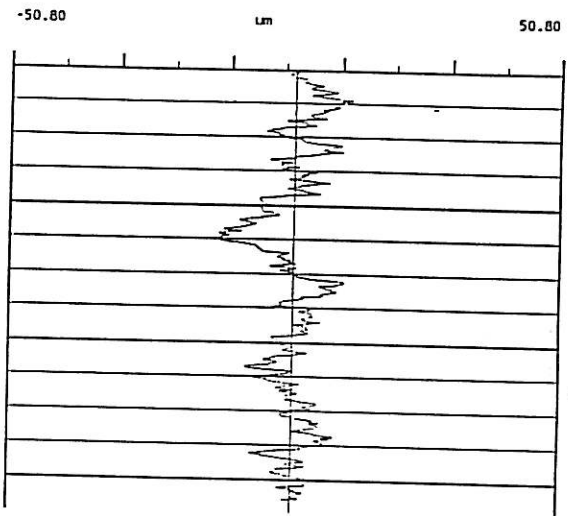


Control

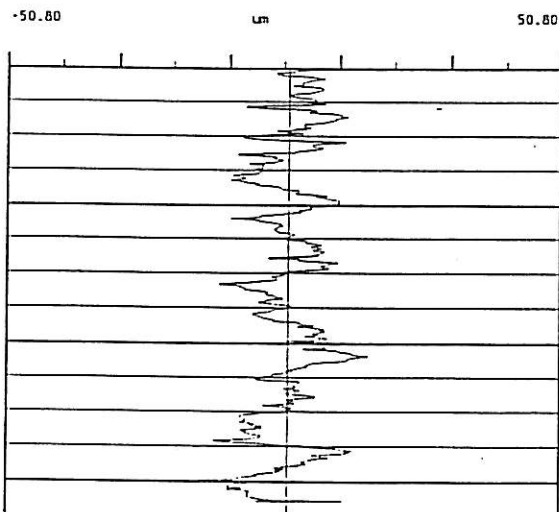
Water



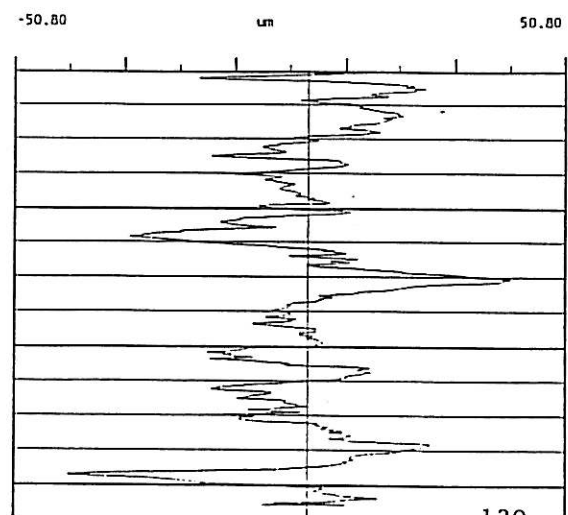
Nut Shells



Glass Beads



Black Beauty



APPENDIX X
MICRODROP ABSORPTION TIME

Appendix X

Summary of measurements of microdrop absorption times. The drop size used was $10 \mu\text{l} \pm 2 \mu\text{L}$ and the dropping distance was 2.5 cm. Data presented are the average of at least five individual measurements, with most of the determinations carried out on sets of twenty drops. The absorption time on a reference glass surface was taken with each set of data and, since it did not vary significantly—taking into account the differences in magnitude with the times measured for the different surfaces—all the values (over 150) were averaged.

Since the absorption time on polished surfaces was close to that of the reference material, the data for these surfaces were not obtained given the limitations of the accuracy of the methodology employed and of time to carry out all the measurements.

1 drop = $10 \mu\text{L} \pm 2 \mu\text{L}$

reference = tg 32 min \pm 1 min

Polished Granite

PG-4-GI	19.6 ± 2.2	min
PG-5-BI	20.0 ± 0.7	
PG-6-BII	21.2 ± 2.0	

Polished Marble

PM-2.3-WI	20.2 ± 2.7	
PM-1.3-GI	21.4 ± 1.4	
PM-1.4-GII	18.2 ± 1.5	
PM-2.1-BI	2.6 ± 0.5	
PM-2.2-BII	5.6 ± 1.1	

Sawn Marble

SM-control	21.2 ± 1.7	
SM-4.3-WI	16.0 ± 1.2	
SM-4.4-WII	12.1 ± 1.9	
SM-3.1-NI	15.3 ± 1.1	
SM-3.2-NII	16.9 ± 2.2	
SM-3.3-GI	11.2 ± 0.7	
SM-3.4-GII	5.6 ± 0.8	
SM-3.3-GI	11.2 ± 0.7	
SM-3.4-GII	5.6 ± 0.8	
SM-4.1-BI	1.0 ± 0.2	
SM-4.2-BII	1.4 ± 0.2	

Sawn Limestone

SL control	1.8 ± 0.4 min	SL-7-WI	7.2 ± 6.5 sec
		SL-8-WII	6.9 ± 5.3
		SL-1-NI	24.5 ± 5.3
		SL-2-NII	22.0 ± 3.2
		SL-3-GI	35.9 ± 6.6
		SL-4-GII	2.6 ± 1.3
		SL-5-BI	1.8 ± 0.2
		SL-6-BII	1.6 ± 0.2 sec

Sawn Sandstone

SS control	9.3 ± 4.4 sec	SS-7-WI	7.8 ± 4.3 sec
		SS-8-WII	3.5 ± 1.5
		SS-1-NI	1.5 ± 0.4 min
		SS-2-NII	1.3 ± 0.2 min
		SS-3-GI	22.6 ± 8.8 sec
		SS-4-GII	1.5 ± 0.2 sec
		SS-5-BI	1.4 ± 0.2 sec
		SS-6-BII	1.8 ± 0.3 sec

Flamed Granite

FG control	9.8 ± 2.3 min	FG-7-WI	13.9 ± 2.2
		FG-8-WII	13.8 ± 0.9
		FG-1-NI	22.8 ± 2.3
		FG-2-NII	21.3 ± 2.8
		FG-3-GI	16.7 ± 1.3
		FG-4-GII	18.7 ± 1.7
		FG-5-BI	15.6 ± 2.3
		FG-6-BII	18.5 ± 1.9

Quarry Tile

QT control	21.1 ± 1.1	QT-3-GI	29.3 ± 0.5
		QT-4-GII	21.3 ± 1.1
		QT-5-BI	12.1 ± 1.4
		QT-6-BII	20.2 ± 1.8

APPENDIX XI
REFLECTED LIGHT IMAGE ANALYSIS - PHASE II

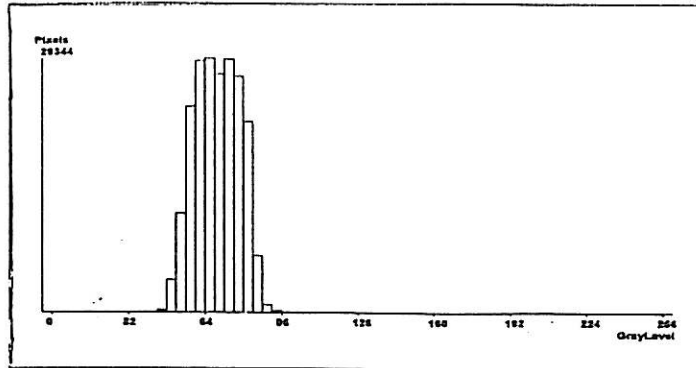
APPENDIX XI

Pixel count of the highest bar of the peak in the histogram obtained by RLIA from the red silicone replicas of the different materials, blasted with water, walnut shells, glass beads and Black Beauty slag at high (I) pressures (100 psi for powdered materials, 2000 psi for water), and low (II) pressures (50 psi for powdered materials, 1000 psi for water). Control areas were only measured on some samples, and the averages listed in Table VI are the overall averages corresponding to these areas.

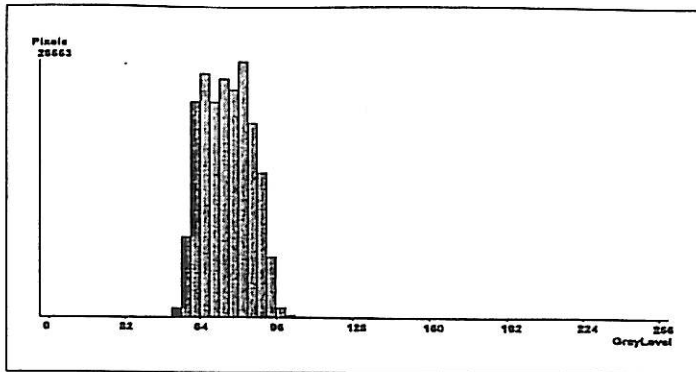
Polished Marble (PM/BIC)		26,446		29,641 (PM/BIIc)	
		24,647		29,344	
				31,699	
		average 28,355 ($\pm 2,793$)			
PM/WI		26,447		PM/WII	31,216
		33,726			29,811
		28,553	29,575 ($\pm 3,745$)		28,531 29,852 ($\pm 1,343$)
PM/NI		32,269		PM/NII	30,110
		27,806			30,285
		33,348	31,141 ($\pm 2,938$)		30,759 30,384 (± 335)
PM/GI		27,846		PM/GII	17,240
		32,408			24,116
		33,639	31,297 ($\pm 3,052$)		22,205 21,187 ($\pm 3,549$)
PM/BI		13,380		PM/BII	15,355
		13,183			14,723
		12,813	13,125 (± 288)		14,467 14,848 (± 457)
Sawn Marble (PM/NIc)		19,935		26,719 (PM/NIIC)	
		20,532		21,652	
		21,461	21,983	average	22,047 ($\pm 2,412$)
SM/WI		22,566		SM/WII	27,200
		23,211			23,661
		23,701	23,159 (± 569)		22,361 24,407 ($\pm 2,504$)
SM/NI		16,914		SM/NII	20,022
		21,307			22,081
		18,337	18,652 ($\pm 2,241$)		22,188 21,430 ($\pm 1,221$)
SM/GI		20,902		SM/GII	15,171
		21,434			15,914
		20,769	21,035 (± 352)		15,315 15,466 (± 394)
SM/BI		13,769		SM/BII	15,501
		12,997			15,565
		14,119	13,628 (± 574)		15,602 15,556 (± 51)

Polished Marble - RLIA histograms for control and areas blasted at high pressures (100 psi for powdered materials, 2000 psi for water).

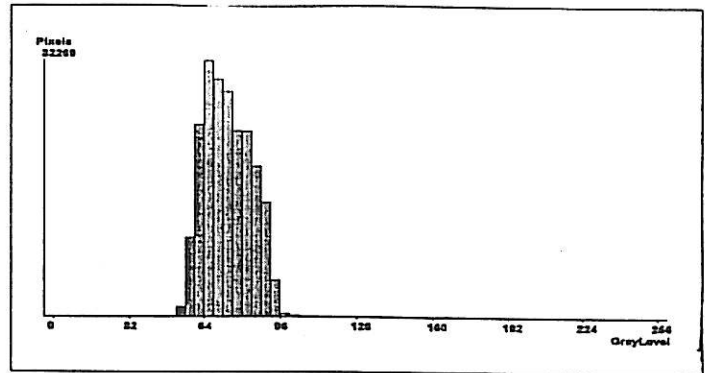
Control (29334 pixels)



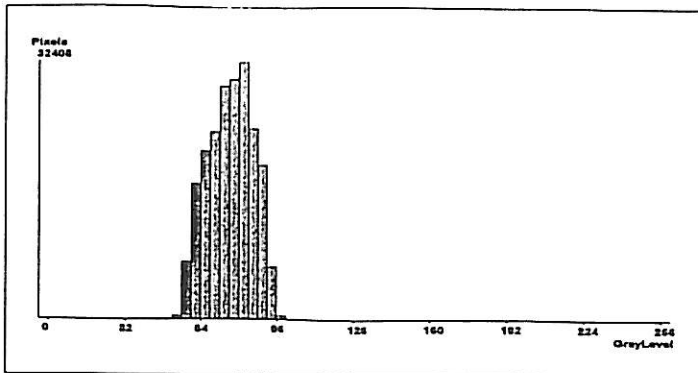
Water (28551 pixels)



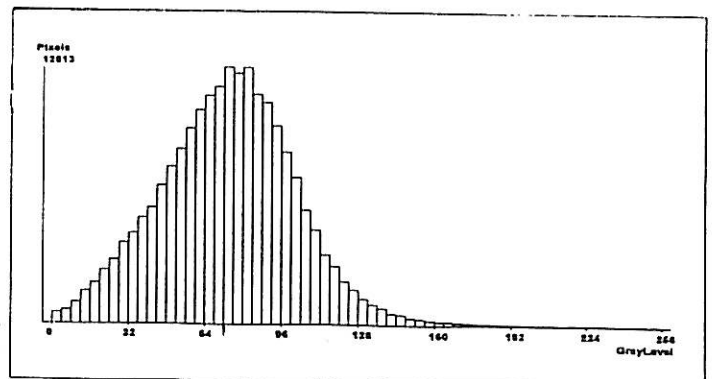
Nut Shells (32269 pixels)



Glass Beads (32408 pixels)

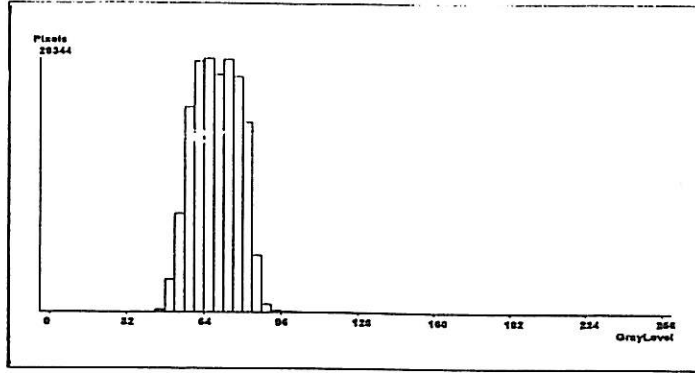


Black Beauty (12813 pixels)

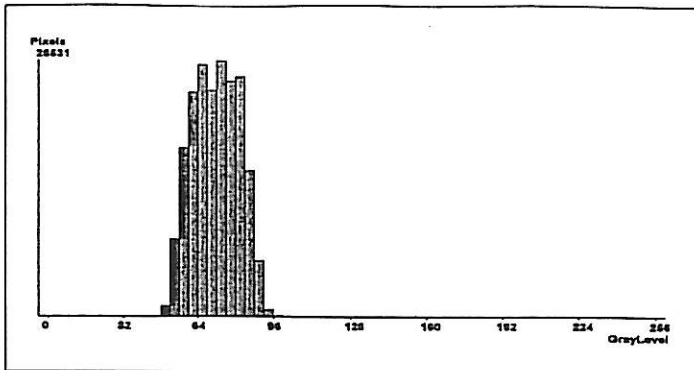


Polished Marble - RLIA histograms for control and areas blasted at low pressures (50 psi for powdered materials, 1000 psi for water).

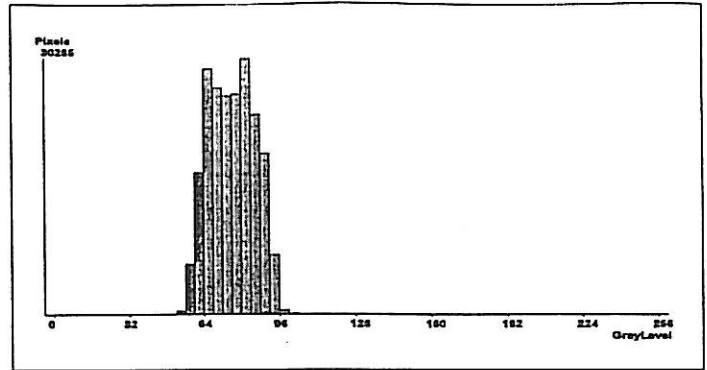
Control (29334 pixels)



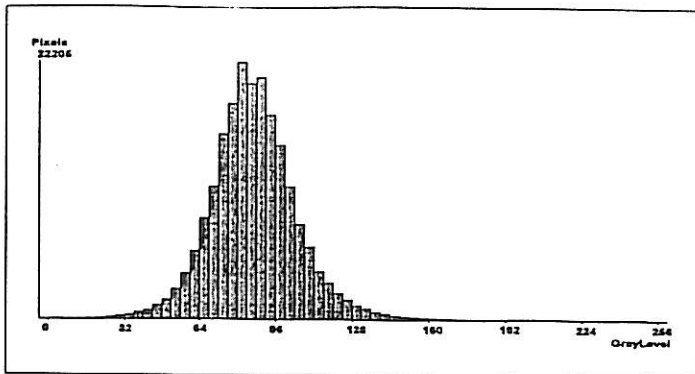
Water (28531 pixels)



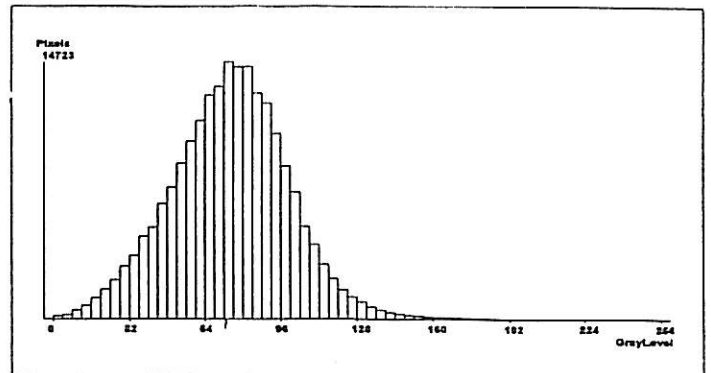
Nut Shells (30285 pixels)



Glass Beads (22205 pixels)

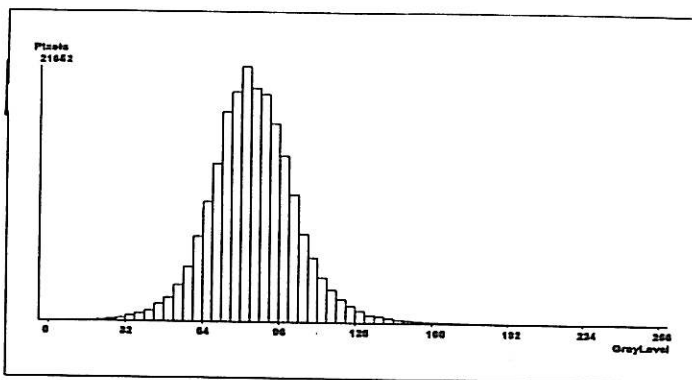


Black Beauty (14723 pixels)

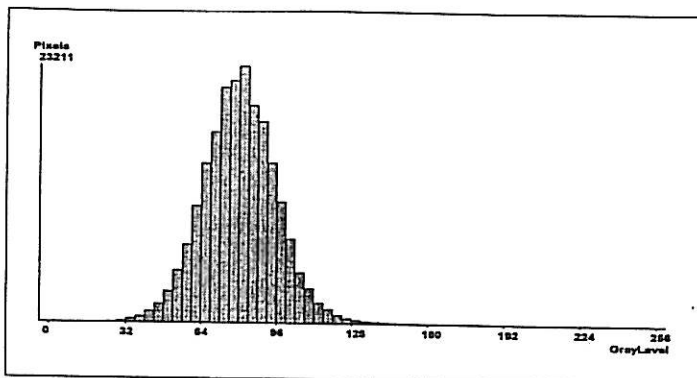


Sawn Marble - RLIA histograms for control and areas blasted at high pressures (100 psi for powdered materials, 2000 psi for water).

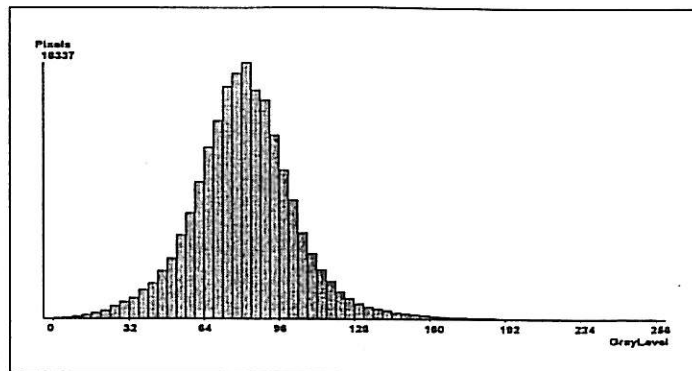
Control (21652 pixels)



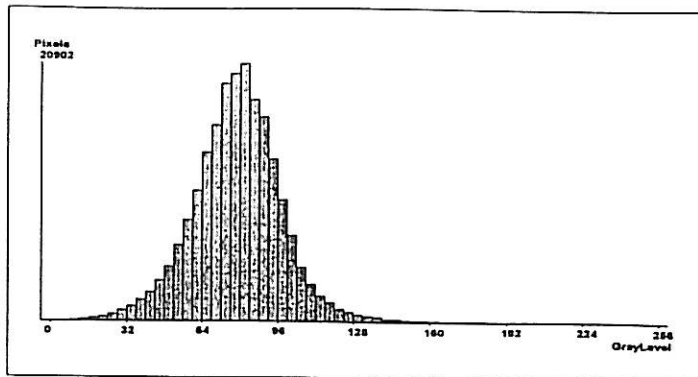
Water (23211 pixels)



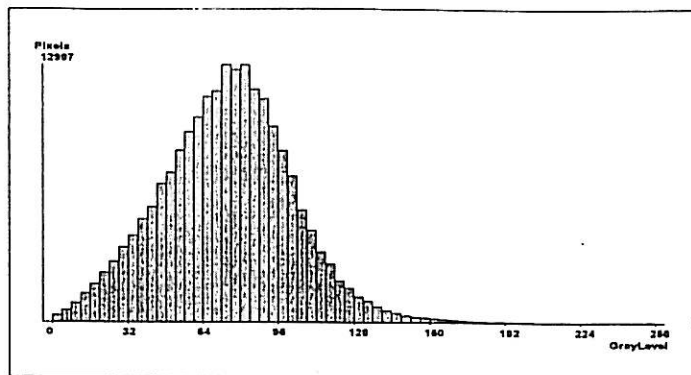
Nut Shells (18337 pixels)



Glass Beads (20902 pixels)

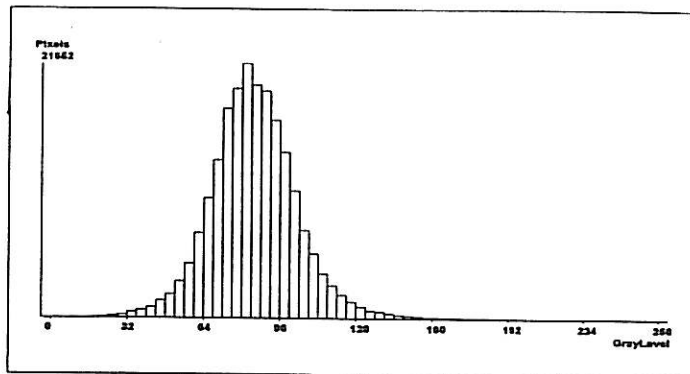


Black Beauty (12997 pixels)

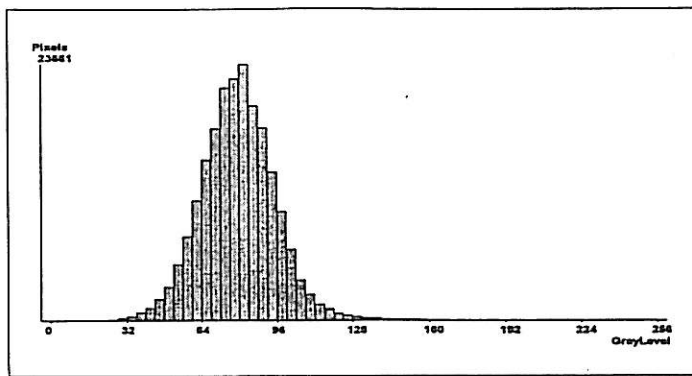


Sawn Marble - RLIA histograms for control and areas blasted at low pressures (50 psi for powdered materials, 1000 psi for water).

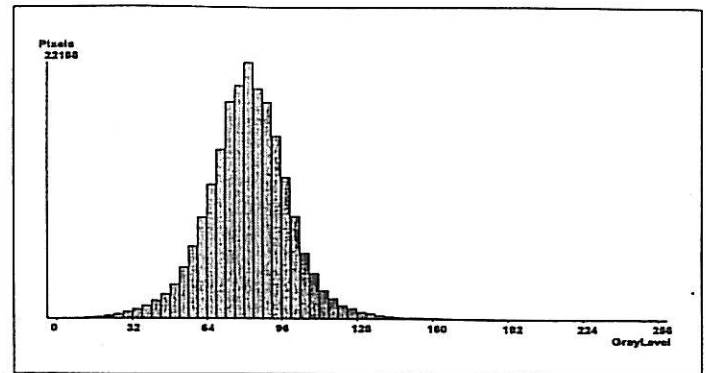
Control (21652 pixels)



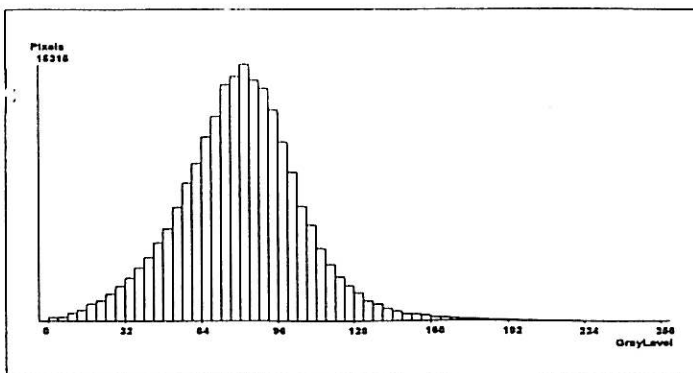
Water (23661 pixels)



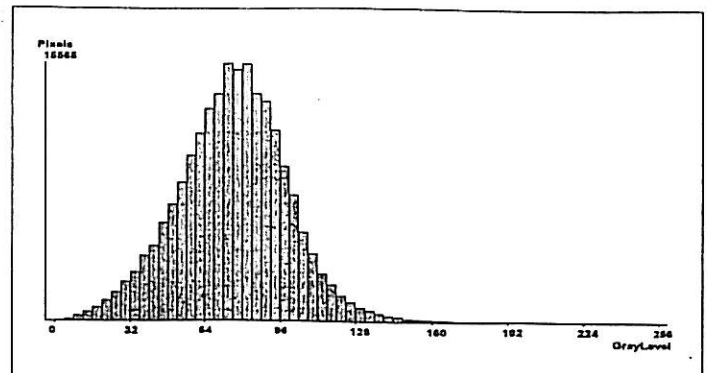
Nut Shells (22188 pixels)



Glass Beads (15315 pixels)



Black Beauty (15565 pixels)



Polished Granite 28,987 (PG/B1c)
 26,007
 30,265 average 28,419 ($\pm 2,185$)

PG/WI	32,035		PG/WII	31,373	
	29,475			28,677	
	36,464	32,658 ($\pm 3,536$)		33,005	31,018 ($\pm 2,185$)

PG/NI	28,727		PG/NII	26,653	
	29,735			32,328	
	28,807	29,089 (± 560)		32,457	30,479 ($\pm 3,314$)

PG/GI	29,553		PG/GII	27,831	
	36,631			29,915	
	35,328	33,837 ($\pm 3,767$)		31,411	29,719 ($\pm 1,798$)

PG/BI	18,830		PG/BII	25,641	
	21,459			26,857	
	18,963	19,750 ($\pm 1,481$)		25,269	25,922 (± 830)

Flamed Granite 14,236 (FG/B1c)
 14,321
 14,812 average 14,456 (± 311)

FG/WI	14,646		FG/WII	13,991	
	14,220			15,215	
	15,636	14,834 (± 726)		14,900	14,702 (± 635)

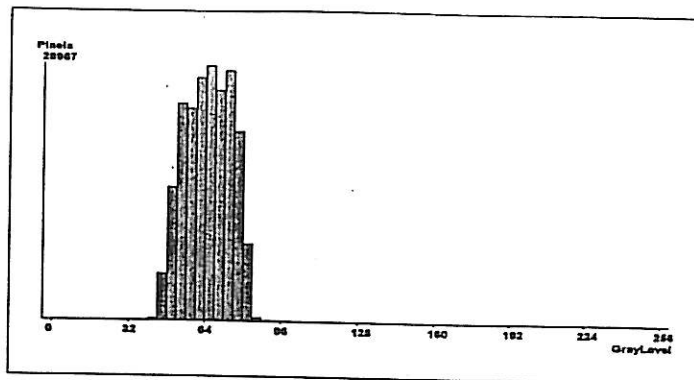
FG/NI	14,378		FG/NII	13,514	
	14,284			14,475	
	14,310	14,324 (± 48)		14,264	14,048 (± 505)

FG/GI	15,498		FG/GII	14,538	
	14,189			14,540	
	14,827	14,838 (± 654)		14,093	14,390 (± 257)

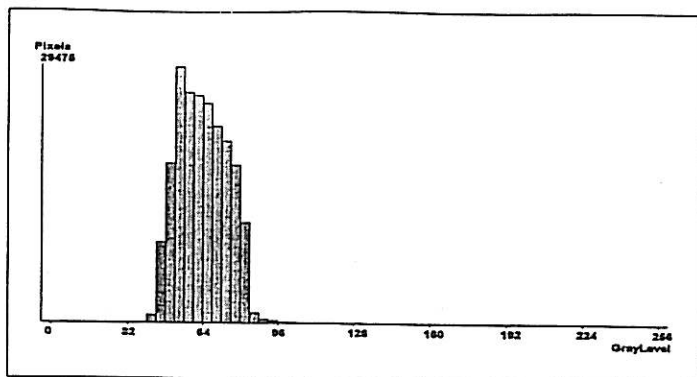
FG/BI	12,997		FG/BII	13,950	
	12,967			12,079	
	12,741	12,901 (± 140)		14,642	13,557 ($\pm 1,326$)

Polished Granite - RLIA histograms for control and areas blasted at high pressures (100 psi for powdered materials, 2000 psi for water).

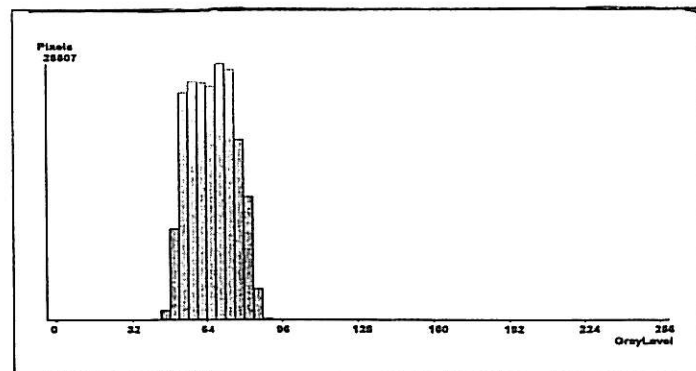
Control (28987 pixels)



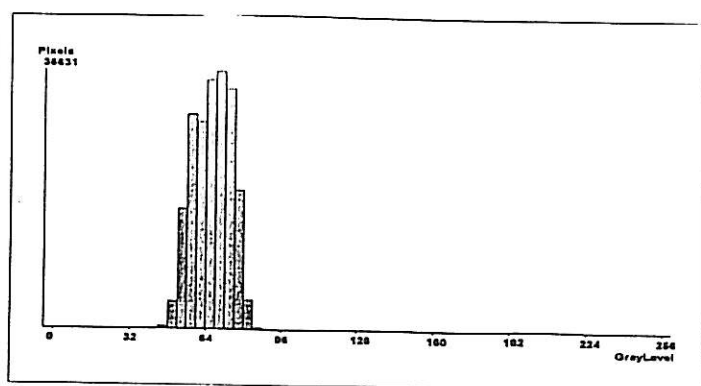
Water (29475 pixels)



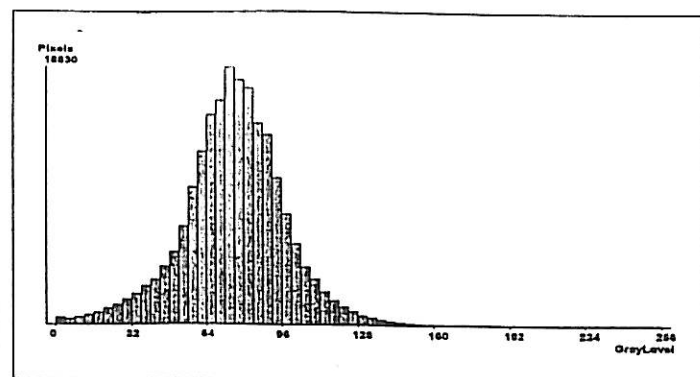
Nut Shells (28807 pixels)



Glass Beads (36631 pixels)

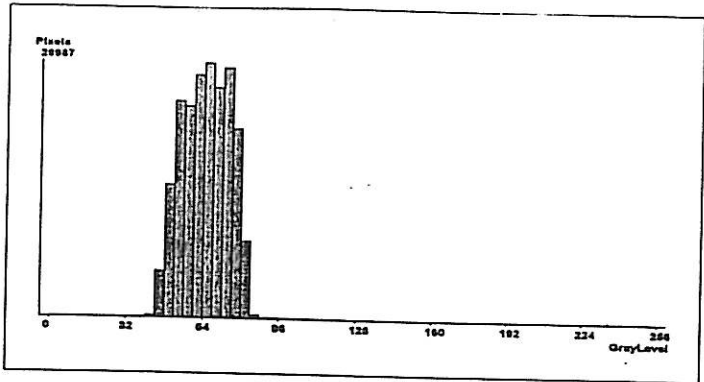


Black Beauty (18830 pixels)

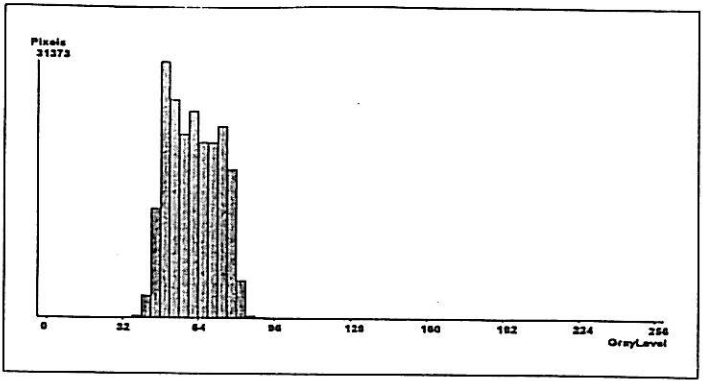


Polished Granite - RLIA histograms for control and areas blasted at low pressures (50 psi for powdered materials, 1000 psi for water).

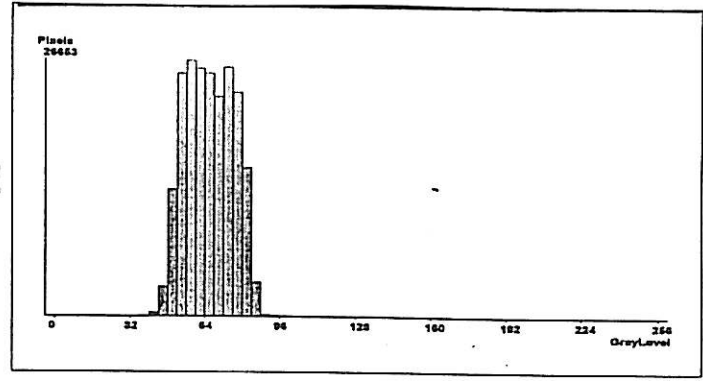
Control (28987 pixels)



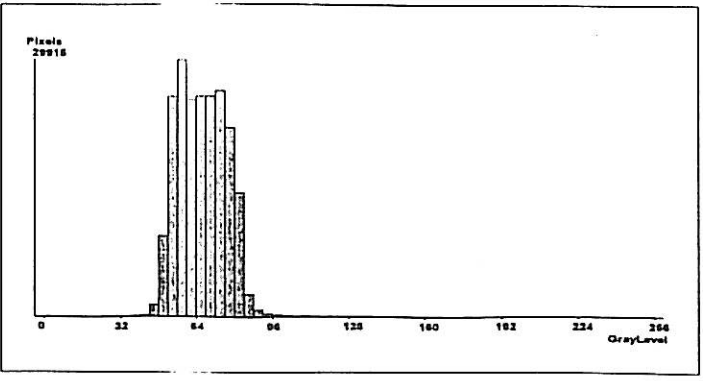
Water (31373 pixels)



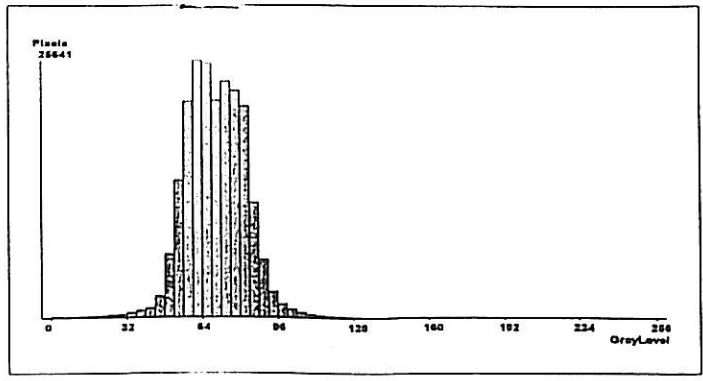
Nut Shells (26653 pixels)



Glass Beads (29915 pixels)

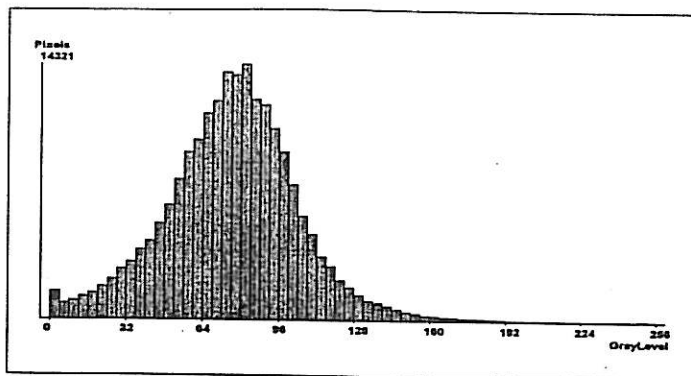


Black Beauty (25641 pixels)

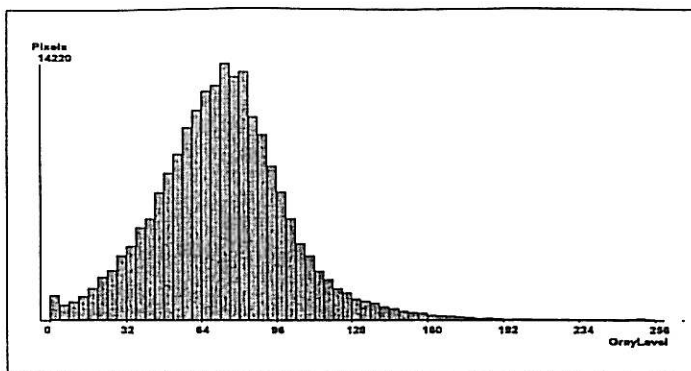


Flame Finished Granite - RLIA histograms for control and areas blasted at high pressures (100 psi for powdered materials, 2000 psi for water).

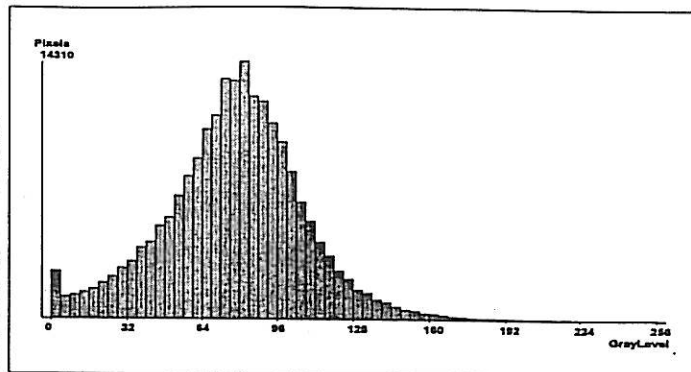
Control (14321 pixels)



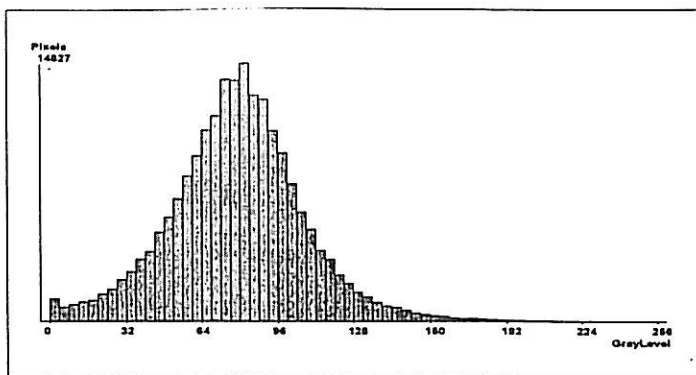
Water (14220 pixels)



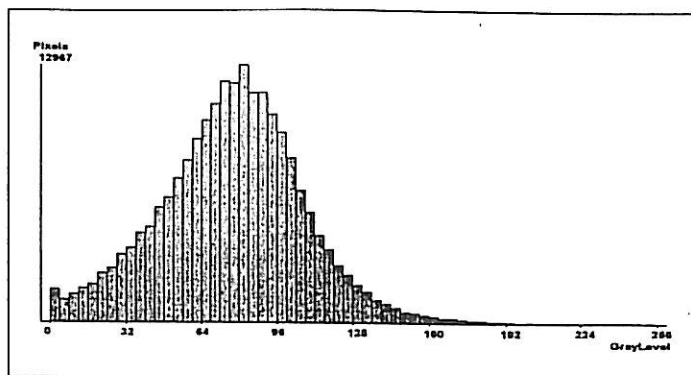
Nut Shells (14320 pixels)



Glass Beads (14827 pixels)

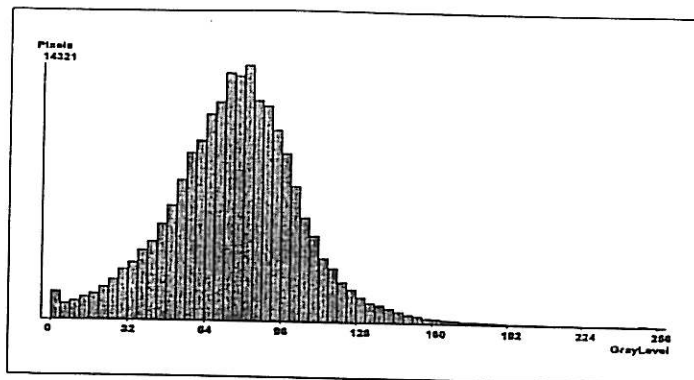


Black Beauty (12967 pixels)

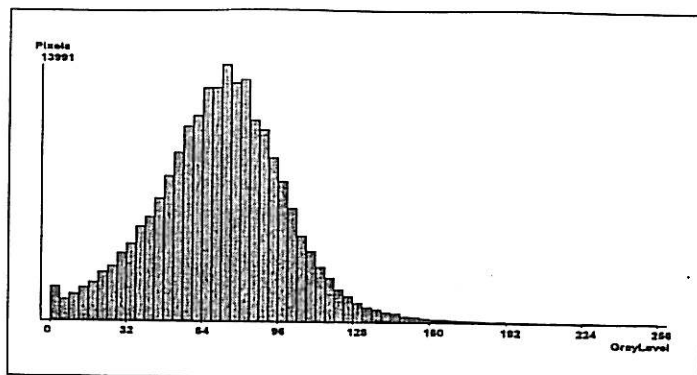


Flame Finished Granite - RLIA histograms for control and areas blasted at low pressures (50 psi for powdered materials, 1000 psi for water).

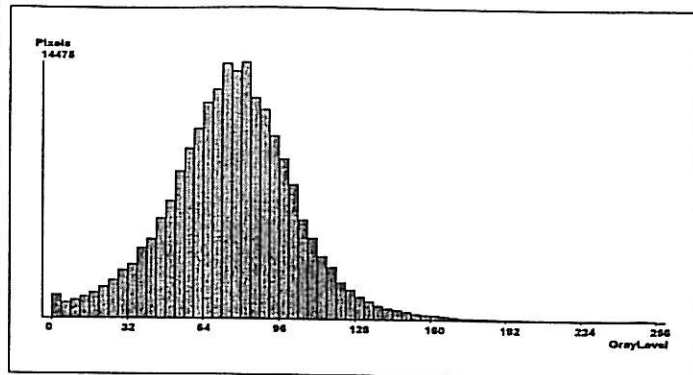
Control (14321 pixels)



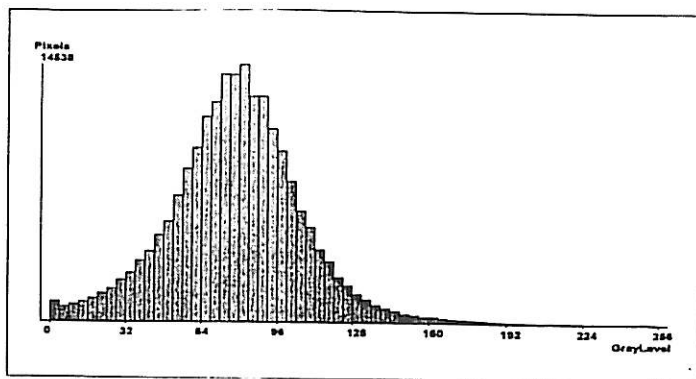
Water (13991 pixels)



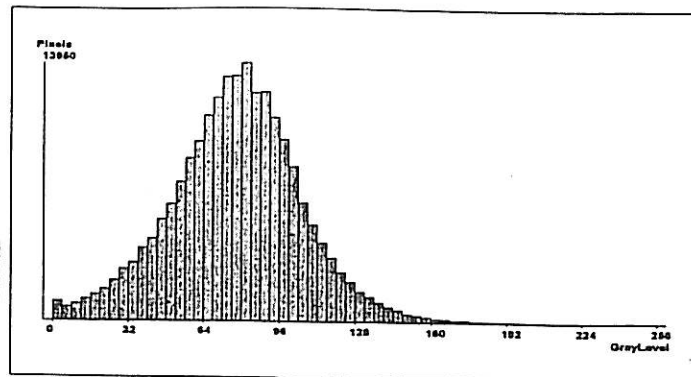
Nut Shells (14475 pixels)



Glass Beads (14538 pixels)



Black Beauty (13950 pixels)



Sawn Limestone (SL/GIc)	10,140		13,461 (SL/WIIc)	
	11,179		13,663	
	12,046		12,934	
			average	12,237 ($\pm 1,383$)

SL/WI	9,696		SL/WII	12,284
	10,181			12,738
	11,611	10,496 (± 995)		12,814
				12,612 (± 286)

SL/NI	8,371		SL/NII	12,372
	7,925			15,427
	8,282	8,192 (± 236)		14,148
				13,982 ($\pm 1,534$)

SL/GI	12,088		SL/GII	9,132
	10,068			8,671
	11,283	11,146 ($\pm 1,017$)		8,362
				8,721 (± 387)

SL/BI	7,676		SL/BII	8,375
	7,456			8,503
	7,539	7,557 (± 111)		7,997
				8,291 (± 263)

Sawn Sandstone (SS/GIc)	8,553		7,105 (SS/NIIc)	
	7,994		7,498	
	7,502		7,951	
			average	7,767 (± 507)

SS/WI	7,627		SS/WII	7,541
	8,191			8,060
	7,792	7,870 (± 290)		7,961
				7,854 (± 275)

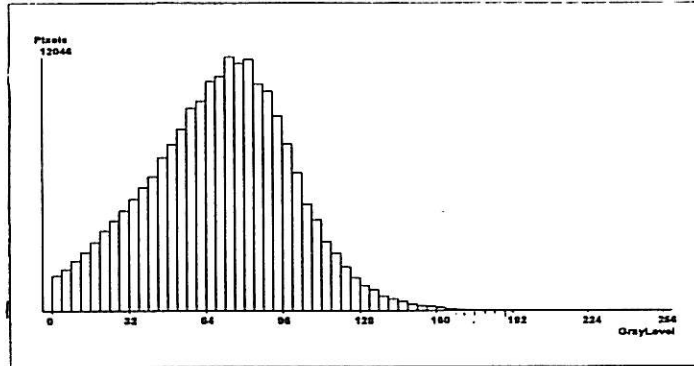
SS/NI	6,714		SS/NII	6,853
	6,184			7,288
	6,540	6,479 (± 270)		6,986
				7,042 (± 223)

SS/GI	7,391		SS/GII	6,484
	7,566			6,226
	7,387	7,448 (± 102)		6,501
				6,403 (± 154)

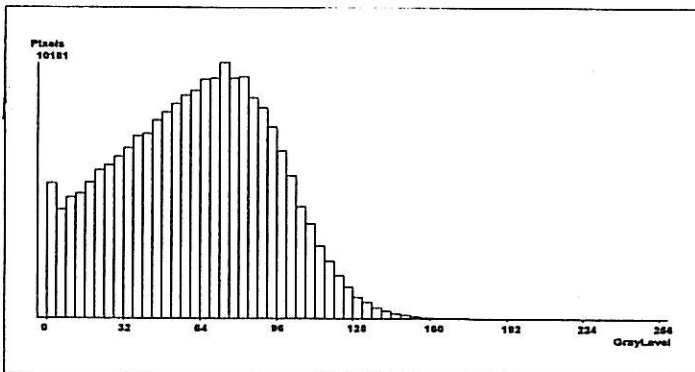
SS/BI	7,564		SS/BII	7,412
	7,298			7,347
	7,075	7,312 (± 245)		7,467
				7,408 (± 60)

Sawn Limestone - RLIA histograms for control and areas blasted at high pressures (100 psi for powdered materials, 2000 psi for water).

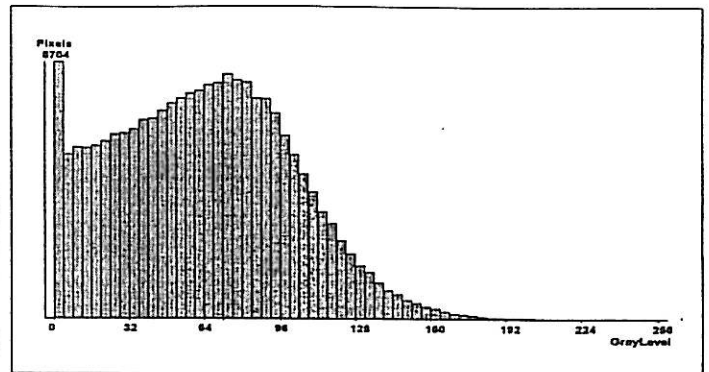
Control (12046 pixels)



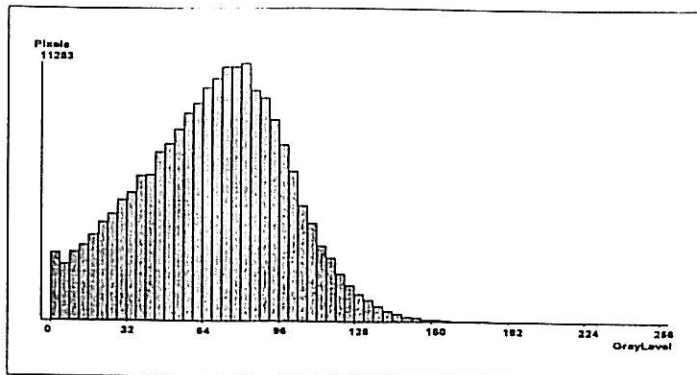
Water (10181 pixels)



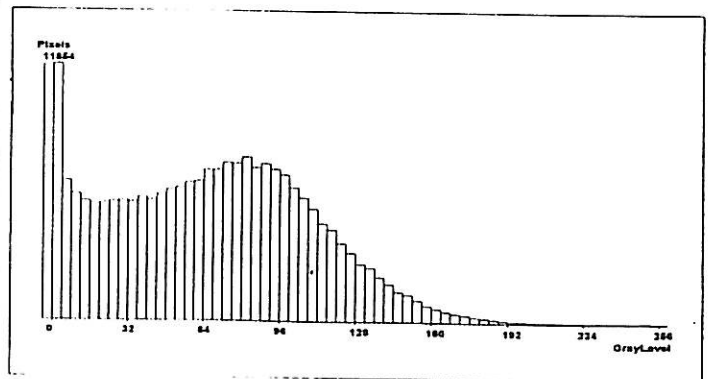
Nut Shells (8282 pixels)



Glass Beads (11283 pixels)

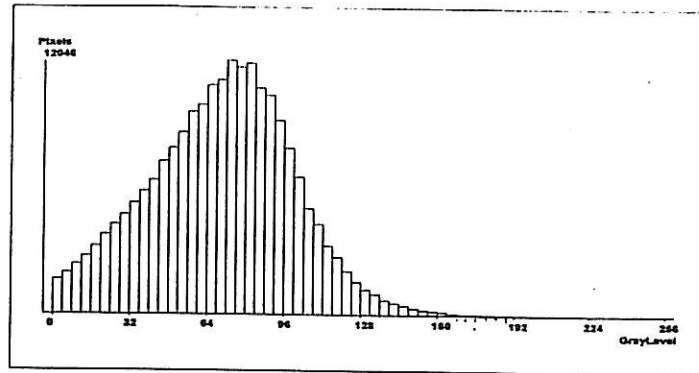


Black Beauty (7539 pixels)

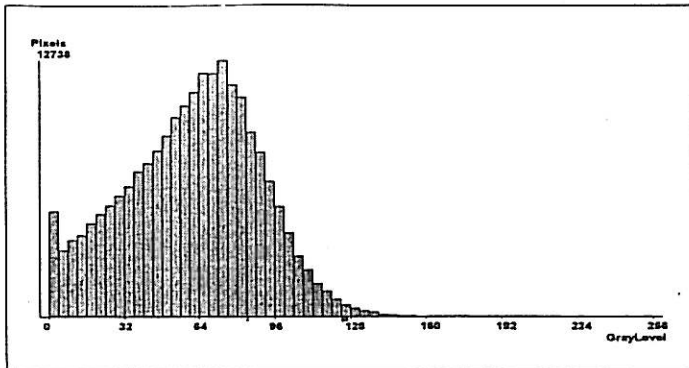


Sawn Limestone - RLIA histograms for control and areas blasted at low pressures (50 psi for powdered materials, 1000 psi for water).

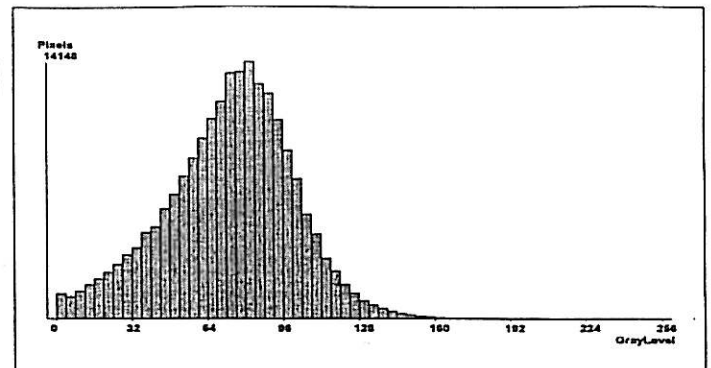
Control (12046 pixels)



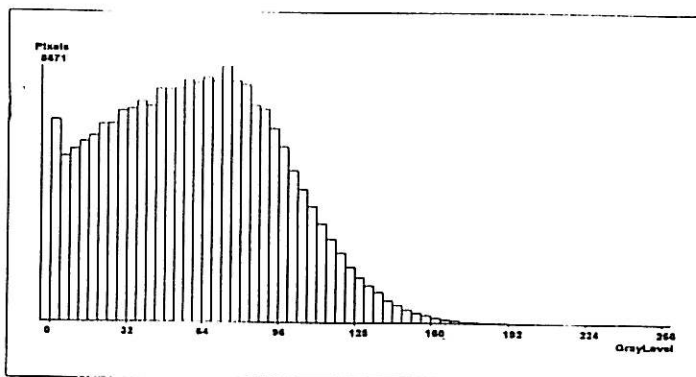
Water (12738 pixels)



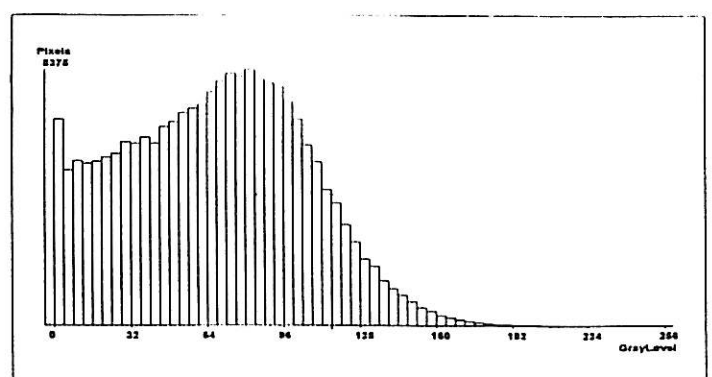
Nut Shells (14148 pixels)



Glass Beads (8671 pixels)

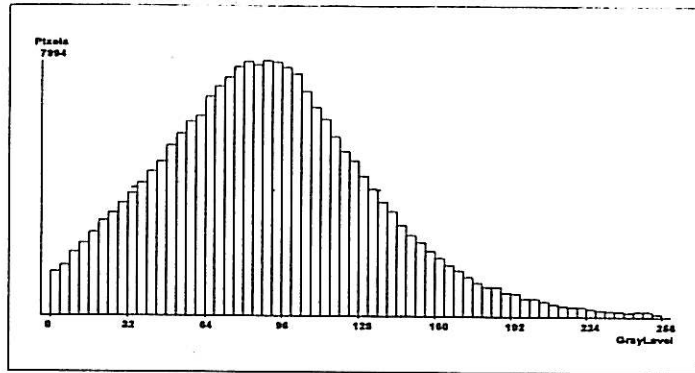


Black Beauty (8375 pixels)

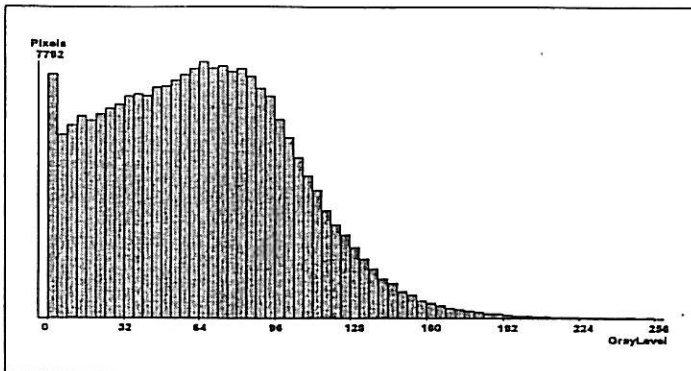


Sawn Sandstone - RLIA histograms for contol and areas blasted at high pressures (100 psi for powdered materials, 2000 psi for water).

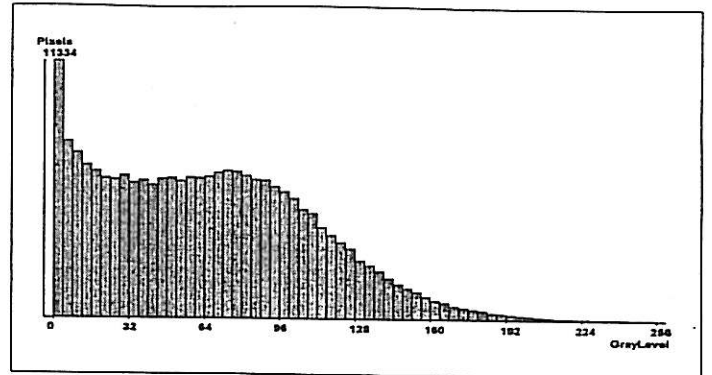
Control (7994 pixels)



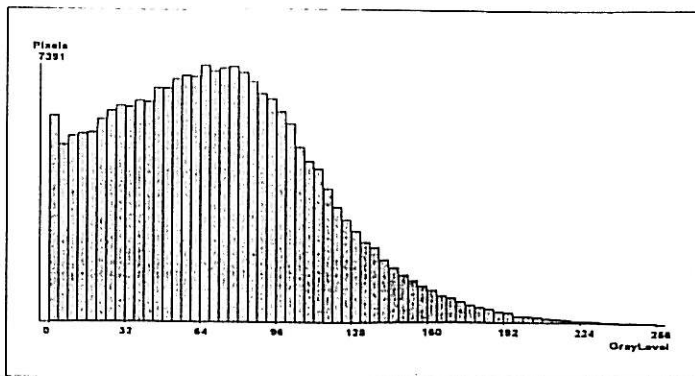
Water (7792 pixels)



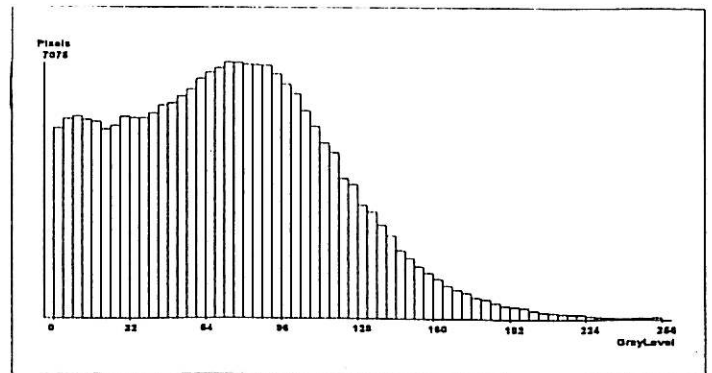
Nut Shells (6540 pixels)



Glass Beads (7391 pixels)

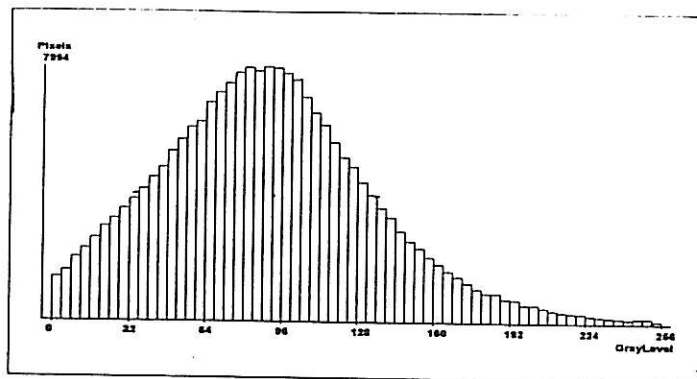


Black Beauty (7075 pixels)

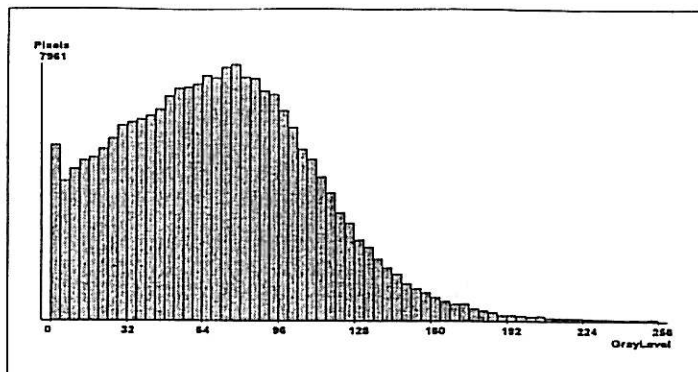


Sawn Sandstone - RLIA histograms for control and areas blasted at low pressures (50 psi for powdered materials, 1000 psi for water).

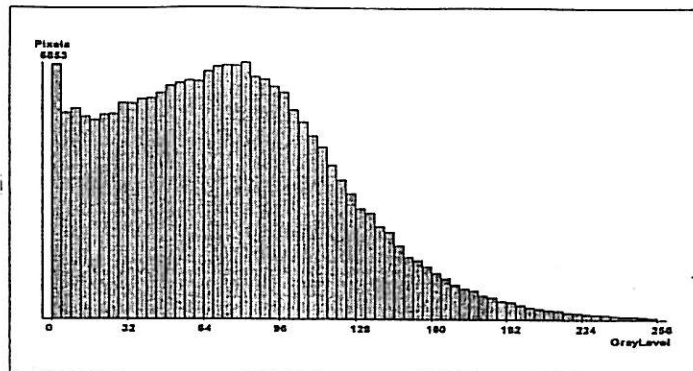
Control (7994 pixels)



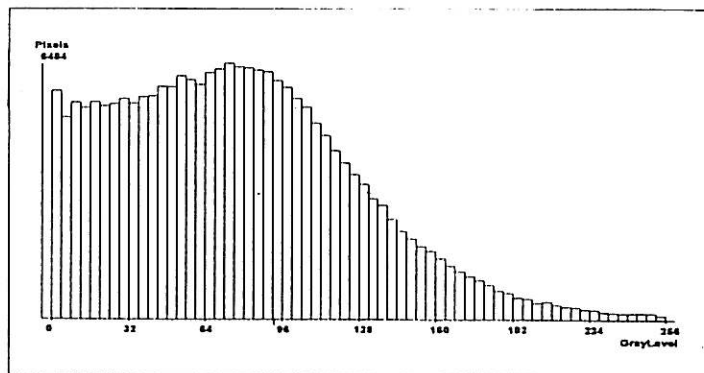
Water (7961 pixels)



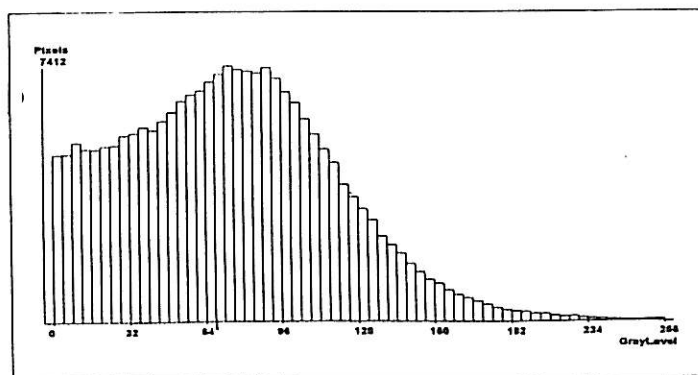
Nut Shells (6853 pixels)



Glass Beads (6484 pixels)



Black Beauty (7412 pixels)



Glazed Tile 38,562 (GT/B1c)
 36,233
 28,763 average 34,519 ($\pm 5,119$)

GT/WI	33,109		GT/WII	29,661	
	26,986			24,750	
	35,407	31,834 ($\pm 4,353$)		30,132	28,181 ($\pm 2,981$)

GT/NI	33,824		GT/NII	26,155	
	29,374			26,892	
	33,300	32,166 ($\pm 2,432$)		30,898	27,981 ($\pm 2,552$)

GT/GI	26,857		GT/GII	30,931	
	35,053			32,561	
	34,509	32,139 ($\pm 4,583$)		29,259	30,917 ($\pm 1,651$)

GT/BI	28,855		GT/BII	34,149	
	25,539			30,260	
	28,323	27,572 ($\pm 1,780$)		27,769	30,726 ($\pm 3,215$)

Quarry Tile 25,812 (QT/B1c)
 24,225
 26,457 average 25,498 ($\pm 1,148$)

QT/WI	26,710		QT/WII	25,423	
	24,793			24,371	
	28,727	26,743 ($\pm 1,967$)		24,898	24,897 (± 526)

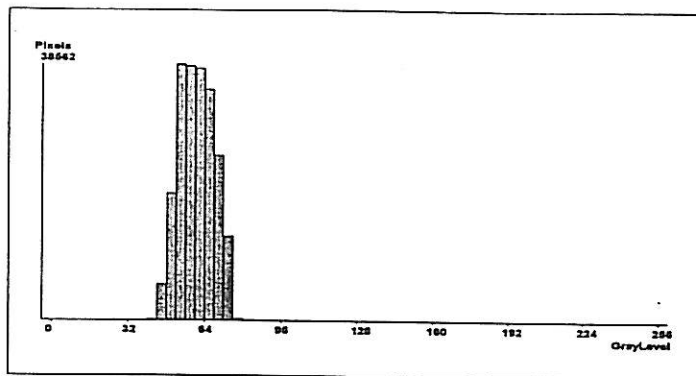
QT/NI	27,365		QT/NII	25,823	
	32,955			26,293	
	28,866	29,728 ($\pm 2,893$)		26,625	26,313 (± 430)

QT/GI	23,598		QT/GII	28,087	
	25,153			27,837	
	24,880	24,543 (± 830)		25,620	27,181 ($\pm 1,358$)

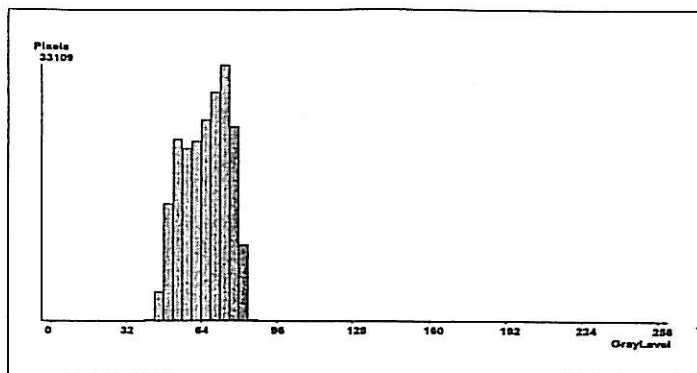
QT/BI	13,649		QT/BII	21,173	
	13,554			16,823	
	13,883	13,695 (± 169)		19,034	19,010 ($\pm 2,175$)

Glazed Tile - RLIA histograms for control and areas blasted at high pressures (100 psi for powdered materials, 2000 psi for water).

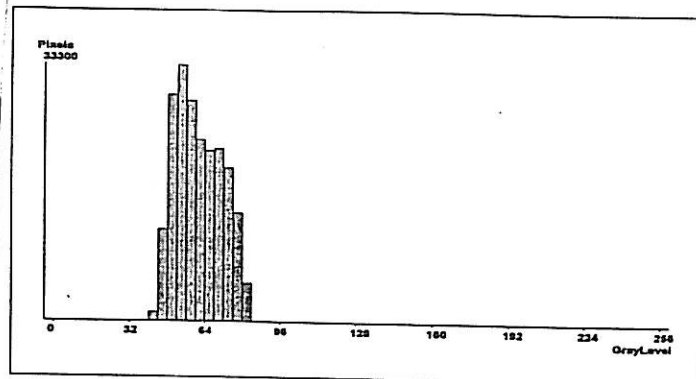
Control (38562 pixels)



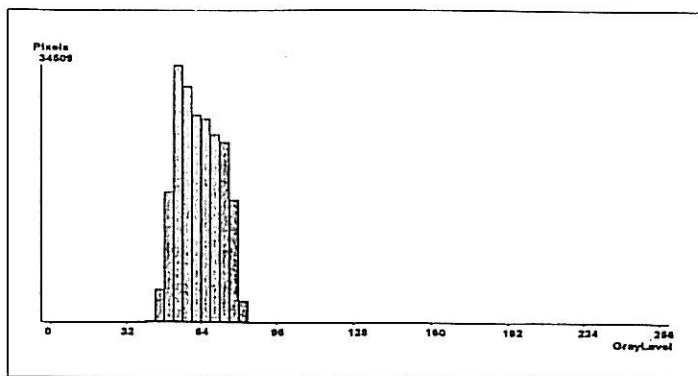
Water (33109 pixels)



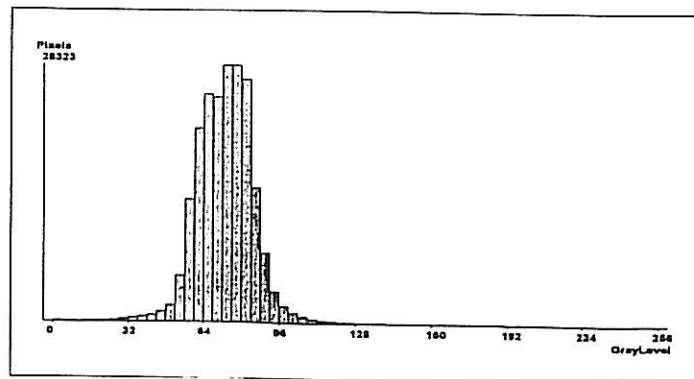
Nut Shells (33300 pixels)



Glass Beads (34509 pixels)

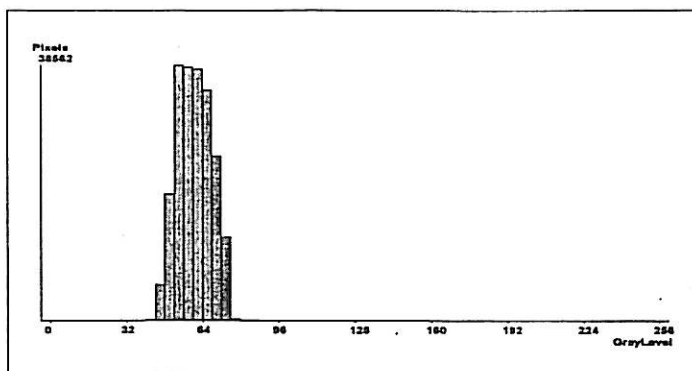


Black Beauty (28323 pixels)

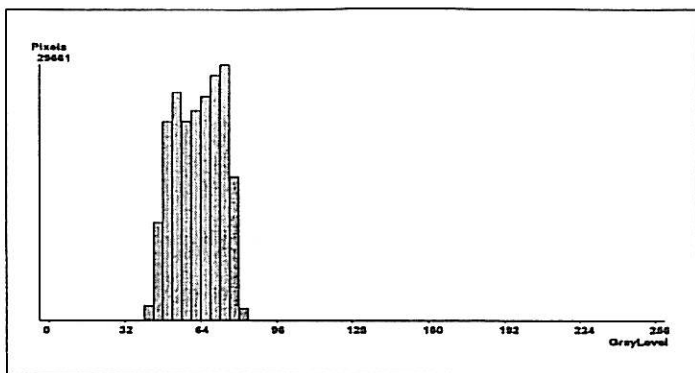


Glazed Tile - RLIA histograms for contol and areas blasted at low pressures (50 psi for powdered materials, 1000 psi for water).

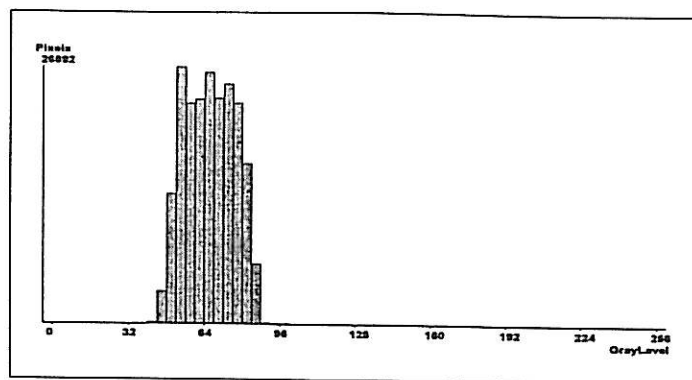
Control (38562 pixels)



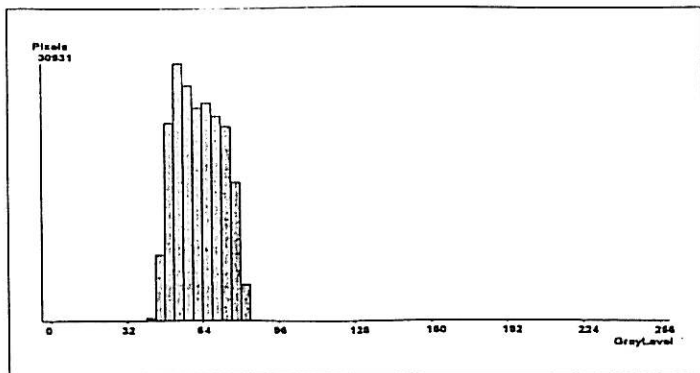
Water (29661 pixels)



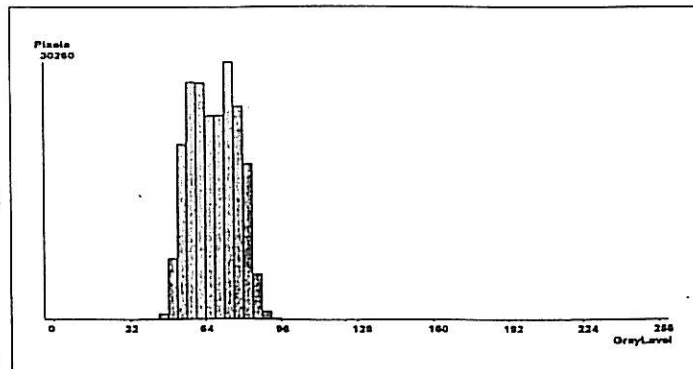
Nut Shells (26892 pixels)



Glass Beads (30931 pixels)

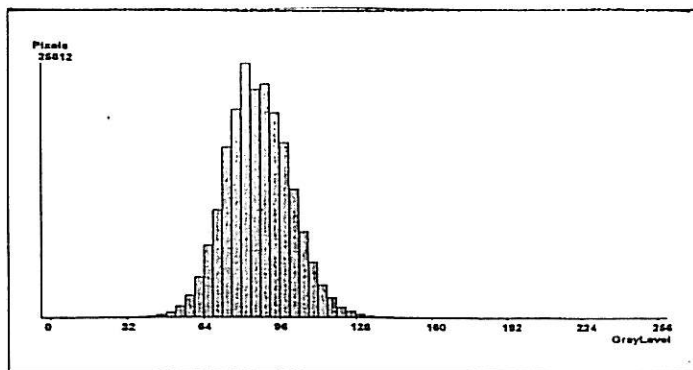


Black Beauty (30260 pixels)

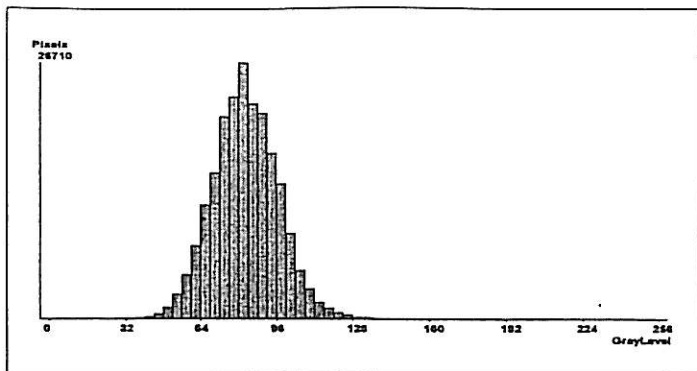


Quarry Tile - RLIA histograms for control and areas blasted at high pressures (100 psi for powdered materials, 2000 psi for water).

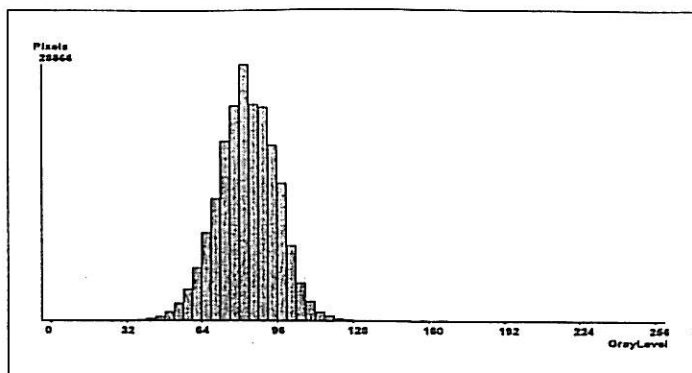
Control (25812 pixels)



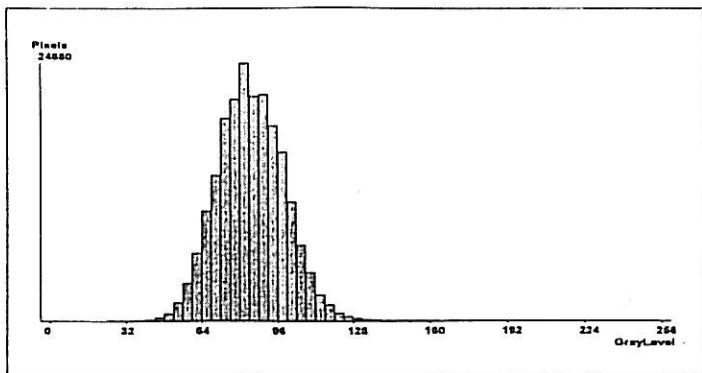
Water (26710 pixels)



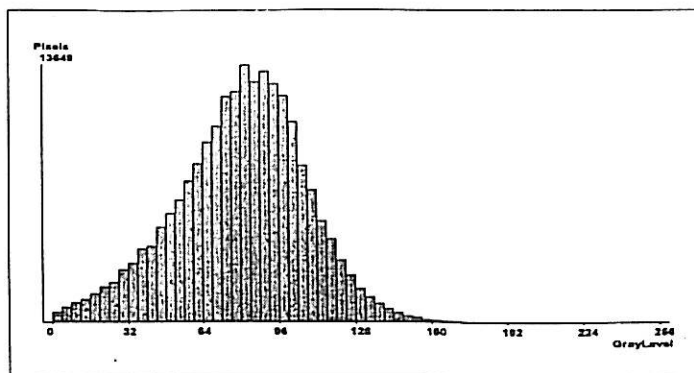
Nut Shells (28866 pixels)



Glass Beads (24880 pixels)

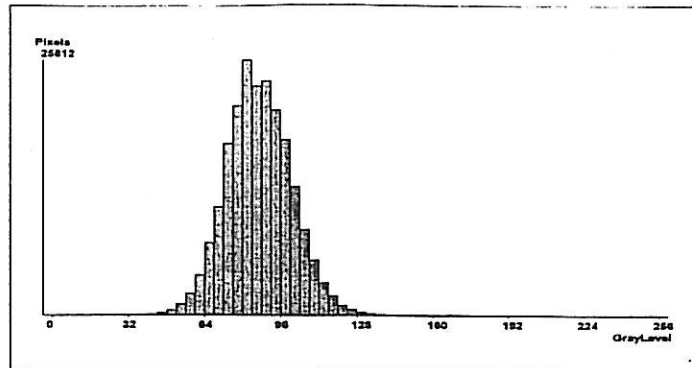


Black Beauty (13649 pixels)

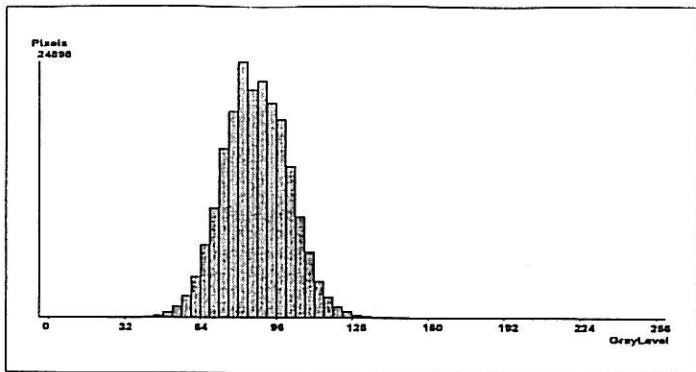


Quarry Tile - RLIA histograms for control and areas blasted at low pressures (50 psi for powdered materials, 1000 psi for water).

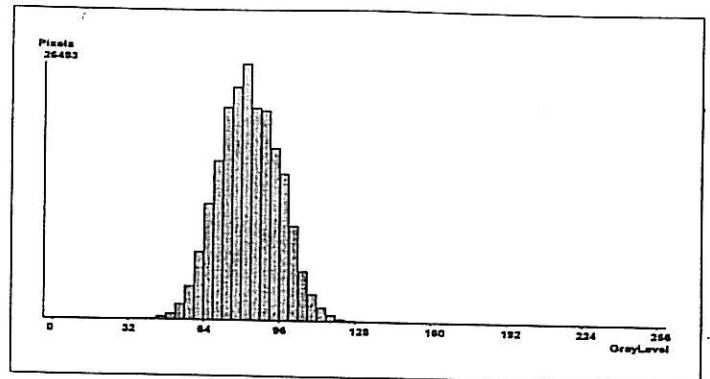
Control (25812 pixels)



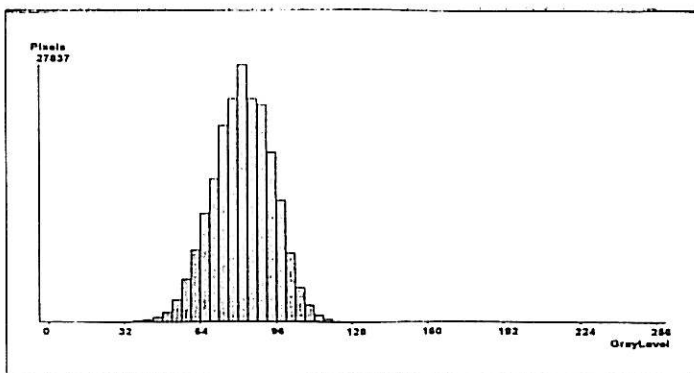
Water (42898 pixels)



Nut Shells (26492 pixels)



Glass Beads (27837 pixels)



Black Beauty (19034 pixels)

